

Deliverable D55 (D7.6)

RI-URBANS booklet summarising information packages from WPs 5-6



RI-URBANS

**Research Infrastructures Services Reinforcing Air
Quality Monitoring Capacities in European Urban &
Industrial Areas (GA n. 101036245)**

By

CSIC, UHEL & ACTRIS-ERIC



7 July 2025

Deliverable D55 (D7.6): RI-URBANS booklet summarising information packages from WPs 5-6

Authors: Xavier Querol & Fulvio Amato (CSIC), Tuukka Petäjä (UHEL) & Giulia Saponaro (ACTRIS ERIC)

Work package (WP)	WP7 Communication, dissemination and exploitation
Deliverable	D55 (D7.6)
Lead beneficiary	ACTRIS ERIC
Deliverable type	<input type="checkbox"/> R (document, report) <input checked="" type="checkbox"/> DEC (websites, patent filings, videos, ...) <input type="checkbox"/> Other: ORDP (open research data pilot)
Dissemination level	<input checked="" type="checkbox"/> PU (public) <input type="checkbox"/> CO (confidential, only members of consortium and European Commission)
Estimated delivery deadline	M48 (30/09/2025)
Actual delivery deadline	07/07/2025
Version	Final
Reviewed by	WP7 Leaders & Project Coordination Team
Accepted by	Project Coordination Team
Comments	<p>This report contains the booklet containing the summary of the Service tools produced by RI-URBANS, the links to each of the 16 specific ST Guidance Documents. Furthermore, it contains chapters on the EU added value of implementing theses by interpreting the EU available compiled urban data for the different advanced pollutants and the applications of the \cdotD measurements, emission inventories and modelling tools. RI-URBANS received an additional financial support from AXA Research Fund and in addition to the electronic file, 1000 printed booklets were produced for dissemination.</p>

Table of Contents

1. About this document.....	1
2. The Booklet.....	2

1. About this document

This report “*RI-URBANS booklet summarising information packages from WPs 5-6*” (D55 (D7.6)) is a product of WP7, and contains the booklet containing the summary of the Service tools produced by RI-URBANS, the links to each of the 16 specific ST Guidance Documents. Furthermore, it contains chapters on the EU added value of implementing theses by interpreting the EU available compiled urban data for the different advanced pollutants and the applications of the ·D measurements, emission inventories and modelling tools. RI-URBANS received an additional financial support from AXA Research Fund and in addition to the electronic file, 1000 printed booklets were produced for dissemination.

17 STs were provided from WP1 (monitoring), WP2 (mapping, citizens and health impact) and WP3 (emission inventories and modelling). Furthermore, for each STs EU available urban data were compiled and interpreted to show the added value and the applications. The 17 STs were tested in WP4 in the 5 pilot studies in 11 cities. From these only 16 STs were considered mature to be finally proposed. All the recommendations of the pilot tests were incorporated and supplied to WP5 and 6 where these were discussed, and 16 guidance documents were produced by WP6. Also, in WP6 a booklet was elaborated summarising the service tools, guidance documents and the links to them, and the added value of the implementation. WP7 worked to give a friendly reading design. This booklet made up the present deliverable report.

This is a public document that will be distributed to all RI-URBANS partners for their use and submitted to the European Commission as RI-URBANS deliverable D55 (D7.6). This document can be downloaded at <https://riurbans.eu/work-package-7/#deliverables-wp7>

The booklet can be directly downloaded from https://riurbans.eu/wp-content/uploads/2025/03/RI-URBANS_AXA-book.pdf

And all the 16 ST guidance documents from: <https://riurbans.eu/project/#service-tools>

2. The Booklet

Guidance documents on measurements and modelling
of novel air quality pollutants in urban Europe:
Summary and added value

with the support of:



Research Fund



Editors: Xavier Querol (CSIC), Fulvio Amato (CSIC), Andrés Alastuey (CSIC), Tuukka Petäjä (UHEL), Katriina Kyllönen (FMI), Rosa Petracca (CNR)

Authors & Reviewers: See Table 2.2.

Cover image created with AI using RECREATE

Research Infrastructures Services Reinforcing Air Quality Monitoring Capacities in European Urban & Industrial AreaS (RI-URBANS)

RI-URBANS (<http://www.RIURBANS.eu>) is supported by the European Commission under the Horizon 2020 – Research and Innovation Framework Programme, H2020-GD-2020, Grant Agreement number: 10103624



Table of Contents

ABBREVIATIONS.....	I
ELEMENTS AND CHEMICAL SPECIES	III
1. ABOUT THIS DOCUMENT	1
2. SUMMARY OF THE SERVICE TOOLS AND OPEN ACCESS TO THE GUIDANCE DOCUMENTS.....	3
3. UFP AND PNSD IN URBAN EUROPE.....	9
3.1 ADDED VALUE OF UFP AND PNSD MEASUREMENTS.....	9
3.2 EMISSION INVENTORIES OF UFP AND PNSD	13
3.3 MODELLING OF UFP AND PNSD	15
3.4 SPECIFIC CHALLENGES IN UFP AND PNSD	16
4. EBC MASS CONCENTRATIONS IN URBAN EUROPE	17
4.1 BLACK CARBON AND AIR QUALITY.....	17
4.2 ADDED VALUE OF MEASURING EBC CONCENTRATION IN EUROPE.....	17
5. PM SPECIATION AND SOURCE APPORTIONMENT IN URBAN EUROPE	21
5.1 PM SPECIATION AND SOURCE APPORTIONMENT IN URBAN EUROPE USING OFF-LINE PM MEASUREMENTS	21
5.1.1 <i>Off-line PM speciation</i>	<i>21</i>
5.1.2 <i>Source apportionment based on off-line PM speciation</i>	<i>24</i>
5.2 NON-REFRACTORY PM1 SPECIATION AND SOURCE APPORTIONMENT IN URBAN EUROPE USING ON-LINE PM MEASUREMENTS.....	25
5.2.1 <i>On-line PM speciation.....</i>	<i>25</i>
5.2.2 <i>Source apportionment based on on-line PM speciation.....</i>	<i>27</i>
6. OXIDATIVE POTENTIAL OF PM IN URBAN EUROPE.....	28
7. NH₃ IN URBAN EUROPE	31
7.1 NH ₃ AND AIR QUALITY	31
7.2 THE ADDED VALUE OF MEASURING NH ₃ IN URBAN EUROPE.....	32
8. VOCs IN URBAN EUROPE	35
8.1 THE COMPLEXITY OF MEASURING VOCs	35
8.2 EMISSIONS OF VOCs.....	36
8.3 THE ADDED VALUE OF MEASURING VOCs IN URBAN EUROPE.....	37
8.3.1 <i>Concentrations of VOCs.....</i>	<i>37</i>
8.3.2 <i>Source apportionment studies of volatile organic compounds in Europe</i>	<i>39</i>
9. VERTICAL PROFILES.....	42
9.1 ATMOSPHERIC BOUNDARY LAYER	42
9.2 VERTICAL PROFILES OF AEROSOLS	43
9.3 IAGOS VERTICAL PROFILES OF POLLUTANTS	45
10. URBAN MAPPING AND CITIZEN SCIENCE	48
10.1 MAPPING OF NOVEL AQ PARAMETERS	48
10.2 MAPPING AND INVOLVEMENT OF CITIZEN SCIENCE.....	50
11. FINAL CONSIDERATIONS.....	52
12. REFERENCES	54

Abbreviations

ABLH	Atmospheric boundary layer height
ACTRIS	Aerosols, Clouds and Trace gases Research InfraStructure
ALC	Automatic lidars and ceilometers
AMS	Aerosol mass spectrometer
API-CIMS	Atmospheric pressure interface CIMS
AQ	Air quality
AQD	Air quality directive
AQEG-UK	UK Air Quality Expert Group
AQMN	Air quality monitoring network
AVOC	Anthropogenic VOC
BBOA	Biomass burning OA
BC	Black carbon
BrC	Brown carbon
BVOC	Biogenic VOC
CAMS	Copernicus Atmosphere Monitoring Service
CBH	Cloud base height
CBL	Convective boundary layer
CEN	European Committee for Standardisation
CHIMERE	Multi-scale chemistry-transport model for atmospheric composition
CIMS	Chemical ionization mass spectrometry
CLe	UNECE long-term Critical Levels
COA	Cooking-like OA
Coal OA	Coal combustion OA
CRDS	Cavity ring-down spectroscopy
CSOA	Cigarette-smoke OA
DMANx	Dynamic model for aerosol nucleation
DWL	Doppler Wind lidars
eBC	Equivalent black carbon
eBC_{lf}	Equivalent black carbon from liquid fuels
eBC_{sf}	Equivalent black carbon from solid fuels
EEA	European Environment Agency
EN	European standard
EPR	Electron paramagnetic resonance
ESFRI	European Strategy Forum on Research Infrastructures
EU	European Union
EURO	European emission standards
FAH	Farming/agricultural hotspot
FTP	File Transfer Protocol
GAW	Global Atmospheric Watch programme by WMO
GC	Gas chromatography
HOA	Hydrocarbon like OA
HFOC	High-finesse optical cavity
HOC	Heavy oil combustion
HPLC	High-performance liquid chromatography
HVOC	Hydrogenated VOC
IAGOS	In-service Aircraft for a Global Observing System
LOA	Local OA
LO-OOA	Less-oxidised oxygenated OA

LUR	Land Use Regression
MIR	Maximum incremental reactivity
NMHC	Non-methane hydrocarbon
MLH	Mixed layer height
MO-OOA	More-oxidised oxygenated OA
MOFP	Maximum ozone formation potential
NAQD	New European Air Quality Directive (formally adopted 14th October 2024)
NMVOC	Non-methane VOC
NR	Non-refractory
OM	Organic matter
OOA	(Generic) oxygenated OA
OP	Oxidative potential
OP^{AA}	Oxidative potential measured through the depletion of the ascorbic acid, a lung anti-oxidant
OP^{DTT}	Oxidative potential measured through the depletion of the dithiothreitol, a lung anti-oxidant's surrogate
OP^{GSH}	Oxidative potential measured through the depletion of the glutathione, a lung anti-oxidant
OP^{OH}	Oxidative potential measured through the formation of hydroxy radical
OP^{ESR}	Oxidative potential measured through the formation of particle-bound free radicals using electron paramagnetic resonance
OP_m	Mass-normalised OP
OP_v	Volume-normalised OP
OVOC	Oxygenated VOC
PAH	Polyaromatic hydrocarbon
PM	Particulate matter
PM_{2.5}	Mass concentration of particles <2.5 µm
PM₁₀	Mass concentration of particles <10 µm
PM_x	PM ₁₀ , PM _{2.5} and PM ₁
PMCAMx-UF	Three-dimensional chemical transport model focusing on the simulation of UFP-PNSD and composition
PMF	Positive matrix factorization
PMF-ME2	Positive matrix factorization with multi-linear engine 2
PN	Particle number
PNC	Particle number concentrations
PNSD	Particle number size distribution
POA	Primary OA
PTR-MS	Proton transfer mass spectrometry
QA/QC	Quality assurance and quality control
RB	Regional background
RBCH	Regional background site close to hotspot
RI-URBANS	Research Infrastructures Services Reinforcing Air Quality Monitoring
ROS	Reactive oxygen species
SCR	Selective catalytic reduction
ShINDOA	Shipping + industry OA
SIA	Secondary inorganic aerosol
SIFT-MS	Selected ion flow tube mass spectrometry
SOA	Secondary organic aerosol
SOAP	SOA formation potential
SP	Spatial
SUB	Sub-urban background

SVOC	Semi-volatile VOC
TEM	Temporal
TOMAS	Two-moment aerosol sectional algorithm
TPN	Total particle number
TR	Traffic
UA	Uric acid assay for OP (OP ^{UA})
UB	Urban background
UFP	Ultrafine particles
UNECE	United Nations Economic Commission for Europe
YSOA	SOA yield
VOC	Volatile organic compounds
WHO	World Health Organization
WMO	World Meteorological Organization
WP	Work package

Elements and chemical species

Al	Aluminium
As	Arsenic
Ba	Barium
Br	Bromine
BTEX	Benzene, toluene, ethylbenzene, and xylenes
C	Carbon
Ca	Calcium
CaSO₄·H₂O	Gypsum
Cd	Cadmium
CH₄	Methane
Cl	Chloride
Co	Cobalt
CO	Carbon monoxide
CO₂	Carbon dioxide
Cr	Chromium
Cu	Copper
DMPO	5,5-dimethyl-1-pyrroline-N-oxide
EC	Elemental carbon
F	Fluoride
FOX	Ferric-xylenol orange
Fe	Iron
H	Hydrogen
H₂O	Water
H₂O₂	Hydrogen peroxide
H₂SO₄	Sulphuric acid
Hg	Mercury
HNO₃	Nitric acid
I	Iodine
K	Potassium
MACR	Methacrolein
Mg	Magnesium
Mn	Manganese
Mo	Molybdenum

MVK	Methyl vinyl ketone
N	Nitrogen
Na	Sodium
NaNO₃	Sodium nitrate
NH₃	Ammonia
NH₄	Ammonium
NH₄HSO₄	Ammonium hydrogen-sulphate
(NH₄)₂SO₄	Ammonium sulphate
NH₄NO₃	Ammonium nitrate
Ni	Nickel
NO	Nitrogen monoxide
NO₂	Nitrogen dioxide
NO₃⁻	Nitrate
NO_x	Nitrogen oxides (NO+NO ₂)
O	Oxygen
O₃	Ozone
OA	Organic aerosol
OC	Organic carbon
OH	Hydroxyl radical
P	Phosphorous
Pb	Lead
R	Alkyl group
Rb	Rubidium
Sb	Antimony
Se	Selenium
Si	Silicon
Sn	Tin
SO₂	Sulphur dioxide
SO₄²⁻	Sulphate
SO_x	Sulphur oxides
Sr	Strontium
Ti	Titanium
V	Vanadium
Y	Yttrium
Zn	Zinc
Zr	Zirconium

1. ABOUT THIS DOCUMENT

This document was prepared as part of the EU-project "Research Infrastructures Services Reinforcing Air Quality (AQ) Monitoring Capacities in European Urban & Industrial Areas" (RI-URBANS, supported by the European Commission under the Horizon 2020 – Research and Innovation Framework Programme, H2020-GD-2020, grant 10103624) that connects the atmospheric observation expertise from the 'Aerosols, Clouds and Trace gases Research InfraStructure' (ACTRIS), and the 'In-service Aircraft for a Global Observing System' (IAGOS), with the urban AQ observation capacities of the regulatory AQ monitoring networks (AQMNs). It is specifically connected to the new European AQ Directive (NAQD) 2024/2881/EC published on 20 November 2024.

The NAQD underlines the importance of emerging pollutants for AQ and the well-being of the citizens. Particularly, novel pollutants such as ultrafine particles (UFP), UFP-number size distribution (PNSD), black carbon (BC) and elemental carbon (EC), as well as ammonia (NH₃) and numerous volatile organic compounds (VOCs), and measurements of tracers of potential toxicity of particulate matter (oxidative potential (OP) of particulate matter (PM)), are required or recommended to be monitored at both rural and urban supersites in order to support scientific understanding of their effects on health and the environment. In order to ensure that the measurements on air pollution are sufficiently representative and comparable across Europe, it is important that standardized measurement techniques and common criteria for the number and location of measuring stations are used for the assessment of ambient AQ.

RI-URBANS produced a number of Service Tools (STs) for specific advanced AQ measurement and modelling variables, a number of these included in Article 10 and Annex VII of the NAQD.

An ST in RI-URBANS is any tool that in the project has been reviewed, in some cases developed, tested, and recommended for advanced AQ assessment in urban areas. These tools can be used to assess AQ in accordance with RI-URBANS AQ monitoring and modelling recommendations for novel pollutants. These recommendations include protocols for measuring advanced AQ variables (derived from ACTRIS and CEN or, in specific cases, proposed when not available) and vertical profiles, mapping protocols, emission inventories, modelling tools, and suggested epidemiological approaches to evaluate the health effects of new pollutants.

This document aims at providing information on the two major fields related with the above issues:

- Information and access links to 16 specific ST documents that have been produced and reviewed in RI-URBANS, and in a number of cases in RI-URBANS/ACTRIS. The section for this aim is shorter because the guidance documents are very detailed and only a very short summary and the link to the specific document are provided.
- Information on the added value of measuring advanced air quality variables for enhanced air quality assessment obtained by compiling existing data sets within the framework of RI-URBANS and, in some cases, RI-URBANS/ACTRIS.

The electronic file of this document, with the links to the files of STs, can be downloaded at <https://riurbans.eu/project/#service-tools>.

We greatly acknowledge the financial support received from AXA Research Fund to increase the outreach.

This RI-URBANS document is the final dissemination document (D55 (D7.6)). Any dissemination of results must indicate that it reflects only the author's view and that the European Commission is not responsible for any use that may be made of the information it contains.

2. SUMMARY OF THE SERVICE TOOLS AND OPEN ACCESS TO THE GUIDANCE DOCUMENTS

As stated above, an ST in RI-URBANS is any tool that in the project has been reviewed, in some cases developed, tested, and recommended for advanced AQ assessment in urban areas. Table 2.1 shows the 16 STs and associated guidance documents (grouped according to their aim/method: surface or profile measurements, source apportionment, health assessment, mapping, emission inventories, and modelling). The specific detailed guidance documents can be downloaded at <https://riurbans.eu/project/#service-tools>. Once accessed through this link, single STs can be visualized/downloaded by clicking in each of six ST groups.

Table 2.1: The 16 STs (grouped according aim/method: surface or profile measurements, source apportionment, health assessment, mapping, emission inventories, and modelling) provided by RI-URBANS for which the respective associated guidance documents can be downloaded at <https://riurbans.eu/project/#service-tools>.

Number	Guidance document topic
Protocols for the measurement of novel AQ pollutants	
ST1	Ultrafine-Particle Number Size Distributions (UFP-PNSD)
ST2	Black Carbon (BC)
ST3	Offline and online particulate matter (PM) speciation
ST4	Oxidative potential of particulate matter (OP of PM)
ST5	Volatile Organic Compounds (VOCs)
ST6	Ammonia (NH ₃)
Methodologies for vertical profiles of pollutants and meteorology	
ST7	Measurements of boundary level height
ST8	Measurements of vertical profiles of aerosols
ST9	Measurements of IAGOS vertical profiles by commercial aircrafts
Methodologies for source apportionment receptor modelling	
ST10	Source apportionment of PM based on offline and online PM speciation
ST11	Source apportionment of UFP, BC, OP and VOCs using receptor modelling
Methodologies for urban mapping of novel AQ pollutants	
ST12	Deterministic urban modelling of fine PM and PNC
ST13	Mapping ultrafine particles and citizen science
Methodologies for evaluating the health effects of novel AQ pollutants	
ST14	Evaluation of health effects of novel AQ parameters
Obtaining emission inventories for novel AQ pollutants	
ST15	First UFP-PNSD and non-exhaust vehicle PM EU emission
Modelling methodologies for novel AQ pollutants	
ST16	UFP-PNSD multiscale modelling

ST1: The aim of this RI-URBANS/ACTRIS document on **UFP and PNSD measurements** (included as mandatory at urban supersites in the NAQD) is to facilitate upscaling of measurement techniques within the AQMNs. It contains an up-to-date report of the harmonised methodologies related to UFP and PNSD measurements, with additional information on sampling and data management. Furthermore, discrepancies between CEN standards and ACTRIS recommendations with AQ guidelines are identified. A Pan-European overview on UFP-PNSD observations is also included with most relevant results reported. Finally, a concise recommendations section on the measurements of UFP and PNSD in urban environments is provided.



ST2: The aim of this RI-URBANS/ACTRIS document on **equivalent BC (eBC) determinations** (mandatory at urban supersites in the NAQD) is to facilitate upscaling of measurement techniques within the AQMNs. It contains an up-to-date report of the harmonised methodologies related to eBC measurements, with additional information on how to obtain eBC data and data management. Furthermore, a few discrepancies with ACTRIS recommendations are identified. A Pan-European overview on eBC observations is also included, with most relevant results reported. Finally, a concise recommendations section on the determination of eBC in urban environments is provided.

ST3: The NAQD (2024/2881/EC) requires or recommends the analysis of specific PM₁₀ and PM_{2.5} components, such as metals (arsenic, As; cadmium, Cd; nickel, Ni; lead, Pb), polyaromatic hydrocarbons (PAH), levoglucosan, elemental and organic carbon (EC and OC) as well as inorganic ions (sulphate, SO₄²⁻; nitrate, NO₃⁻; chloride Cl⁻; ammonium NH₄⁺; calcium, Ca²⁺; potassium, K⁺; magnesium, Mg²⁺; sodium, Na⁺). Protocols for specific sampling and analytical reference methods are supplied to this end in the NAQD, which shall be followed. However, in addition to these, for an advanced AQ assessment, including source apportionment, additional PM inorganic and organic components might be required. This guidance document by RI-URBANS/ACTRIS supplies detailed recommendations for **offline** (24 h sampling followed by laboratory analyses) **and online** (<1 h and without laboratory analyses) **PM speciation**. A Pan-European report on PM speciation is also included, with most relevant results reported. Finally, a concise recommendations section is provided.

ST4: This RI-URBANS document describes the steps needed to conduct **measurements of oxidative potential of particulate matter (OP of PM)**, which is recommended by the NAQD. The ST provides an update on the state of the art on this harmonisation. This guidance document describes the different OP assays. It also provides information of the most recent studies comparing data and elucidates its connection with emission sources, chemical composition and size of PM. Furthermore, it gives recommendations to follow in the implementation of OP of PM measurements according to the conclusions obtained in the first international inter-laboratory comparison exercise developed in the framework of the RI-URBANS project. Finally, it shares a simplified measurement protocol developed for the most widely used **OP-dithiothreitol (DTT)** assay where the most critical steps have been optimised and harmonised in the framework of a dedicated task of RI-URBANS by a set of expert laboratories.

ST5: Annex VII of the NAQD recommends the measurement of 45 **VOC species** that are precursors of ozone (O₃). The aim of this RI-URBANS/ACTRIS guidance document is to facilitate upscaling of measurement techniques for VOCs within AQMNs. It provides an up-to-date summary of the methodologies related to VOCs, summarizes recent scientific synthesis of Pan-European observations and provides recommendations on the measurements of VOCs.

ST6: In the NAQD, measurements of **NH₃** are requested for rural supersites, but not for the urban ones, where this is only recommended. However, in the urban pollution hotspots, NH₃ measurements are very relevant to evaluate possible effects of AQ policy actions to abate fine particulate matter (PM_{2.5}), since this pollutant has a key role in the generation of secondary PM. This RI-URBANS guidance document reviews the methods for measuring NH₃ ambient concentrations, compiles and interprets spatial and time variability based on the datasets from 69 European sites, and gives recommendations on the measurement of NH₃.

ST7: Currently, most AQMNs miss information about important processes and quantities in the vertical dimension that are necessary to better understand surface-level pollution data. The vertical dimension is

especially relevant when considering potential non-local sources of aerosols (e.g. those arriving via medium-to-long-range transport) or for evaluating vertical dilution of locally emitted pollutants (for example to forecast exceedances of specific daily limit values), among others. This RI-URBANS/ACTRIS guidance document highlights the added value provided by information from measurements of **atmospheric boundary layer** height and dynamics. The main instruments allowing these measurements are briefly outlined, as well as the operation requirements. The document presents a few selected examples of measurements and retrievals that are applied in different RI-URBANS pilot cities and beyond.

ST8: Similarly, to ST7, this RI-URBANS/ACTRIS guidance document focuses on the added value of vertical measurements. The aim of this document is to facilitate the consideration of **aerosol profiling** within AQMNs. A concise summary of the currently available methodologies is provided, focusing on very precise methods, as well as a synthesis of Pan-European observations.

ST9: RI-URBANS connects the atmospheric observation expertise from IAGOS to the urban air quality. This document describes the available AQ parameters from IAGOS profiling, the data access, and examples of the use of **IAGOS profiles** over RI-URBANS pilot cities.

ST10: This RI-URBANS/ACTRIS guidance document offers an overview of state-of-the-art procedures to conduct Positive Matrix Factorization (PMF) analyses for **the source apportionment of PM₁₀ and PM_{2.5}**, as well as submicron organic aerosols (OA), the major fraction of fine aerosols, and trace elements, which are good tracers for a wide variety of PM sources.

ST11: This RI-URBANS/ACTRIS guidance document offers overviews on the **source apportionment of online measurement data of UFP-PNSD, BC, online non-refractory PM speciation, and VOCs as well as offline OP of PM**. The added value of obtaining results of receptor modelling for these novel AQ pollutants is shown by supplying the respective Pan-European overviews.

ST12: This RI-URBANS guidance document focuses on the application of **deterministic modelling for mapping PM and UFP at urban scale**. Pollutants such as NO₂, PM_{2.5}, BC and UFP may strongly impact the health of the population, with their concentrations being often particularly high over cities, with strong urban heterogeneities. In cities, concentration of NO₂, BC and particle number (PN) and to a lesser extent PM_{2.5} are particularly high along traffic axes and in streets. To estimate the outdoor concentration exposure of the population, maps are required at spatial scales below 100 m, at the minimum, to be able to differentiate the street from the urban background concentrations. Hourly time resolution is desirable.

ST13: This RI-URBANS guidance document describes methods that AQMNs, researchers and other groups can use to develop **fine spatial resolution maps of urban air pollution derived from monitoring**. The methods described in this document are complementary to routine monitoring with reference equipment at one or a few monitoring sites across the city. The described methods are also complementary to deterministic dispersion models which are often applied by AQ agencies for regulatory purposes. The methods for involvement of citizen science for such mappings are also reviewed.

ST14: This RI-URBANS document guides on **the steps needed to conduct an epidemiological analysis linking novel AQ pollutants** with health effects. Estimates of short-term associations between air pollution and health are usually based on studying the relationship between daily variations of air pollutant concentrations and daily counts of health outcomes such as mortality and/or morbidity (e.g. hospital admissions or hospital visits by various causes). This document reports on the different options that can be followed to conduct

epidemiological studies, the data needs and the statistical methodologies that can be applied. Lastly, it illustrates, using the data compiled by the RI-URBANS project, the feasibility of implementing such analyses and the added value of the novel AQ pollutants to determine health effects.

ST15: This RI-URBANS document guides on the steps needed to produce **consistent emission inventories for regional and urban scale modelling** applications. It describes the specific improvements that have been made to existing European emission inventories for RI-URBANS at a horizontal resolution of $\sim 6 \times 6 \text{ km}^2$ to better represent road transport emissions and include estimations of UFP, among others. This document also describes a downscaling tool to detail the European emission dataset to a $1 \times 1 \text{ km}^2$ resolution over urban areas in a consistent way. The specific **RI-URBANS emission inventories are elaborated for: UFP-PNSD, non-exhaust PM, other anthropogenic sources of PM and its components, including BC, and NO_x , SO_x (sulphur oxides), NH_3 and VOCs**. The European wide emission inventories can be obtained directly through access to an FTP repository, or by requesting them via email (Jeroen.Kuenen@tno.nl or Marya.ElMalki@tno.nl), while urban ($1 \times 1 \text{ km}^2$) emission datasets for Amsterdam, Athens, Birmingham and Helsinki can be obtained by the same FTP repository or by requesting them via email (eathana@noa.gr).

ST16: This RI-URBANS document focuses on guidance to **adequately model the spatial-temporal variation of UFP and PNSD**. To this end, primary UFP-PNSD emission inventories are required (see [ST15](#) on the first UFP-PNSD EU emission inventory), but also complex physical-chemical processes for nucleation should be implemented in the modelling tools. Multiscale approaches are required to account for emission and particle formation if the urban UFP-PNSD are intended to be modelled. This document summarises methodologies for multiscale modelling of UFP using two approaches, PMCAMx-UF (a three-dimensional chemical transport model focusing on the simulation of the UFP-PNSD and composition; Jung et al., 2010) and CHIMERE (a multi-scale chemistry-transport model for atmospheric composition analysis and forecast).

All the STs summarized above have been developed and reviewed by a large group of experts in the field of AQ management and research. The authors and reviewers are listed in Table 2.2. These STs have been produced RI-URBANS by experts from work packages WP1, WP2 and WP3, but also from WP4 by including results of the pilot testing of the STs.

Table 2.2: The authors and reviewers of the sixteen Service Tools.

Number	Authors	Reviewers
Protocols for the measurement of novel AQ pollutants		
ST1	Merixell García-Marlès (CSIC), Pedro Trecehera (CSIC), Xiansheng Liu (CSIC), (CNRS), Tuukka Petäjä (UHEL), Roy Harrison (UoB), Phillip Hopke (U Clarkson), Alfred Wiedensohler (TROPOS), Andrés Alastuey (CSIC), Xavier Querol (CSIC)	Karri Saarnio (FMI), Elli Suhonen (FMI), Oliver Bischof (TSI), Carsten Kykal (TSI), Sebastian Schmitt (TSI), Torsten Tritscher (TSI), Joonas Vanhanen (Airmodus), Aki Pajunoja (Airmodus), Imre Salma (ELTE), Katrianne Lehtipalo (UHEL), Christoph Hüglin (EMPA)
ST2	Marjan Savadkoohi (CSIC), Marco Pandolfi (CSIC), Andrés Alastuey (CSIC), Tuukka Petäjä (UHEL), Jean-Philippe Putaud (JRC), Olivier Favez (INERIS), Xavier Querol (CSIC)	Hilkka Timonen (FMI), Karri Saarnio (FMI), Katriina Kyllönen (FMI), Elli Suhonen (FMI), Christoph Hüglin (EMPA)
ST3	Andrés Alastuey (CSIC), Xiansheng Liu (CSIC), Barend L. Van Drooge (CSIC), Clara Jaén	Hilkka Timonen (FMI), Katriina Kyllönen (FMI), Elli Suhonen (FMI), Falk Mothes



	(CSIC), Marta Via (CSIC), Benjamin Chazeau (AMU/PSI), Anja Tremper (ICL), Manos Manousakas (PSI), André S.H. Prevot (PSI), Jean-Eudes Petit (CNRS), Jean-Philippe Putaud (EC-JRC), Olivier Favez (INERIS), Xavier Querol (CSIC)	(TROPOS), Anja Tremper (ICL), Gang Chen (ICL), Hasna Chebaicheb (INERIS)
ST4	Pamela Dominutti (CNRS), Jean-Luc Jaffrezo (CNRS), Roy Harrison (UoB), Xavier Querol (CSIC), Gaëlle Uzu (CNRS)	Katriina Kyllönen (FMI), Elli Suhonen (FMI), Tuukka Petäjä (UHEL)
ST5	Thérèse Salameh (IMT Nord Europe), Xiansheng Liu (CSIC), Xavier Querol (CSIC)	Katriina Kyllönen (FMI), Jean-Philippe Putaud (JRC), Heidi Hellén (FMI), Elli Suhonen (FMI)
ST6	Marsailidh M. Twigg (CEH), Katriina Kyllönen (FMI), Ulla Makkonen (FMI), Xiansheng Liu (CSIC), Tuukka Petäjä (UHEL), Xavier Querol (CSIC)	Wenche Aas (NILU), Jean Philippe Putaud (JRC)
Methodologies for vertical profiles of pollutants and meteorology		
ST7	Simone Kotthaus (CNRS), Melania Van Hove (CNRS), Martial Haeffelin (CNRS), Francesca Barnaba (CNR), Annachiara Bellini (CNR, now at ARPA VdA), Lucia Mona (CNR)	Xavier Querol (CSIC), Ewan O'Connor (FMI), Adolfo Comerón (UPC), Iwona Stachlewska (UW), Arnoud Apituley (KNMI)
ST8	Lucia Mona (CNR), Doina Nicolae (INOE), Francesca Barnaba (CNR), Annachiara Bellini (CNR, now ARPA VdA) Simone Kotthaus (CNRS), Martial Haeffelin (CNRS)	Xavier Querol (CSIC), Ewan O'Connor (FMI), Adolfo Comerón (UPC), Iwona Stachlewska (UW), Arnoud Apituley (KNMI), Andreas Petzold (Jülich)
ST9	Hannah Clark (IAGOS-CNR), Christoph Mahnke (ZJ), Andreas Petzold (FZJ)	Xavier Querol (CSIC), Christoph Gerbig (MPI-BGC)
Methodologies for source apportionment receptor modelling		
ST10	Fulvio Amato (CSIC), Marta Via (CSIC), Mannos Manousakas (PSI), Benjamin Chazeau (AMU), Gang Chen (ICL), Barend L. van Drooge (CSIC), Jean-Luc Jaffrezo (UGA), Olivier Favez (INERIS), Cristina Colombi (ARPA Lombardia), Eleonora Cuccia (ARPA Lombardia), Guido Lanzani (ARPA Lombardia), André S.H. Prevot (PSI), Andrés Alastuey (CSIC), Xavier Querol (CSIC)	J. Eudes Petit (CNRS), Katriina Kyllönen (FMI), Hilikka Timonen (FMI), Anja Tremper (ICL), Elli Suhonen (FMI)
ST11	BC: Marjan Savadkoohi (CSIC), Marco Pandolfi (CSIC), Olivier Favez (INERIS), Mohamed Gherras (INERIS), Andres Alastuey (CSIC), Tuukka Petäjä (UHEL), Xavier Querol (CSIC) UFP-PNSD: Meritxell Garcia-Marlès (CSIC), Phil Hopke (U Clarkson), Roy Harrison (UoB), Andres Alastuey (CSIC), Tuukka Petäjä (UHEL), Xavier Querol (CSIC) OP of PM: Gaëlle Uzu (IGE), Kaspar Daellenbach (PSI), Vy Dinh Ngoc Thuy (IGE), André Prevot (PSI), Jean-Luc Jaffrezo (IGE) VOC: Thérèse Salameh (IMT Nord Europe), Marvin Dufresne (IMT Nord Europe), Marten	Xavier Querol (CSIC), Katriina Kyllönen (FMI), Imre Salma (ELTE), Olivier Favez (INERIS), Hilikka Timonen (FMI), Heidi Hellén (FMI), Elli Suhonen (FMI)



	In't Veld (CSIC, RIVM), Stéphane Sauvage (IMT Nord Europe), Michelle Jessy Müller (EMPA), Stefan Reimann (EMPA)	
Methodologies for urban mapping of novel AQ pollutants		
ST12	Karine Sartelet (ENPC), Jian Zhong (UoB), Eleni Athanasopoulou (NOA), Lya Lugon (ENPC), Soo-Jin Park (ENPC), Roy Harrison (UoB)	Augustin Colette (INERIS), Elli Suhonen (FMI)
ST13	Gerard Hoek (UU), Jules Kerckhoffs (UU), Martine van Poppel (VITO), Jelle Hofman (VITO), Roy Harrison (UoB), Sef van den Elshout (DCMR)	Tuukka Petäjä (UHEL), Xavier Querol (CSIC), Elli Suhonen (FMI)
Methodologies for evaluating the health effects of novel AQ pollutants		
ST14	Vanessa Nogueira dos Santos (ISGlobal), Ioar Rivas (ISGlobal), Xavier Basagaña (ISGlobal)	Roy Harrison (UoB), Gerard Hoek (UU), Xavier Querol (CSIC), Elli Suhonen (FMI)
Obtaining emission inventories for novel AQ pollutants		
ST15	Jeroen Kuenen (TNO), Eleni Athanasopoulou (NOA), Marc Guevara (BSC)	Augustin Colette (INERIS), Maria Kanakidou (FORTH), Elli Suhonen (FMI)
Modelling methodologies for novel AQ pollutants		
ST16	Evangelia Siouti (FORTH), Karine Sartelet (ENPC), Elena Poulikidi (FORTH), David Patoulas (FORTH), Lya Lugon (ENPC), Spyros N. Pandis (FORTH)	Augustin Colette (INERIS), Maria Kanakidou (FORTH), Elli Suhonen (FMI), Martijn Schaap (TNO), Xavier Querol (CSIC)

3. UFP AND PNSD IN URBAN EUROPE

'Ultrafine particles' means the particle number concentrations (PNC) of aerosol particles with a diameter less than or equal to 100 nm in unit volume. According to the NAQD 2024/2881/EC (following the definition by WHO, 2021), UFPs are defined as PNC per cubic centimetre (cm³) for a size range with a lower limit of 10 nm (defined as 50% detection efficiency D_{p50}) and with no restriction on the upper limit. Since the fraction of particles larger than 100 nm typically accounts only for 10–30% (Trechera et al., 2023), measuring PNCs without an upper size limit is used as a surrogate of UFP.

PNC and PNSD measurements are harmonized by CEN standards and ACTRIS measurement guidelines as described in [ST1](#). The RI-URBANS/ACTRIS' guidance document for the measurement of UFP (PNC) and PNSD can be downloaded from the RI-URBANS webpage. This ST describes the relevant measurement methods, quality control, data management as well as recommendations for them. There is also an additional guidance chapter on source apportionment of UFP-PNSD in the website of RI-URBANS ([ST11](#)), the first EU UFP-PNSD emission inventory ([ST15](#)) and a guidance document for UFP-PNSD multiscale modelling ([ST16](#)).

The [ST1](#) provides also a thorough analysis of UFP and PNSD variability within European urban environments, the identification of similarities and major differences; and the evaluation of relationships with other pollutants, such as BC, PM_x (PM₁₀, PM_{2.5}, PM₁), and gaseous pollutants (SO₂, NO_x, O₃, CO), and with meteorological parameters.

Comprehensive observations encouraged by NAQD at supersites will facilitate co-located measurements of UFP and PNSD as well as the previously regulated AQD parameters. The harmonized and quality-controlled measurements will allow quantification of health impacts on the general population linked to UFP, PM_{2.5} and other air pollutants separately.

PNSD data can be converted to lung-deposited surface area (LDSA), which provides a metric that connects to the lung-exposure. Liu et al. (2023) and Garcia-Marlès et al. (2024a) provide a pan-European analysis of the variability in LDSA in urban environments. Further measurements initiated by the NAQD in traffic and urban background sites will provide new data for understanding the health impacts of air pollution.

3.1 Added value of UFP and PNSD measurements

It is widely recognised that exposure to PM negatively impacts human health (Trechera et al., 2023; WHO, 2021). Several studies have also shown that UFP can penetrate deeply into the respiratory system, thus causing respiratory and cardiovascular diseases in humans (Cassee et al., 2019, and references therein). In the range <10 nm, a rapidly increasing fraction of particles are lost by diffusion in the nose, oral cavity, and trachea. The sizes of UFPs not only allow them to reach the deeper parts of the respiratory system, but a fraction of these can reach the alveoli, translocate and reach the circulatory system, and, from there, they can reach any organ in the body, or directly reach the brain by translocating the olfactory bulb of the brain (Cassee et al., 2019, and references therein). The new World Health Organization AQ Guidelines (WHO, 2021) identify UFP concentration as a relevant AQ parameter and find that, although there is a body of evidence for the health effects of UFPs, results are still inconsistent. Cassee et al. (2019) and Rivas et al. (2021) reported that this inconsistency may be, at least in part, due to methodological differences in measurements, to the lack of representation of human exposure to UFPs resulting from the use of only a single monitoring station per city in most studies, and the different sources contributing to UFP concentrations in other cities/regions. Although the WHO (2021) does not provide guideline values, the monitoring of concentrations of UFPs and

BC is recommended to allow a more accurate evaluation of their health effects. However, WHO (2021) provides a good practice statement, in which they state that low ambient air concentration can be considered to be $<1000 \text{ \# cm}^{-3}$ and high concentration $>10000 \text{ \# cm}^{-3}$ as a 24h mean value.

RI-URBANS carried out a compilation and interpretation of 27 long datasets of UFP-PNSDs in urban Europe (Trechera et al., 2023). The results showed that UFP concentrations are typically higher closer to source areas, such as traffic and industrial hotspots and the concentrations are lower in urban and suburban background areas (Figure 3.1). The diurnal cycle at traffic sites follows anthropogenic traffic and combustion source patterns with a contribution of photochemical production of nanoparticles during daytime. Night-time concentrations are lower due to lower UFP emissions. Typically, UFP concentrations in urban environments are higher during wintertime due to reduced vertical mixing and increased anthropogenic sources.

Focusing on urban background sites the highest annual averaged PNCs were recorded in eastern and southern Europe (11200 to 10300 \# cm^{-3}) and two central European sites (close to 10000 \# cm^{-3}), followed by central-southern Europe (8900 to 6200 \# cm^{-3}) and north and north-western Europe and Switzerland (4500 to 3500 \# cm^{-3}) (Figure 3.2).

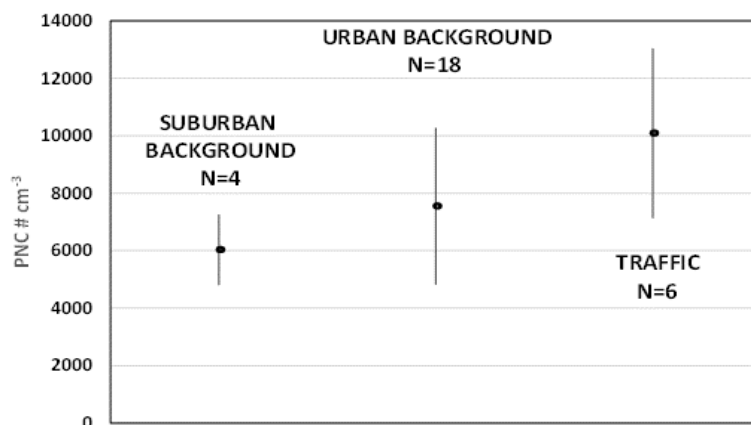


Figure 3.1: Average UFP concentrations and standard deviation ranges of suburban and urban background and traffic sites. Data from Trechera et al., 2023.

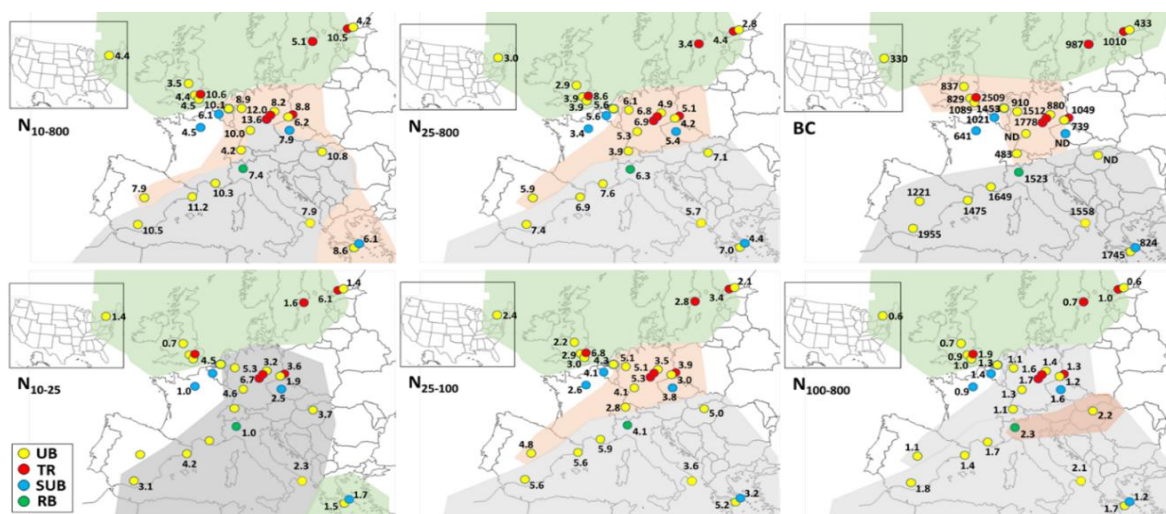


Figure 3.2: Regional variability of averaged 2017–2019 particle number concentrations (in # cm⁻³ 10³) size fractions (in # cm⁻³ 10³) and black carbon (BC in ng m⁻³) in Europe. For the size fraction of 10–25 nm (N_{10-25}), only sites with a lower size detection limit of 10–14 nm are included. UB, Urban background; TR, traffic; SUB, Suburban background; RB, Regional background. Modified from Trechera et al. (2023).

PNSD measurements were used for source contribution analyses of urban UFP. Garcia-Marlès et al. (2024a) summarized the pan-European source apportionment analysis based on PNSD (Figure 3.3). Focusing on European urban background and traffic sites, traffic-related UFP contributions dominate PNC, followed by photochemical nucleation or new particle formation producing particles close to the detection limit of the instrument (10 nm). Shipping and aviation might also contribute to increasing UFP concentrations with a prevalence of the lowest mode (Diesch et al., 2013; Lorentz et al., 2019; Stacey et al., 2021). The UFP sources also include biomass burning, urban background sources, industrial emissions, mixed sources, dust and unknown sources (Hopke et al., 2022).

Long-term data on UFP and PNSD in different European urban environments will allow analysis of trends in the concentrations and PNSD. As shown in Garcia-Marlès et al. (2024a, b), this can be used to quantify impacts of new AQ policies, such as implementation of EURO5/EURO6 engine emission policies, impact of local low-emission zones or quantifying the changes in AQ and air pollution exposure during electrification of the traffic fleet. The long-term UFP and PNSD data can help to identify emerging needs, such as the one of applying controls for semi volatile VOCs (SVOCs) in the diesel filter traps. During the regeneration cycles they emit SVOCs that cause nucleation of UFP very close to the exhaust emissions. The results from Garcia-Marlès et al. (2024a, b) showed that the traffic nucleation source did not have a consistent decreasing trend, while the diesel contribution and Aitken and accumulation modes did (Figure 3.4).

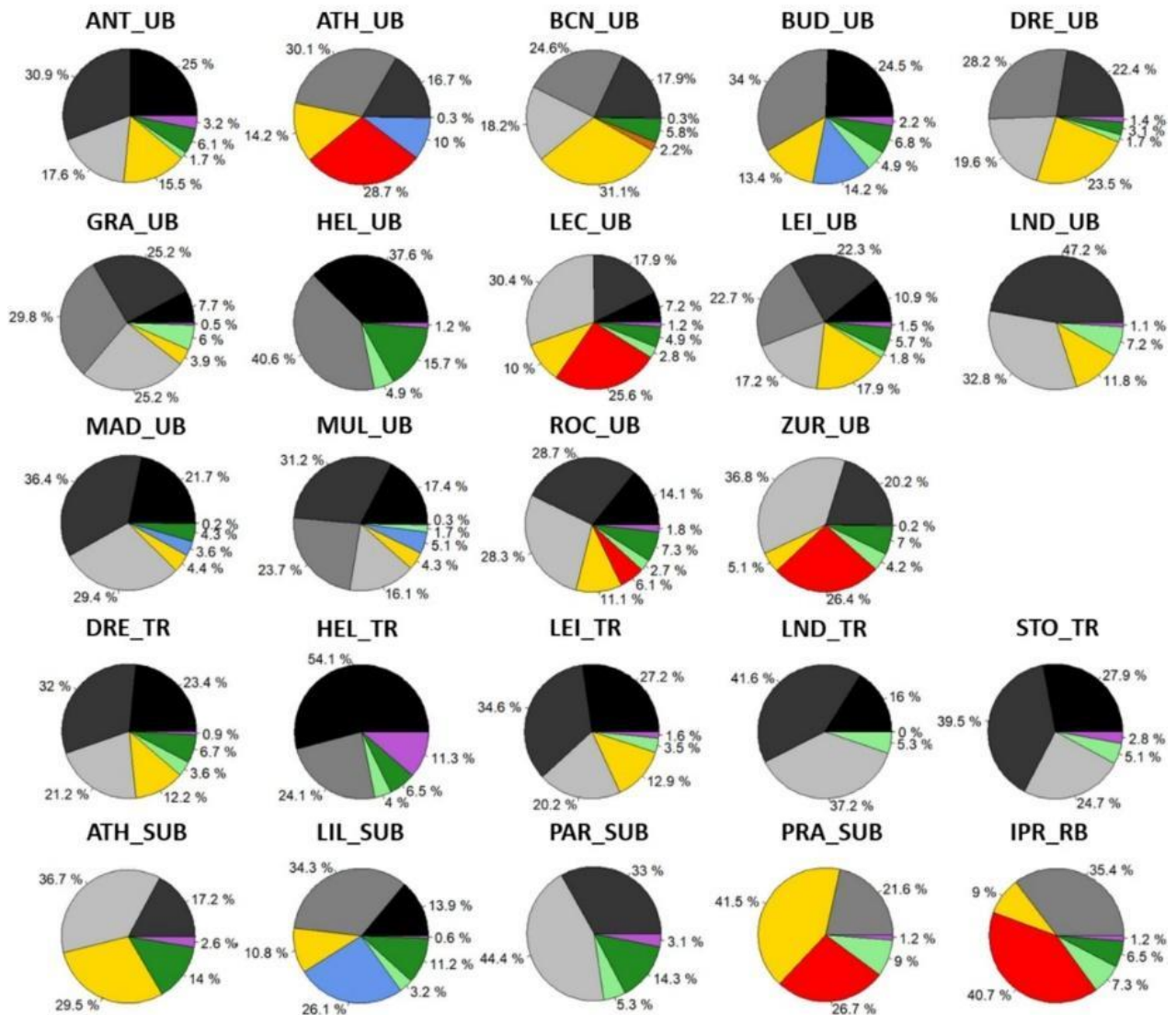


Figure 3.3: Results of the source apportionment of PNCs based on PNSD time series from 24 supersites in urban Europe. Figure from Garcia-Marlès et al. (2024b). UB and SUB, urban and suburban background; RB, regional background; TR, traffic sites. Antwerp (ANT_UB), Athens (ATH_UB), Barcelona (BCN_UB), Budapest (BUD_UB), Dresden (DRE_UB), Granada (GRA_UB), Helsinki (HEL_UB), Lecce (LEC_UB), Leipzig (LEI_UB), London (LND_UB), Madrid (MAD_UB), Mülheim (MUL_UB), Zurich (ZUR_UB), and Rochester (ROC_UB) in New York State in USA. Dresden (DRE_TR), Helsinki (HEL_TR), Leipzig (LEI_TR), London (LND_TR) and Stockholm (STO_TR). Athens (ATH_SUB), Lille (LIL_SUB), Paris (PAR_SUB) and Prague (PRA_SUB). Ispra (IPR_RB).

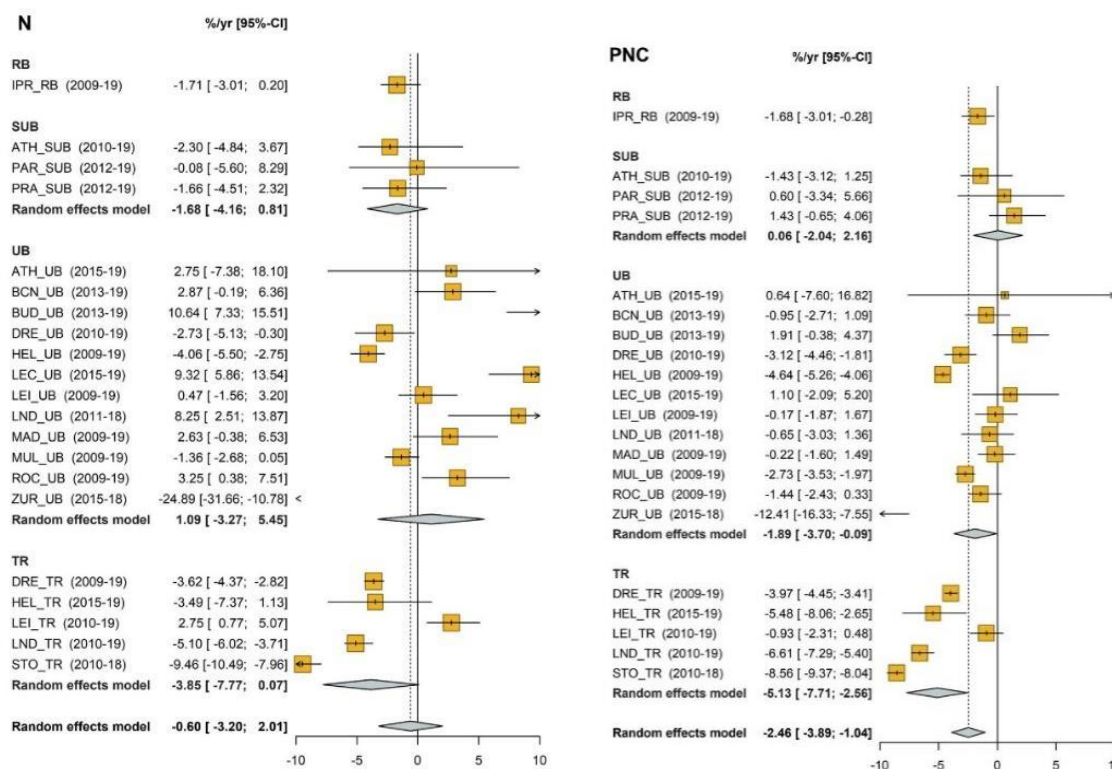


Figure 3.4: Results of the trend analysis and subsequent meta-analysis for Nucleation mode particle concentration (N), and total particle number concentrations (PNC). Trends are calculated using the Theil-Sen method. The dashed lined represents the global meta-analysis. Random effects model is the mean effect calculated for each site type. UB and SUB, urban and suburban background; RB, regional background; TR, traffic sites. Antwerp (ANT_UB), Athens (ATH_UB), Barcelona (BCN_UB), Budapest (BUD_UB), Dresden (DRE_UB), Granada (GRA_UB), Helsinki (HEL_UB), Ispra (IPR_RB), Lecce (LEC_UB), Leipzig (LEI_UB), London (LND_UB), Madrid (MAD_UB), Mülheim (MUL_UB), Zurich (ZUR_UB), and Rochester (ROC_UB) in New York State in USA. Dresden (DRE_TR), Helsinki (HEL_TR), Leipzig (LEI_TR), London (LND_TR) and Stockholm (STO_TR). Athens (ATH_SUB), Lille (LIL_SUB), Paris (PAR_SUB) and Prague (PRA_SUB). Figure from Garcia-Marlès et al. (2024a).

3.2 Emission inventories of UFP and PNSD

ST15 elaborated European wide emission inventories (at a horizontal resolution of $\sim 6 \times 6 \text{ km}^2$) and urban ones ($1 \times 1 \text{ km}^2$ for the urban areas of Amsterdam, Athens, Birmingham and Helsinki) for UFP-PNSD, non-exhaust PM, other anthropogenic sources of PM and its components, including BC, and NO_x , SO_x , NH_3 and VOCs. Figure 3.5 shows as an example the contribution of the different sub-sources in road transport to total emissions in 2019 according to this inventory. It shows that – depending on the pollutant – cold start emissions vary between 3% and 18% of UFP emissions, whereas for PM_{10} the non-exhaust accounts for 60% of total emissions, while for $\text{PM}_{2.5}$ this share is around 45%. For total particle number, TPN (equivalent to UFP) the hot engine emissions reach 95% of TPN from road traffic. Other examples are shown in Figure 3.6, which compares TPN and $\text{PM}_{2.5}$ emissions for the different sectors, with domestic combustion > energy and industry >> waste and agriculture being the main contributors for $\text{PM}_{2.5}$ and shipping > road transport > energy and industry >> aviation for TPN.

Contribution to road transport total emissions

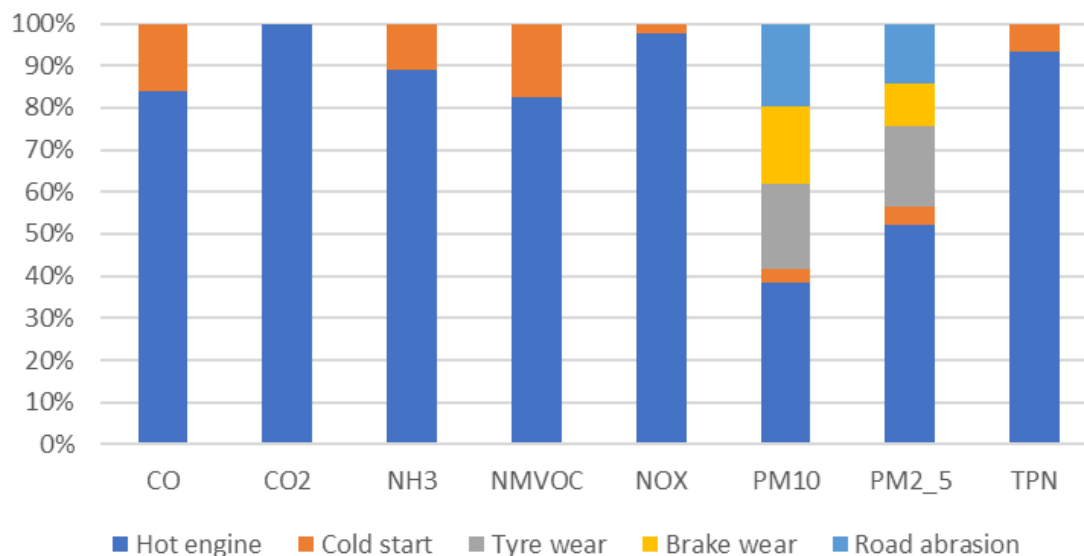


Figure 3.5: Contribution of different sources in road transport to total emissions for relevant pollutants. Exhaust emissions are split between hot engines and cold start contribution. TPN, total particle number, equivalent to UFP number concentrations (ST15).

PM2.5 and TPN emissions in 2019 (total for Europe)

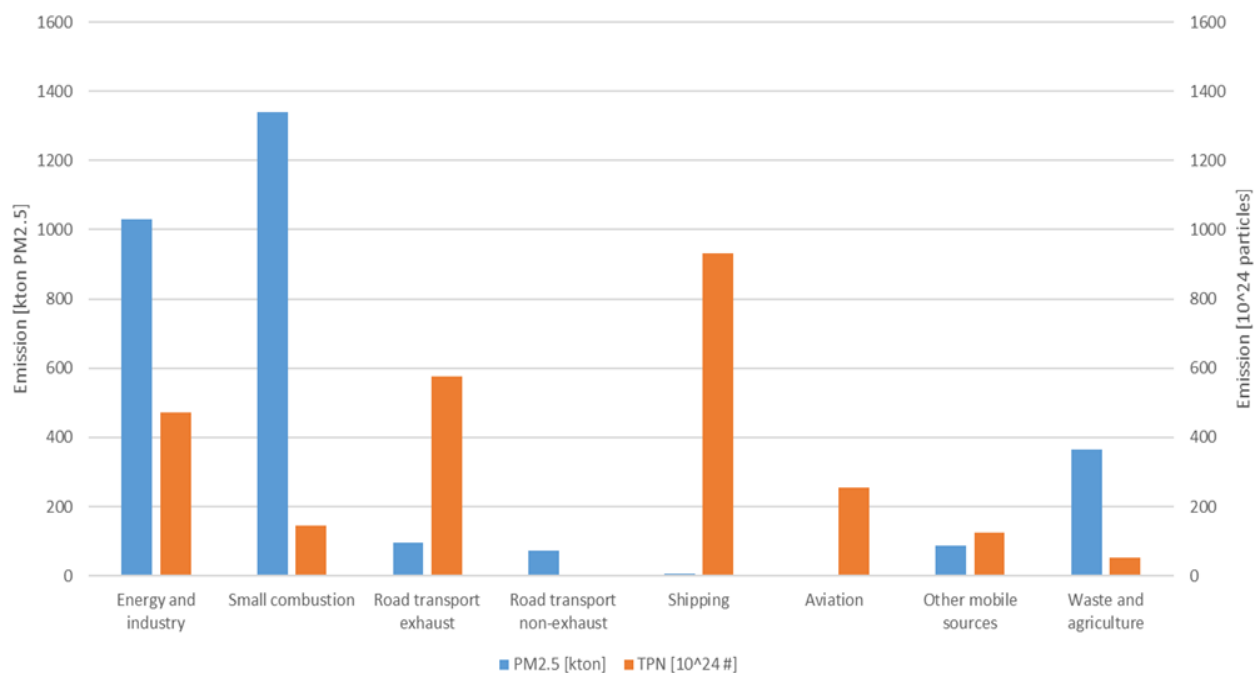


Figure 3.6: Comparison between PM_{2.5} (in kt) and total particle number (TPN, equivalent to UFP) emissions (in 10^{24} #) (ST15).

3.3 Modelling of UFP and PNSD

[ST16](#) is a guidance document for the multiscale modelling of UFP-PNSD using deterministic tools. Here an example is presented for the Athens region using PMCAMx-UF. This is a three-dimensional chemical transport model that simulates both the PNSD and the mass/composition distribution of the multicomponent atmospheric aerosol (Jung et al., 2010). The simulation of the aerosol microphysics is handled by the updated version of the Dynamic Model for Aerosol Nucleation (DMANx), which includes the processes of condensation, evaporation, nucleation, and coagulation assuming an internally mixed aerosol (Patoulias et al., 2015). DMANx includes the Two-Moment Aerosol Sectional (TOMAS) algorithm, which tracks both mass and number concentrations simultaneously and can use the desired nucleation theory to simulate particles starting from nuclei sizes.

Figure 3.7 displays the UFP source contributions (in %) over Athens for the summer. The major contributor to UFP is nucleation for the whole modelling domain while diesel also has an important impact in the city centre, and shipping has a great effect on the number concentration on the coast of Athens.

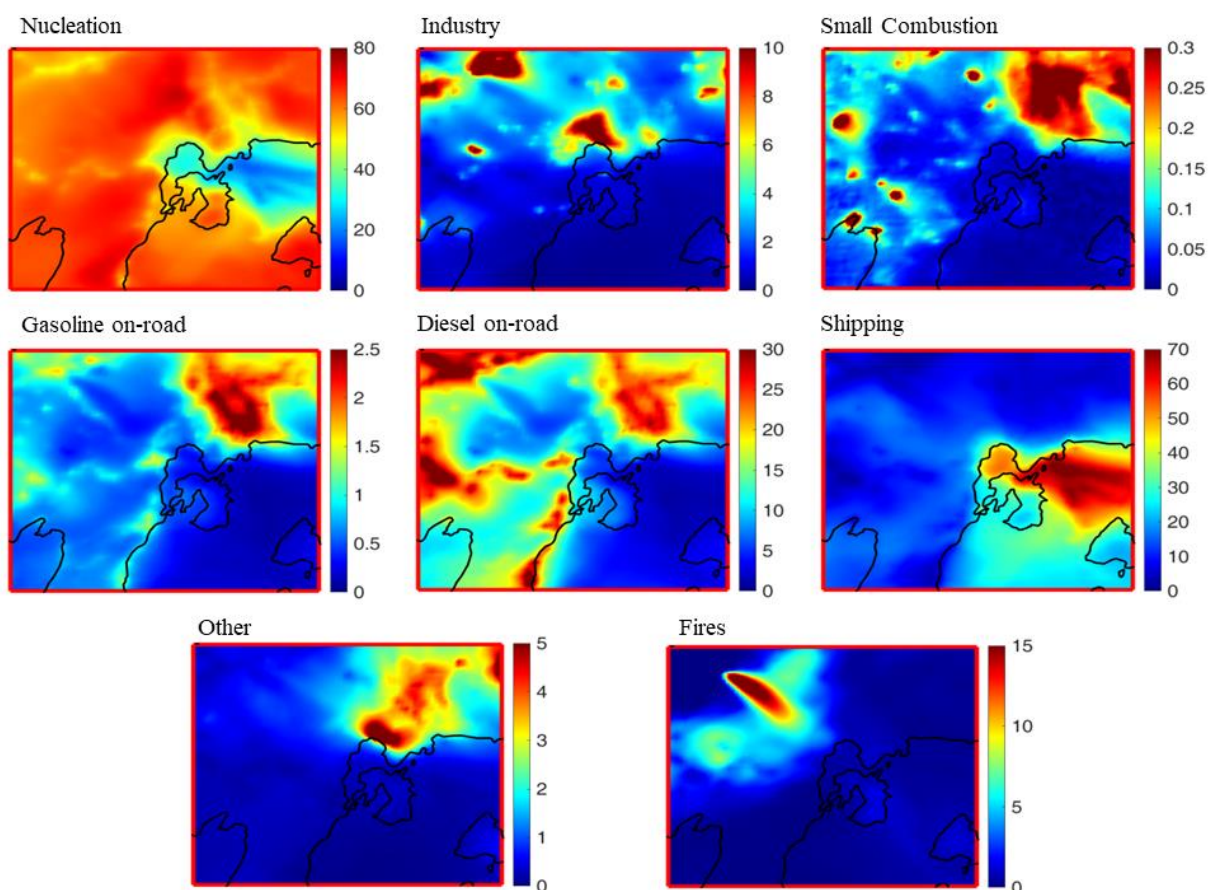


Figure 3.7: Predicted source contributions of UFP to the total size range of 10–800 nm (N_{10-800}) over Athens for the summer of 2019 using PMCAMx-UF. Domestic biomass burning emissions are not included.

3.4 Specific challenges in UFP and PNSD

Long-term measurements of UFP-PNSD are difficult due to complex instrumentation and >90% data coverage is a challenge. Recently, Hopke et al. (2024) and Vörösmarty et al. (2024) carried out studies that cover 15 and 11 years of data, respectively, with a high data coverage. Also, data coverage reported by Trechera et al. (2023) for sites from Budapest, Helsinki, Ispra, Leipzig, Mulheim, Paris, Rochester, reached >90% data coverage but the other 22 sites included in the study did not. A specific attention should be placed on maintenance and follow-up of the UFP and PNSD instruments to reach the required data coverage.

Reliable measurement of UFP and PNSD requires specific sampling as the UFP are rapidly lost in long sampling lines. UFP and PNSD measurements require drying of the sampled particles in order to produce harmonized and comparable data.

There are also challenges in having enough trained and skilled personnel, and for covering the associated costs of personnel and instrumentation, as well as for having an appropriate external calibration and traceability.

Emission inventories and modelling still need improvements to accurately reproduce experimental data on UFP-PNSD, but tools are already available and implemented.

4. eBC MASS CONCENTRATIONS IN URBAN EUROPE

The NAQD (2024/2881/EC) defines ‘black carbon’ (BC) as carbonaceous aerosols measured by light absorption. The directive addresses BC as an air pollutant of emerging concern and recommends BC to be measured at monitoring supersites in urban and at least half of the rural supersite locations co-located with other air pollutants. The term equivalent BC (eBC) is used when BC data in the unit $\mu\text{g m}^{-3}$ are obtained from absorption measurement by using conversion factors that have been obtained from simultaneous elemental carbon (EC) measurements.

The definitions and methodologies for deriving atmospheric eBC concentrations from optical measurements are described in [ST2](#) including recommendations for the instrument choice, method, quality control and data management.

4.1 Black Carbon and air quality

Black carbon (BC) is a component of fine particulate matter mass ($\text{PM}_{2.5}$). It originates predominantly from incomplete combustion of fossil fuels, biofuels, and biomass. BC influences both AQ and climate.

In the climate perspective, BC is one of the short-lived climate forcers influencing the radiative balance of the atmosphere. BC strongly absorbs sunlight and therefore contributes to global warming (IPCC, 2021). Deposition of BC on bright surfaces such as snow can lead to enhanced melting of snow and ice. Such feedback speeds up climate change (Bond et al., 2013). The lifetime of BC in the atmosphere varies from hours to weeks and therefore reduction of the BC emissions and concentrations can help to tackle climate change in a rapid fashion.

Studies of AQ have identified BC as a component that has negative health impacts, particularly the epidemiological evidence demonstrates a strong association between BC exposure and increased cardiopulmonary morbidity and mortality. Toxicological studies further indicate that BC acts as a universal carrier for a wide range of chemicals, which vary in toxicity and can impact human health (Janssen et al., 2012), therefore reducing exposure to BC is expected to yield significant health benefits. The reduction is co-beneficial for both AQ and climate.

The BC emissions in EU-27 countries have decreased from 345 to 193 Gg in 2000–2021, which is a decrease of 44% (EEA, 2021). The EU-27 BC emissions originate from heating (37%), road traffic (23%), waste burning (19%), agriculture (8%), industry (8%), non-road transport (3%) and energy production (2%).

4.2 Added value of measuring eBC concentration in Europe

For eBC there is not a reference method and needs harmonisation of measurement protocols and data treatment. In the framework of RI-URBANS, Savadkoohi et al. (2023) evaluated the long-term phenomenology of eBC by compiling datasets on eBC mass concentrations from 50 European monitoring sites, covering various periods between 2006 and 2022. These 50 measurement sites included 23 urban background (UB), 18 traffic (TR), 7 suburban background (SUB), and 2 regional background (RB) sites across 29 cities in 11 European countries (Figure 4.1).

The harmonized dataset indicated a significant decreasing trend in eBC mass concentrations between the classification of environments, generally ranked as $\text{TR} > \text{UB} > \text{SUB} > \text{RB}$. However, there were exceptions, such as high eBC values observed at a rural site in the Po Valley (Northern Italy), known for its PM pollution. Average eBC mass concentrations varied from $3.4 \mu\text{g m}^{-3}$ at a traffic site in Milan, Italy, to $0.17 \mu\text{g m}^{-3}$ at a

regional background site in Hyytiälä, Finland, based on data from 2017–2019. A notable north–south gradient in eBC mass concentrations, in line with other pollutants like NO₂ or PM_{2.5}, reflected regional differences in emissions. Seasonal variability in eBC mass concentrations was evident, with the highest levels observed during winter at the above Milan traffic site ($5.2 \pm 2.8 \mu\text{g m}^{-3}$) and the lowest in summer at the Finnish regional background site ($0.1 \pm 0.1 \mu\text{g m}^{-3}$).

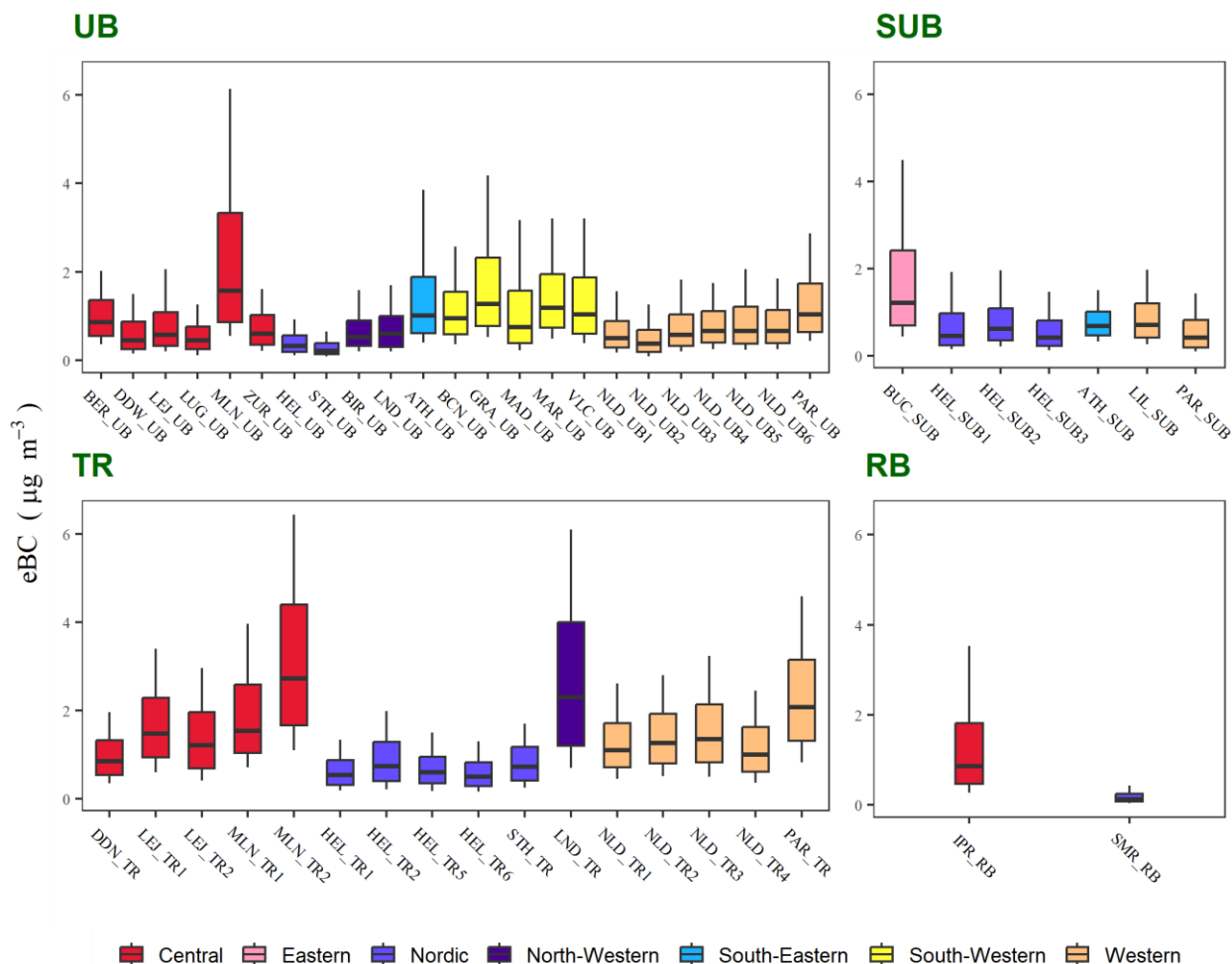


Figure 4.1: Variability of hourly averaged eBC mass concentrations at 50 sites between 2017 and 2019 categorized by the type of site and region. Modified from Savadkoohi et al. (2023).

RI-URBANS [ST11](#) provides a methodology for source apportionment allowing to differentiate the BC data to two BC sources, solid fuel emissions and liquid fuel emissions based on the methodology presented in Sandradewi et al. (2008) and (Zotter et al. 2017). Savadkoohi et al. (2024) gives recommendations for reporting eBC mass concentrations based on long-term pan-European in-situ observations. Figure 4.2 shows the results of the eBC source apportionment in urban Europe provided by Savadkoohi et al. (2023). It shows the regional variations in the relative contributions of eBC from liquid fuels (eBC_{lf}, mostly road traffic) and eBC from solid fuels (eBC_{sf}, mostly biomass burning), with an increasing trend in the eBC_{lf} from Northern to Central, Western, and South-Western Europe.

Long-term observations and source apportionment of BC can allow analysis of trends in emission sources and atmospheric concentrations. For example, Figure 4.3 shows a decreasing trend in eBC_{lf} in Barcelona, which is likely a consequence of implementation of diesel particle filters by EURO5/V and 6/VI. On the contrary, $eBC(sf)$ concentrations follow an increase at the sites influenced by domestic burning. The long-term observations of eBC in the urban areas will allow quantification of impacts of vehicle fleet electrification as the eBC emissions will likely continue to decrease as the combustion engines will become sparser.

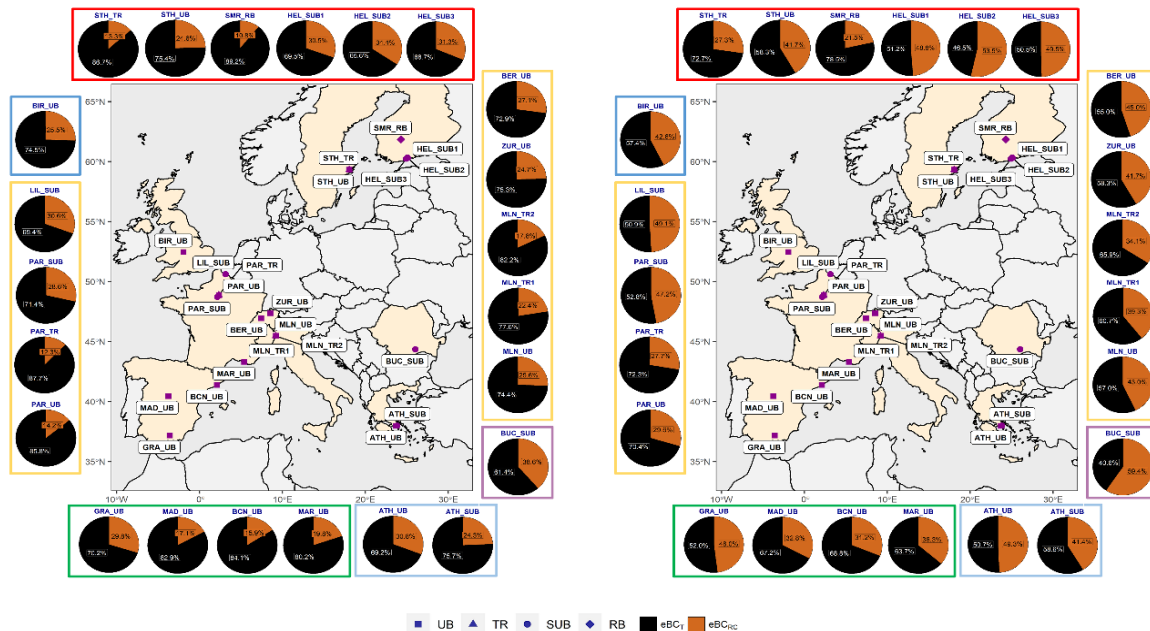


Figure 4.2: The results of the analysis of eBC mass concentrations for 23 European sites used over 2017–2019. Modified from Savadkoobi et al. (2023).

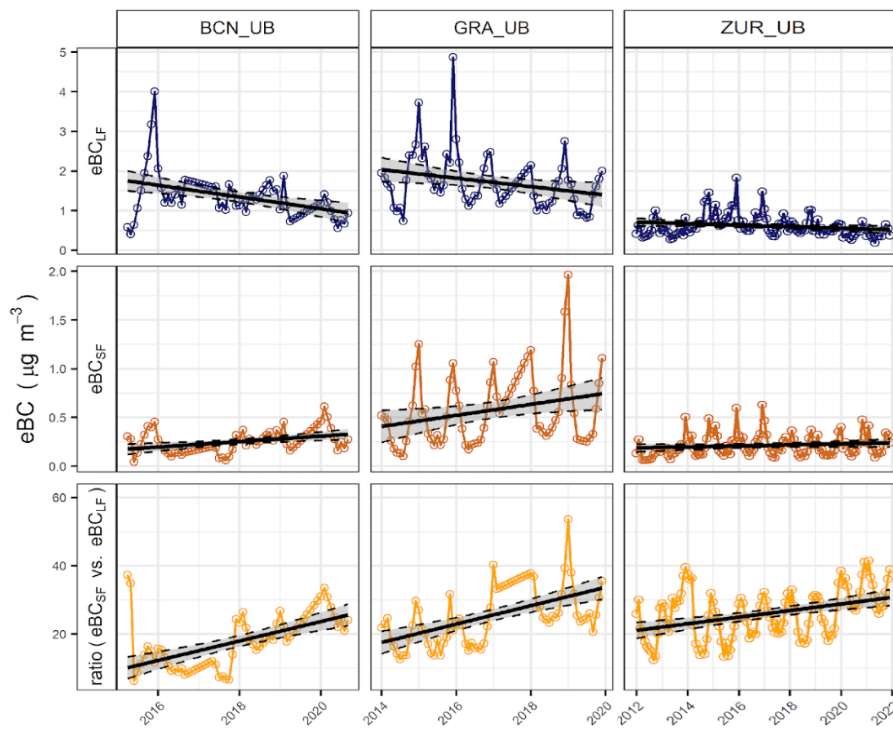


Figure 4.3: The results of the 2012–2022 trend analysis of eBC_{f} and eBC_{sf} mass concentrations, and the ratio among these, for urban background sites of Barcelona, Granada and Zurich (BCN, GRA, ZUR). Figure from Savadkoohi et al. (2023).

Spatial mapping of BC in the urban areas can be explored with the help of citizen science as some of the BC measurements outside the supersites can be done with small BC sensors. In RI-URBANS, the citizen science approach is summarized in **ST13** (mapping UFP and citizen science). This approach can raise awareness of the urban citizens to air pollution issues.

The observations on BC concentrations together with other air pollutants will enable quantification of health impacts in an unprecedented manner. BC particles are linked to toxicity and the exposure to traffic related BC will likely decrease in the coming decades.

5. PM SPECIATION AND SOURCE APPORTIONMENT IN URBAN EUROPE

Atmospheric suspended particulate matter (PM) is defined as a complex mixture of solid and liquid particles suspended in the air (Mészáros, 1993). The complexity of PM arises from i) the mix of origins, sizes and compositions of the solid and liquid particles, ii) the changes that particles might undergo after emission; and iii) possible sampling artefacts. PM can be classified as primary and secondary, if it is emitted directly into the atmosphere, or formed into the atmosphere from gaseous precursors, respectively. PM can be also classified as natural or anthropogenic according to its emission sources.

In AQ, PM mass has historically been split in the fine (<2.5 µm, PM_{2.5}) and coarse (2.5-10 µm, PM_{2.5-10}) fractions. Current AQ standards fix limit values for PM₁₀ and PM_{2.5}, for the mass concentration of particles (in µg m⁻³) with aerodynamic diameters less than 10 µm and 2.5 µm (50% cut-off), respectively. In scientific studies, PM₁ (diameter <1 µm) is also often measured and analysed.

PM_{2.5} are the AQ pollutants with the highest impact on the premature mortality attributable to air pollution in E-27 (EEA, 2023).

[ST3](#) compiles detailed information for guiding PM speciation analysis to obtain adequate PM speciation datasets that can be used for complete source apportionment studies. Both offline and online PM speciation measurements are included in the guidance document. Furthermore, detailed guidance on PM source apportionment receptor modelling applied to PM speciation is included in [ST10](#), for both offline and online measurement methods.

5.1 PM speciation and source apportionment in urban Europe using off-line PM measurements

5.1.1 Off-line PM speciation

The major constituents of PM are classically differentiated as follows:

- **Mineral matter** consists mostly of oxides of elements, such as Si, Al, Fe, Ca, Na, Mg, K, Ti, P, and Mn, arising from wind production of suspended soil particles (desert dust, pavement erosion), construction and demolition works, in addition to some industrial emissions (such as the ceramic and cement industry). The maximum of mineral matter emissions is usually in the coarse mode.
- **Sea salt** is mostly composed of Cl⁻ and Na⁺ together with a fraction of SO₄²⁻ and Mg²⁺. These have a dominant mode in the coarse fraction.
- **Organic matter (OM)** is a very complex mixture of organic compounds arising from primary combustion sources e.g. hydrocarbons from vehicle exhaust emissions, levoglucosan and polyaromatic hydrocarbons from biomass burning, and many other compounds such as nicotine from smoking and azelaic acid from cooking. In addition, organic matter includes secondary compounds such as carboxylic acids formed from oxidation of gaseous precursors in the atmosphere and polymers of those. OM primarily occurs in the fine fraction.
- **Elemental carbon (EC)** is graphitic or amorphous carbon produced by incomplete combustion of fuels, from vehicles, biomass and coal burning. EC dominant mode is in the fine fraction.
- **Inorganic ions NO₃⁻, SO₄²⁻, and NH₄⁺** constitute the secondary inorganic aerosol (SIA) from the atmospheric oxidation of gaseous NO_x and SO₂, respectively, followed by a reaction with gaseous NH₃. These occur as NH₄NO₃, NH₄HSO₄ and/or (NH₄)₂SO₄ in the fine fractions of PM. The two first precursors arise from emission of combustion processes, while NH₃ is primarily emitted from agriculture and farming (EEA, 2022). Part of the Cl⁻ can contribute to SIA in the form of NH₄Cl in regions where anthropogenic HCl emissions

are relevant. These have a dominant mode in the fine fraction. SIA can occur in the coarse mode where NaNO_3 can form from nitric acid and sea salt.

- **Trace elements** consist of a wide variety of elements (such as As, Cd, Ni, Pb, V, Zn) with different origin, toxicity and size distribution, present in the low concentration (in the ng m^{-3} range). The sources of trace elements include e.g. combustion, non-exhaust emissions (tyre dust, brake dust), exhaust emissions, and industrial emissions. These have a dominant role typically in the fine fraction, but those from traffic have a high load in the coarse mode. These and some organic compounds, such as PAHs are key components in PM speciation because some are carcinogenic and others have relevant toxic effects; but also, because these are key tracers for advanced source apportionment studies using receptor modelling.
- **Undetermined fraction** is the PM mass determined by gravimetry that is not accounted for by the sum of the concentrations of all the above PM components, because there are light atoms (typically H, N, O) whose contributions are not properly determined. For instance, crystallisation water accounts for 21% of gypsum ($\text{CaSO}_4 \cdot 2\text{H}_2\text{O}$) molecular mass. PM bound water can still contribute significantly to the gravimetric mass if hygroscopic constituents are present, Furthermore, there might be heteroatoms that are not properly quantified in e.g. organic matter.

RI-URBANS compiled datasets of trace elements from 55 sites provided by AQMNs, research projects, and research supersites (Liu et al., 2025a). The datasets span a decade, covering the years 2013 to 2022, with a series of data for each site covering a minimum of one year. The data come essentially from 7 countries: France (24 sites), Italy (9), Spain (8), Switzerland (5), UK (5), Portugal (3), and Greece (1). Thus, the first result from the analysis of this compilation is the scarcity of long-term detailed PM speciation datasets in urban Europe. Details of the datasets, measurement protocols and species analysed are given in [ST3](#).

Major PM components

In the UB sites, OC had an average concentration (of the averages of the sites) of $6.0 \pm 5.4 \mu\text{g m}^{-3}$, EC around $1.3 \pm 1.3 \mu\text{g m}^{-3}$, NO_3^- $2.2 \pm 3.0 \mu\text{g m}^{-3}$, SO_4^{2-} $1.8 \pm 1.4 \mu\text{g m}^{-3}$ and NH_4^+ around $0.82 \pm 1.1 \mu\text{g m}^{-3}$. Median concentrations of Ca^{2+} , Fe, Na^+ , Cl^- , Al, K^+ , and Mg^{2+} reached around 0.40 ± 0.44 , 0.40 ± 0.40 , 0.33 ± 0.49 , 0.30 ± 0.70 , 0.25 ± 0.38 , 0.18 ± 0.24 , and $0.04 \pm 0.05 \mu\text{g m}^{-3}$, respectively.

Overall, the concentration of major PM10 constituents varied across different environment types (Table 5.1), reflecting the influence of specific human activities and natural processes. Specifically, the concentrations of OC and EC were observed to be higher in UB, TR, UI (urban industrial), and SUB environments compared to RB areas, resulting from higher emissions from combustion sources (e.g. traffic, industries, and residential heating) at the former. At RB sites, the OC/EC ratio is significantly higher than at other site types, reflecting the larger contribution to OC from both anthropogenic and biogenic secondary organic aerosol (SOA). Thus, a high proportion of OC has a regional origin, while EC is more local (traffic and biomass burning).

For metal ions and elements, the concentrations of Na^+ , Mg^{2+} , Al, and Fe were higher at UI and TR environments due to industrial and vehicular emissions. Intermediate concentrations were found in UB and SUB due to the influence of traffic and construction activities. In contrast, RB areas had lower metal ion and element concentrations, resulting from less industrial activity and lower traffic density. K^+ and Ca^{2+} concentrations were higher in SUB, UB, and UI due to more biomass burning and construction activities compared to rural areas. Chloride (Cl^-) concentrations were higher in UI due to industrial processes, with intermediate levels in TR and SUB, and the lowest in RB.

In terms of secondary inorganic compounds, SO_4^{2-} concentrations did not show significant differences across environments, reflecting that SO_4^{2-} is formed from the oxidation of SO_2 , and mainly produced by cloud processing, which is actually a large-scale process. NO_3^- and NH_4^+ concentrations were higher in TR and RB most probably due to the proximity of the vehicle emissions and the high NH_3 concentrations found in some RB sites due to agriculture and farming emissions (Liu et al., 2024a), respectively, with intermediate levels in UB and UI, and lowest in SUB.

Table 5.1 shows the average concentration range of major PM components, considering the average for each site for the IND, TR, UB, SUB, and RB sites, for PM10 and PM2.5. The ranges of the two PM sizes are not directly comparable because not many sites are reporting PM10 and PM2.5 data. However, the table might be used as a reference of the usual concentrations found in the different environments.

Trace elements

Twenty trace elements in PM10 were selected for this overview, including As, Ba, Br, Cd, Co, Cr, Cu, Hg, Mn, Mo, Ni, Pb, Rb, Se, Sr, Ti, V, Y, Zn, and Zr. Among these, Cd, As, Cr, and Ni are classified as carcinogenic elements (WHO, 2007). It is worth mentioning that Sn and Sb were not included because these elements were not determined or detected in a number of sites where wet chemistry methods were not applied, but these are relevant for source apportionment analyses.

AQ limit/target values for trace elements in European AQ Directives are set up only for As (6 ng m^{-3}), Pb (500 ng m^{-3}), Cd (5 ng m^{-3}), and Ni (20 ng m^{-3}) listed in 2008/50/EC and 2004/107/CE. The average concentrations of As, Pb, Cd, and Ni all complied with EU standards. The highest concentrations were recorded for Zn, Cu and Ti (40 ± 48 , 23 ± 34 and $20 \pm 29 \text{ ng m}^{-3}$, respectively), followed by Mn and Ba (12 ± 25 and $11 \pm 15 \text{ ng m}^{-3}$, respectively), all of them being conventionally attributed to brake-wear, tyre-wear and road dust resuspension in urban environments (Amato et al., 2016). Inhalation of these trace elements poses significant health risks. For instance, As, Cd, and Ni are known carcinogens, with exposure linked to lung and bladder cancers (WHO, 2007). Zn, Cu, and Mn, while essential in small amounts, can cause toxicity at higher concentrations, leading to respiratory and cardiovascular problems (Wu et al., 2019). Overall, the presence of these toxic metals in PM highlights the need for stricter regulatory measures and continuous monitoring to mitigate adverse health effects on urban populations. Table 5.2 shows the average concentration range of trace elements, considering the average for each site for the IND, TR, UB, SUB, and RB sites, for PM10 and PM2.5.

Table 5.1: Average concentration range of major PM components, considering the average for each site for industrial (IND), traffic (TR), urban background (UB), suburban background (SUB) and regional background (RB) sites, in $\mu\text{g m}^{-3}$, for PM10 and PM2.5. ND, not determined. Data from Liu et al. (2025a).

	PM10					PM2.5				
	IND	TR	UB	SUB	RB	IND	TR	UB	SUB	RB
OC	2.2-6.0	2.9-18*	2.1-19*	2.4-33*	1.8-2.3		1.9-4.3	1.0-4.9	2.7-5.4	
EC	0.7-2.1	0.3-4.6*	0.2-4.5*	0.4-3.9	0.2-0.2		0.6-1.4	0.2-1.2	0.3-1.1	
SO ₄ ²⁻	1.7-3.8	1.2-3.1	0.7-2.8	0.5-4.0	2.0-2.2		0.5-1.7	0.5-2.0	1.5-3.1	
NO ₃ ⁻	1.1-6.5	1.2-6.4	0.7-7.9*	0.7-5.4	3.0-3.2		0.1-5.1	0.1-6.9*	0.2-0.8	
NH ₄ ⁺	0.1-2.3	0.3-2.4	0.2-3.3*	0.1-1.7	1.2-1.3		0.4-1.9	0.5-2.4*	0.6-0.8	
Cl ⁻	0.2-0.4	0.1-3.5	0.2-1.2	0.3-0.8	ND		0.01-0.1	<0.01-0.1	<0.01-0.1	
Na	0.4-1.3	0.1-2.0	0.1-0.9	0.2-0.8	ND		0.02-0.1	0.0-0.1	0.1-0.1	
Mg	0.2-0.4	0.1-0.4	0.0-0.9	0.1-0.4	ND		0.01-0.02	0.0-0.6	0.0-0.2	
Ca	1.7-2.7	0.3-1.2	0.2-1.6	0.2-0.8	ND		0.05-0.2	0.1-0.2	0.1-0.2	
Si	ND	0.3-1.3	0.2-1.3	0.2-1.0	ND		<0.05-0.1	0.1-0.7	0.1-0.3	
Al	0.1-1.3	0.1-0.8	0.0-1.1	0.0-0.6	0.1-0.1		<0.05-0.1	0.0-0.2	0.0-0.1	
Fe	0.3-3.9	0.3-1.4	0.1-1.2	0.0-1.1	0.1-0.2		0.1-0.5	0.0-0.2	0.1-0.1	
K	0.2-1.4	0.2-0.4	0.2-1.3	0.2-1.5	ND		0.1-0.5	0.0-0.6	0.1-0.2	
Levogluconan	0.1-0.3	0.2-0.8	0.1-3.2*	0.2-0.9	0.1-0.1		0.03-0.3	0.0-1.1	<0.1-0.3	

* Highest values of the range are due to winter measurement campaigns

Table 5.2: Average concentration range of trace elements, considering the average for each site, in industrial (IND), traffic (TR), urban background (UB), suburban background (SUB) and regional background (RB) sites, in ng m⁻³, for PM10 and PM2.5. ND, not determined. Data from Liu et al. (2024b).

	PM10					PM2.5				
	IND	TR	UB	SUB	RB	IND	TR	UB	SUB	RB
As	<0.1-10	<0.1-9.2	<0.1-7.9	<0.1-28	<0.1-4.1		0.2-0.7	<0.1-1.6	<0.1-0.4	
Ba	<0.1-61	<0.1-133	<0.1-416	<0.1-344	0.1-20		<0.1-6.7	<0.1-24.7	4.0-7.9	
Br	<0.1-2.3	<0.1-734	<0.1-160	<0.1-23	<0.1-3.0		ND	ND	ND	
Cd	<0.1-6.6	<0.1-5.2	<0.1-9.3	<0.1-7.0	<0.1-0.7		<0.1-0.2	<0.1-0.1	3.2-3.7	
Co	<0.1-2.7	<0.1-2.2	<0.1-47	<0.1-110	<0.1-0.2		<0.1-0.1	<0.1-0.1	<0.1-0.1	
Cr	<0.1-32	<0.1-51	<0.1-200	<0.1-122	<0.1-34		0.5-2.3	<0.1-2.9	0.8-1.3	
Cu	<0.1-349	<0.1-215	<0.1-1087	<0.1-117	<0.1-1.5		7.9-15	0.7-16.2	2.4-5.1	
Hg	<0.1-55	<0.1-216	<0.1-50	0.5-56	0.1-35.2		ND	ND	ND	
Mn	<0.1-118	<0.1-149	<0.1-185	<0.1-91	<0.1-28		2.1-7.8	0.1-3.8	2.0-3.3	
Mo	<0.1-46	<0.1-177	<0.1-57	<0.1-5.0	<0.1-0.1		<0.1-3.2	<0.1-1.6	<0.1-2.2	
Ni	<0.1-95	<0.1-261	<0.1-64	<0.1-318	<0.1-0.1		<0.1-0.9	<0.1-2.5	1.6-4.9	
Pb	<0.1-967	<0.1-312	<0.1-306	<0.1-149	<0.1-3.6		0.8-5.2	0.5-4.9	2.6-4.4	
Rb	0.1-15	<0.1-45	<0.1-35	<0.1-18	<0.1-8.1		0.2-1.3	0.1-1.3	0.5-0.9	
Se	<0.1-62	<0.1-32	<0.1-211	<0.1-57	0.1-119		<0.1-0.1	<0.1-0.1	0.4-0.5	
Sr	<0.1-92	<0.1-130	<0.1-147	<0.1-100	<0.1-1.8		<0.1-5.2	<0.1-1.6	0.7-1.5	
Ti	<0.1-516	<0.1-620	<0.1-345	0.1-521	<0.1-1.6		0.7-6.1	<0.1-0.1	3.3-10	
V	0.1-118	<0.1-34	<0.1-64	<0.1-23	0.2-4.7		0.1-0.3	<0.1-0.5	1.5-2.9	
Y	<0.1-2.8	<0.1-11	<0.1-7.6	<0.1-3.0	ND		<0.1-0.3	<0.1-0.3	ND	
Zn	<0.1-1034	0.1-575	<0.1-1983	<0.1-356	1.8-56		7.0-26	3.5-30	9.2-11	
Zr	<0.1-23	<0.1-23	<0.1-18	<0.1-10	ND		<0.1-5.2	<0.1-8.1	<0.1-11	

5.1.2 Source apportionment based on off-line PM speciation

Source receptor modelling using Positive Matrix Factorisation (PMF, Paatero and Tapper, 1994; Paatero and Hopke, 2009) was applied to the off-line PM speciation datasets compiled. Liu et al. (2025a) and [ST10](#) report details of the protocols recommended and applied to this end. As shown in Figure 5.1, solutions with 5–9 PM10 factors (source contributors) provided the most suitable and reliable outcomes across the 24 monitoring sites, which were identified. In summary, sources of ambient PM10 have been grouped into 7 categories:

- Road traffic (including exhaust and non-exhaust vehicle emissions).
- Biomass burning, a crustal source.
- SIA+SOA.

- Industrial sources.
- Sea-salt source (in most cases loaded with aged anthropogenic PM).
- A mixed fuel-oil combustion (with or without shipping).
- Other specific sources.

Their source contributions to PM₁₀ for each city widely vary according to local and regional emission patterns and climate characteristics. Details of the datasets, source profiles and locations are given in Liu et al. (2025a).

These results suggest that EU-wide offline PM speciation datasets can support advanced policy assessments at EU, regional, and local levels. Additionally, policies aimed at reducing PM may need to be tailored to the specific climates and cities across Europe. In Central Europe, nitrate (deep blue in Figure 5.1) makes a significant contribution to PM, whereas its contribution is much lower in Southern Europe. Road traffic (black in the figure) is a notable source of PM₁₀ across all cities, though its contribution varies widely. Biomass burning is a major source in most locations, and in many cases, it is the largest contributor.

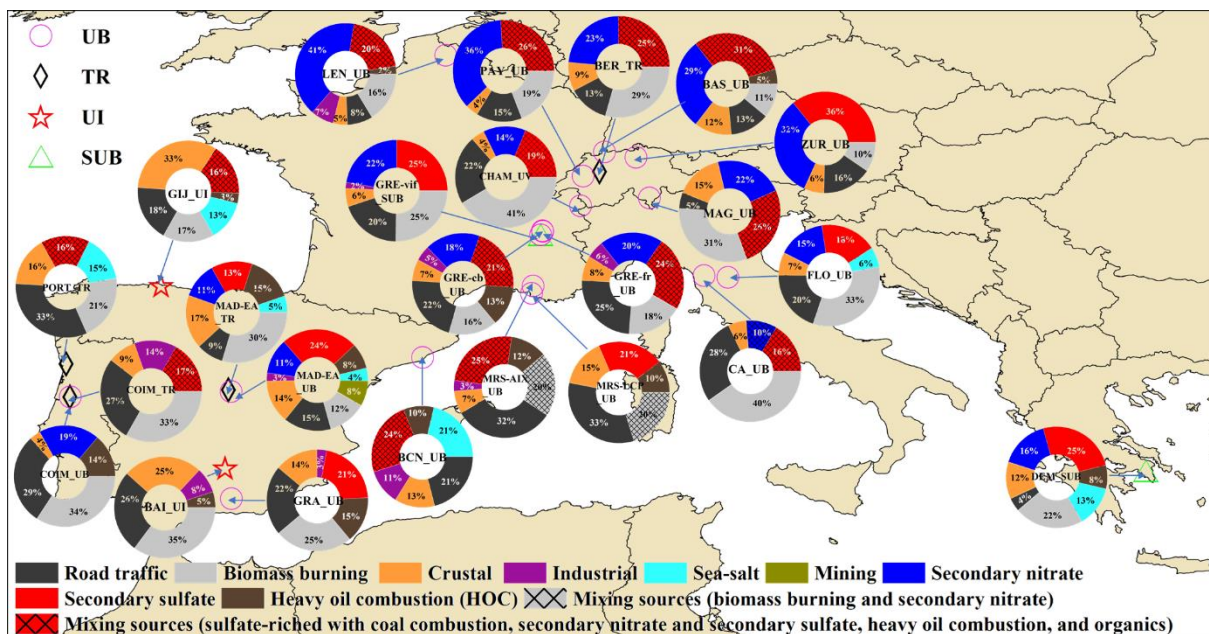


Figure 5.1: Quantitative source apportionment (with PMF) of mean PM₁₀ concentrations for 24 locations across 6 countries in Europe. Figure from Liu et al. (2025a).

5.2 Non-refractory PM₁ speciation and source apportionment in urban Europe using on-line PM measurements

5.2.1 On-line PM speciation

RI-URBANS also compiled available datasets of urban long-term measurements of the non-refractory (NR) PM₁ measured with Aerosol Chemical Speciation Monitors (ACSM). These datasets were obtained in the period covering from 2011 to 2023, with different duration, and were provided to RI-URBANS by AQMNs, research infrastructures (such as ACTRIS) and single research institutes. These included 26 UB sites, and additionally 5 SUB, 3 TR and 1 RB sites.

Regarding NR-PM₁ composition, the main component was organic aerosol (OA) at all sites. The average, standard deviation, and ranges (average ± standard deviation, min–max %) of each species (for a set of sites excluding Birmingham (PM_{2.5} instead of PM₁) and without stations, were:

- OA: 55±10%, 40–67%
- SO₄²⁻: 18±8%, 9–48%
- NO₃⁻: 16±5%, 6–26%
- NH₄⁺: 10±3%, 5–19%
- Cl⁻: 1±1%, <0.1–6%

The 35 sites were classified into four groups according to the chemical compositions shown in Figure 5.2:

- SO₄²⁻ << NO₃⁻: Typically, continental or high-latitude sites, where winter stagnation episodes are frequent and/or severe, or with high traffic influence.
- SO₄²⁻ >> NO₃⁻: Typically, with sea influence and in lower latitudes, where SO₄²⁻ is photochemically produced from dimethyl sulphate and/or shipping emissions.
- SO₄²⁻ ≈ NO₃⁻: Typically, intermediate sites, with similar concentrations in summer and winter.
- High Cl⁻: Only three sites (Padova, Milano, Bologna) were identified with high Cl⁻, and this was in the Po Valley region known for elevated PM levels. These three datasets presented very high NR-PM₁ concentrations and high amounts of NO₃⁻, with the exception of Padova which is closer to the coast and more SO₄²⁻ dominated. These results can be biased because Padova and Milano data is only for winter, but in any case, the Po Valley is known as a European hotspot for PM accumulation due to the orographic and meteorological conditions, multiple sources of PM and recirculating breeze regimes which cause severe winter pollution episodes (Scotto et al., 2021).

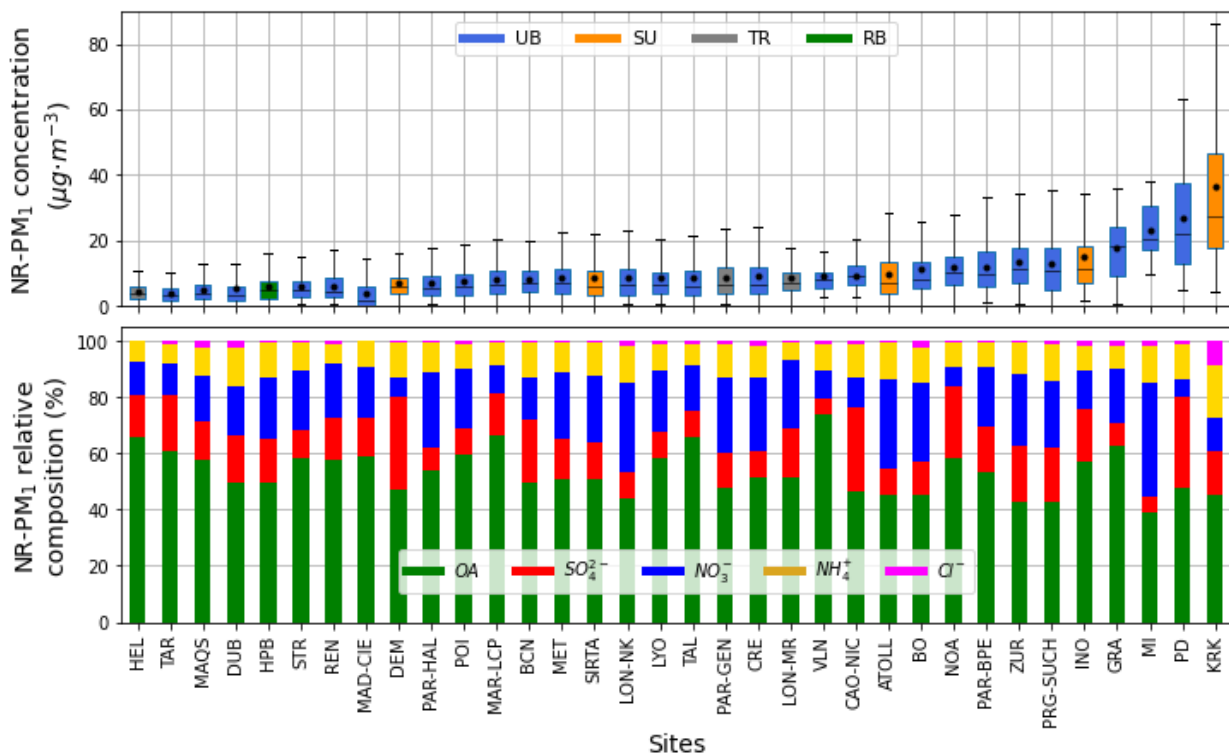


Figure 5.2: (a) NR-PM₁ concentrations boxplots. (b) Relative composition of NR-PM₁ compounds. Both graphs are ordered by growing mean concentration of NR-PM₁. Upper: Concentration boxplots include average (circle), median, quartiles 25 and 75%, and minimum and maximum. Lower: Relative composition of NR-PM₁ compounds. Both graphs are ordered by growing mean concentration of non-refractory-PM₁.

5.2.2 Source apportionment based on on-line PM speciation

PMF-ME2 receptor modelling was applied to 19 datasets of NR-PM₁ on-line speciation measurements (see [ST10](#) for detailed methodology used) for OA apportionment. Primary sources of the OA include hydrocarbon like OA (HOA, and also HOA1, HOA2), biomass burning OA (BBOA), cooking-like OA (COA), amine OA (amine-OA), wood, coal, and peat OA, coal combustion OA (Coal OA), shipping + industry OA (SHINDOA), local OA (LOA); primary OA (POA), and cigarette-smoke OA (CSOA). Amongst secondary OA there are less-oxidised oxygenated OA (LO-OOA), more-oxidised oxygenated OA (MO-OOA), and generic oxygenated OA (OOA). Also, there are different mixings of OOA+BB (OOA_BB, OOA_BBaq).

The proportion of SOA amongst all the sites was 41–92% of the OA, with a mean and standard deviation of 65% and 13%, respectively. As it can be seen in Figure 5.3 the regional background site, Hohenpeissenberg, was the one with the lowest proportion of primaries, as expected from remote background sites. Contrarily, the urban background sites presented the minimum SOA/OA ratios, even though there is a high variability of sources amongst sites.

For POA there were a few sites whose BBOA was the dominant POA. All the Po Valley sites were POA-BBOA-dominated. Conversely, although traffic was not the main primary source at almost any site (HOA), it was present at every site, even in the remote background ones, implying that traffic was not only a local source but also an OA source of regional influence. In addition, COA was also a relevant source, especially in urban background locations and in one traffic site, but it was not detected at suburban sites. This implied that this source was unstable under transport conditions from the most densely populated areas to city outskirts. Coal combustion was a relevant source only in Dublin and Krakow, although in the latter it was the most prominent primary source. Other primary sources present in this study in minor proportions were amine-OA, wood and peat burning, Shipping + Industry OA, local OA, a generic primary OA source, and cigarette smoke OA.

Regarding SOA, all sites achieved the differentiation of two main SOA factors differentiated upon their degree of oxidation into Less Oxidised-OOA and More Oxidised-OOA, except for the Granada and Padova sites, probably because of the campaigns being short and in winter. In summer, according to various SA studies, the OOA is easy to differentiate, with the formation of LO-OOA due to the enhancement of photochemical reactions and of MO-OOA which denotes a more aged and regional origin (Canonaco et al., 2015; Via et al., 2021). In Zurich, both OOA and LO-OOA/MO-OOA pairs were present because both SOA factors were differentiated in the warmer periods but not in the colder seasons. The Bologna site also achieved the differentiation of two more OOAs related to BBOA emissions giving the capacity of the aerosol mass spectrometer (AMS) to resolve individual species.

Details of the datasets, source profiles and specific source apportionment results are given in [ST10](#).

The results show clearly that NR-PM₁ on-line speciation measurements and source apportionment applied to the resulting dataset is a very useful tool to determine the source contributions to OA, a main (if not the main) PM_{2.5} component, and assess policies for PM abatement. Even if measurements are done for PM₁ for measurement protocols, the OA of PM_{2.5} and PM₁ are mostly equivalent. Furthermore, it can inform AQMNs

managers on a near-real-time mode to show the composition and source apportionment of PM in specific pollution episodes and then support policy decisions for short term actions.

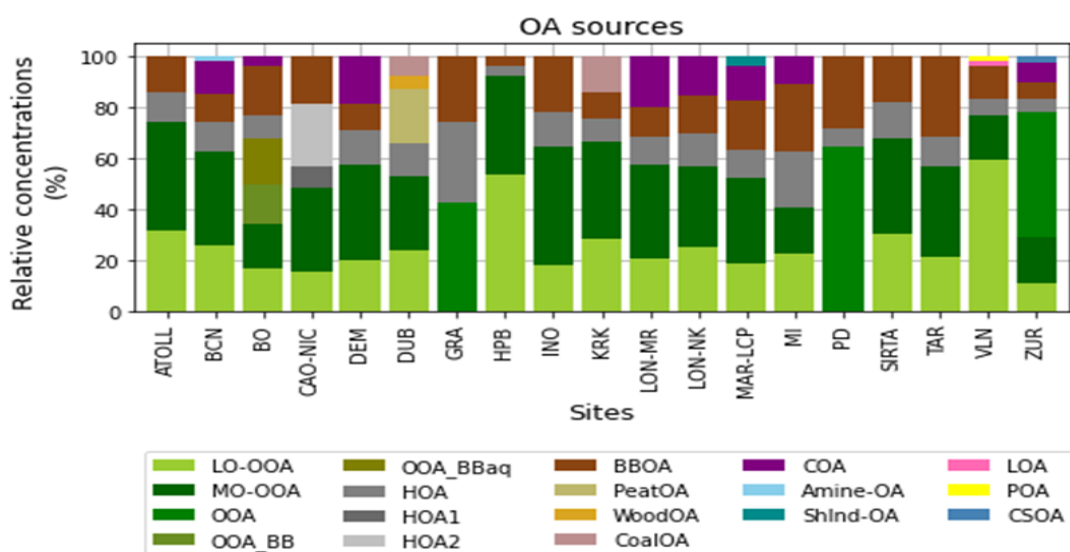


Figure 5.3: Relative mean site OA composition of all sites providing source apportionment results.

6. OXIDATIVE POTENTIAL OF PM IN URBAN EUROPE

Health effects attributable to PM are complex and diverse, and overall, PM_{2.5} is now considered to be the largest environmental contributor to adverse health effects globally (WHO, 2021). PM may act through different mechanisms such as oxidative stress and inflammation, genomic alterations, impaired nervous system function, epigenetic alterations, among others. Thus, it is not possible to cover all these effects by monitoring a single AQ parameter.

Oxidative potential of particulate matter (OP of PM) represents the capacity of PM to invoke oxidative reactions or to generate reactive oxygen species (ROS) in a biological media (Bates et al., 2015; and Uzu et al., 2011, among others). The ROS can be carried on by the PM or be induced/produced from their interactions with the biological system (e.g., fluids, cells, and tissues) and be quantified by different methodologies (Goldsmith et al., 1997; and Sarnat et al., 2016, among others). Oxidative potential can be calculated for different target molecules, such as 1,4-dithiothreitol (OP^{DTT}), ascorbic acid (OP^{AA}), glutathione (OP^{GSH}), uric acid (OP^{UA}), and 2,7-dichlorodihydrofluorescein (OP^{DCFH}), among the most used. These are known as depletion OP assays (Janssen et al., 2014). Furthermore, the (OP^{ESR}) assay measures OP based on the ability of PM to generate hydroxyl radicals (●OH) in the presence of hydrogen peroxide (H₂O₂), and the spin trap 5,5-dimethyl-1-pyrroline-N-oxide (DMPO) (Janssen et al., 2014). The OP^{OH} assay measures the formation of the radical hydroxyl (●OH) in surrogate lung fluid containing the major lung antioxidants, while the Electron Paramagnetic Resonance (EPR) assay measures particle-bound free radicals (Shen et al., 2022).

OP is usually a kinetic measurement based on the depletion rate of anti-oxidants or surrogates when in contact with PM. OP can be mass-normalised (OP_m, expressed in nmolAnti-Ox.min⁻¹µg⁻¹) representing the inherent capacity of one µg of PM to oxidise the lung and is related to the “harmfulness” of such PM. Alternatively, OP can be volume-normalised (OP_v, expressed in nmolAnti-Ox.min⁻¹.m⁻³) related to the exposure of populations to atmospheric oxidant compounds. Note that OP_v of PM is often abbreviated in OP of PM and OP_m also called “intrinsic OP” in scientific literature.

ST4 reviews the available OP measurements and proposes a simplified RI-URBANS measurement protocol with the OP^{DTT} assay (Dominutti, et al., 2024) and also reports on OP^{DTT} and OP^{AA} levels in urban Europe. Figure 6.1 shows a summary of OP^{DTT} and OP^{AA} values reported in urban Europe, with the highest ones being reached in road traffic sites and cities with high biomass burning contributions. All these results point out that both OP^{AA} and OP^{DTT} are sensitive to organic species and metals carried out by PM but to a different extent. In fact, OP^{DTT} – a thiol-based assay, displays a more balanced response to all atmospheric compounds than OP^{AA}, being more specific to a few specific species (mainly metallic, or biomass-burning compounds related). The combinations of both OP^{DTT} and OP^{AA} is evaluated as a good approach to characterise OP of PM. However, despite the development of several acellular assays to evaluate OP of PM, there exists a lack of consensus regarding methodologies and protocols for the OP of PM measurement, as well as the quantification and calibration procedures, hindering inter-study comparisons.

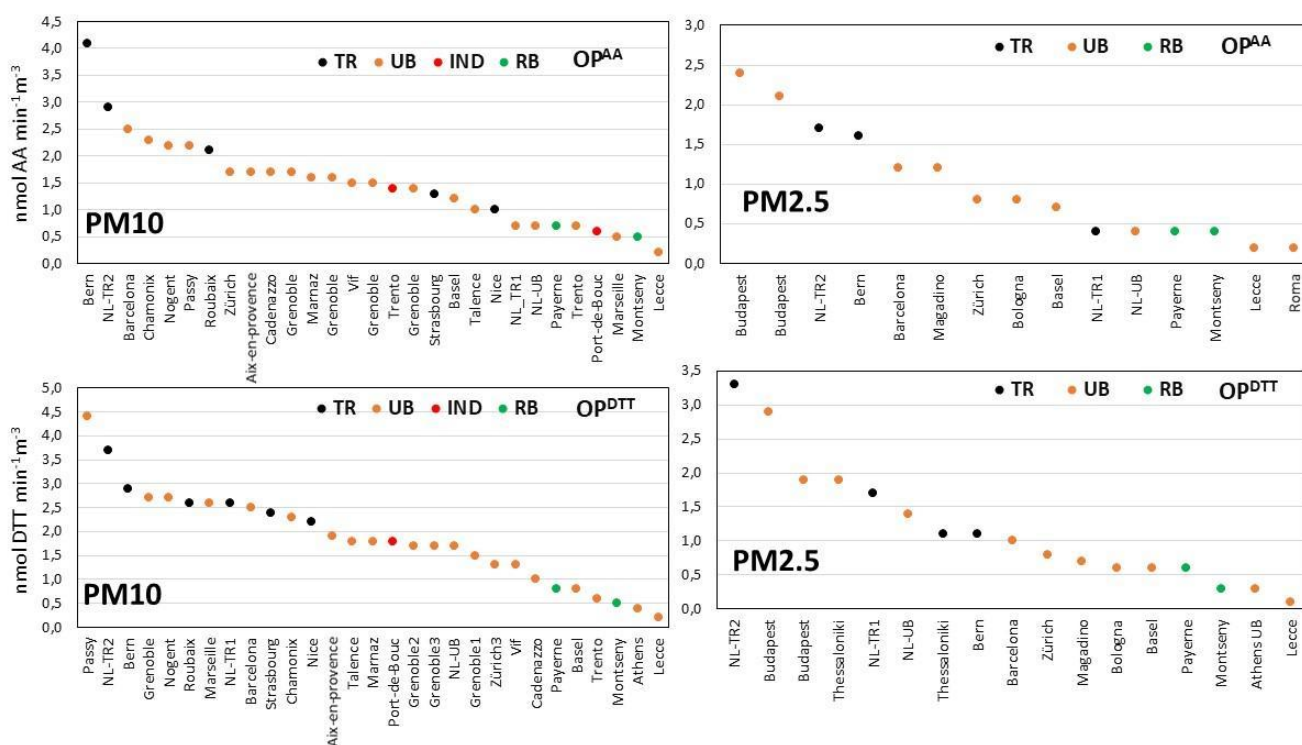


Figure 6.1: OP^{AA} and OP^{DTT} volume of PM mean values (nmol min⁻¹ m⁻³) in (mostly) urban sites, reported by Janssen et al. (2014), Argyropoulos et al. (2016), Visentin et al. (2016), Paraskevopoulou et al. (2019), Pietrogrande et al. (2019, and references therein), Weber (2021), Weber et al. (2021), Grange et al. (2022), Dominutti et al. (2023), In 't Veld et al. (2023a) and Vörösmarty et al. (2023).

ST11 reviews the methodology for source apportionment of OP of PM, which is based on PMF source apportionment applied to PM speciation datasets followed by multilinear regression to assign collocated measurements of OP to PMF sources. Figure 6.2 shows results of the source apportionment of OP of PM₁₀ from an urban Alpine city in France (Dominutti et al., 2023). This included the assessment of well-established assays like AA, DTT, and DCFH, alongside novel assays such as Ferric-Xylenol Orange (FOX) and direct ROS quantification via OH radical. The main findings underscored the significant influence of seasonality on source contributions and OP activities. In winter, when anthropogenic emissions dominate, all OP assays exhibited strong agreement. Conversely, in warmer months, with reduced anthropogenic influence, biogenic and

secondary organic-related aerosols exerted a greater impact. Additionally, we observed varying sensitivities of each OP assay to PM₁₀ sources, likely reflecting differences in chemical composition and processes (Dominutti et al., 2023, Figure 5).

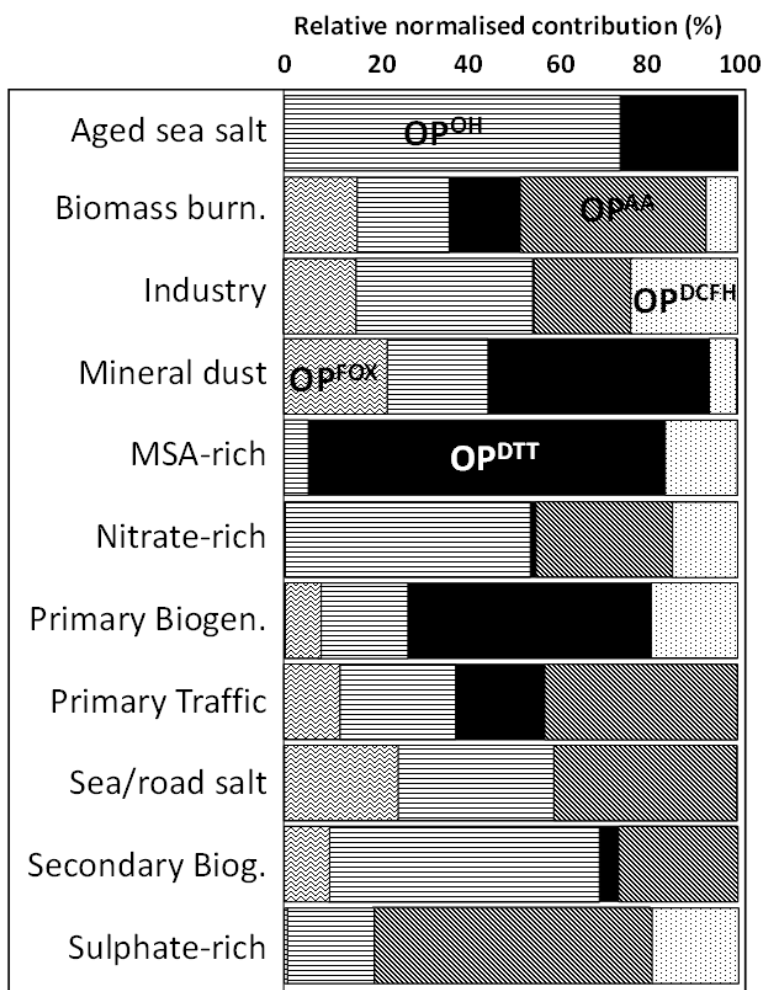


Figure 6.2: OP sensitivity contribution of each PM source. Relative normalised contribution of OP assays to the PM₁₀ sources. Colours represent each OP test evaluated (adopted from Dominutti et al., 2023).

7. NH₃ IN URBAN EUROPE

Ammonia (NH₃) is an alkaline gaseous pollutant of high relevance for AQ. Ammonia increases the formation of secondary PM, and, per se, it negatively impacts ecosystems.

The NAQD (2024/2881, Art 10 and Annex VII) requires the measurement of NH₃ at the rural supersites, but only recommends it at the urban ones. In RI-URBANS, we strongly recommend conducting these measurements at urban sites due to the significant role this pollutant plays in policies aimed at reducing urban PM_{2.5} concentrations. Nitrate (NO₃⁻) concentrations in PM tend to be higher in cities than in the surrounding rural sites, while this is not the case for most studies on sulphate in PM_{2.5} (in 't Veld et al., 2022), this suggesting the relevance of urban NH₃ for ammonium nitrate (NH₄NO₃). [ST6](#) offers comprehensive guidance and recommendations on implementing NH₃ measurements, covering a wide range of offline and online methods with different time resolution, instrumental costs and complexity of running the measurements. This ST also contains a section on the added value of implementing these measurements in urban Europe. In the following section, we summarize the results of compiling and evaluating available NH₃ measurements, primarily from urban areas.

7.1 NH₃ and air quality

In the urban background areas of European cities, 70% of the PM_{2.5} arise from secondary inorganic (SIA) and secondary organic aerosols (SOA) (Amato et al., 2016). Emitted sulphur dioxide (SO₂) and nitrogen oxides (NO_x) undergo atmospheric oxidation reactions that generate gaseous sulphuric (H₂SO₄) and nitric acid (HNO₃). Once formed, these react with NH₃ to generate ammonium sulphate (NH₄HSO₄ and (NH₄)₂SO₄) and ammonium nitrate (NH₄NO₃), two major components of PM_{2.5} (Figure 7.1). PM_{2.5} reduction can become challenging with increasing (or stable) NH₃ concentrations, in situations where NH₃ availability is the limiting factor in SIA formation (i.e. HNO₃ is in excess). Furthermore, NH₃ might interact with volatile organic compounds (VOCs) and SOA to produce NH₄⁺-bearing SOA (Hao et al., 2020, and references therein), which contributes to increase the aerosol radiative forcing (brown carbon, BrC; Bones et al., 2010) and to stabilize SOA in PM (Paciga et al., 2014). It has been demonstrated the abating NH₃ emissions is a cost-effective measure for mitigating PM_{2.5} (Gu et al., 2021). Furthermore, Lelieveld et al. (2015) attributed premature mortality to NH₃-derived SIA in Europe, Russia and East Asia, assuming all particles are of equal toxicity. Although in some cases, (NH₄)₂SO₄ and NH₄NO₃ in PM_{2.5} are considered as the PM components with the lowest potential for health effects, WHO (2013) stated that there is no evidence to exclude health effects for these components.

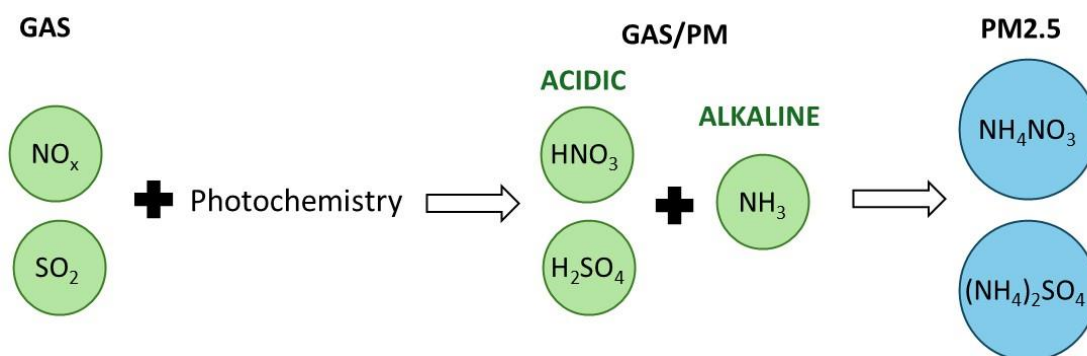


Figure 7.1: Atmospheric processes yielding to the formation of secondary inorganic PM_{2.5}.

NH₃ might also have important effects on ecosystems by causing foliar injury on vegetation, with a sensitivity that follows native vegetation > forests > agricultural crops (Krupa, 2003). Other impacts on vegetation include growth and productivity, tissue content of nutrients and toxic elements, drought and frost tolerance, responses to insect pests and disease-causing microorganisms (pathogens), development of beneficial root symbiotic or mycorrhizal associations and inter species competition or biodiversity. High levels of nitrogen (N) deposition, due to high NH₃ ((NH₄)₂SO₄, NH₄HSO₄ and NH₄NO₃) contribute to eutrophication of ecosystems by N saturation and the consequent negative effects (Hettelingh et al., 2017).

Unlike the AQ criteria pollutants, NH₃ does not have AQ standards in Europe. However, a number of Member States set thresholds for the protection of vegetation, or recommended targets are proposed (UNECE, 2007; Cape et al., 2009). Thus, UNECE long-term Critical Levels (CLE) have been set at 1 µg m⁻³ for lichens and bryophytes and at 3 µg m⁻³ for higher plants.

In the EU-27, agriculture and farming are the leading contributors to the NH₃ emission inventory, accounting for 94% of total NH₃ emissions in 2020. Other sources, including industry, road transportation, and solid waste management, each contribute approximately 1% (EEA, 2022). However, in urban and industrial areas, where SO₂ and NO_x emissions are high, high NH₃ concentrations from local sources might contribute to the increase of PM_{2.5}. Relevant urban sources of NH₃ are waste management, traffic and fugitive emissions from sewerage systems (Reche et al., 2012, 2015; Pandolfi et al., 2012).

In urban areas, the contribution of NH₃ derived from traffic sources have a potential for an increase due to the widespread implementation of selective catalytic reduction (SCR) NO_x-controls in the new EURO 6/VI diesel vehicles (Hopke and Querol, 2022), which uses urea or NH₃ as catalysts to reduce NO₂ tail-pipe emissions. In fact, Reche et al. (2022) reported increases in urban NH₃ concentrations in Barcelona in 2011–2020 probably due to the increase of emissions from traffic and waste management.

7.2 The added value of measuring NH₃ in urban Europe

In the framework of RI-URBANS, Liu et al. (2024a) compiled 69 datasets of NH₃ concentrations from European regional, suburban and urban background (RB, SUB and UB, respectively), industrial (IND) and traffic sites (TR). These included 36 sites from Spain, 15 from France, 12 from Italy, five from the UK and one from Finland. Most of the data was from non-rural sites (UB, 15; SUB, 12; TR, 12; IND, 5), but although the focus was on urban and farming/agricultural hotspots, 15 RB datasets were also collected to better interpret NH₃ spatial and temporal variability. Remote sensing data (Van Damme et al., 2018) was used to identify the spatial extension of farming/agricultural NH₃ hotspots (FAHs). Furthermore, arbitrarily, RB sites reaching average concentration >1.5 µg/m³ were also classified as FAHs, and these were named Regional Background sites Close to Hotspot (RBCH). A wide range of instrumentation was used to measure NH₃ concentrations, including active denuders, passive samplers, online chemiluminescence gas chromatography-mass spectrometry, optical CRDS (cavity ring-down spectroscopy), optical HFOC (high-finesse optical cavity), and annular denuder equipped with online ion chromatography.

The average of all sites reached $8.0 \pm 8.9 \mu\text{g m}^{-3}$, with minimum and maximum of 0.2 and $54.4 \mu\text{g m}^{-3}$. The vast majority of the sites exceeded the UNECE Cle threshold of $1 \mu\text{g m}^{-3}$ set for NH_3 to protect ecosystems and the $3 \mu\text{g m}^{-3}$ threshold for other vegetation.

For the group of sites excluding FAHs (non-FAHs, Figure 4a and Figure 5), the mean concentration reached $3.2 \pm 1.8 \mu\text{g/m}^3$. For these non-FAH sites, the highest annual average concentrations, 4.7 ± 3.2 and $4.5 \pm 1.0 \mu\text{g/m}^3$, were recorded at IND and TR sites, 3.3 ± 1.5 and $2.7 \pm 1.3 \mu\text{g/m}^3$ at UB and SUB sites, and $1.0 \pm 0.3 \mu\text{g/m}^3$ at an RB site (Figure 7.2). Thus, NH_3 levels were higher at TR sites compared to UB sites, owing probably to NH_3 slip from vehicles. This possibility highlights the importance of considering the implementation of NH_3 emission limits for all times of vehicles (as requested in the forthcoming EURO 7/VII standards), especially because such limits currently apply only to heavy-duty vehicles (EURO VI) in the EU. Furthermore, UB sites might receive NH_3 contributions from other sources, such as waste management and sewage systems that could also significantly impact urban NH_3 levels (Pandolfi et al., 2012; Reche et al., 2012). Therefore, in non-FAHs, IND, TR and UB sites urban sources are the main contributors to NH_3 ambient concentrations, and probably not always these are adequately accounted in the emission inventories.

When considering only FAHs (Figure 7.2), NH_3 concentrations were similar at SUB, RBCH, UB, TR sites ($14\text{--}15 \mu\text{g/m}^3$), and $10.0 \pm 2.3 \mu\text{g/m}^3$ at the IND sites. Thus, in this case, SUB and RBCH reached slightly higher NH_3 concentrations, probably because in these FAH sites, very large volumes of NH_3 are emitted by nearby agriculture and livestock (Sutton et al., 2022). Thus, UB-FAH NH_3 average concentration ($14.0 \pm 5.3 \mu\text{g/m}^3$) was 4-fold higher than the one for UB-non-FAH sites ($3.3 \pm 1.5 \mu\text{g/m}^3$).

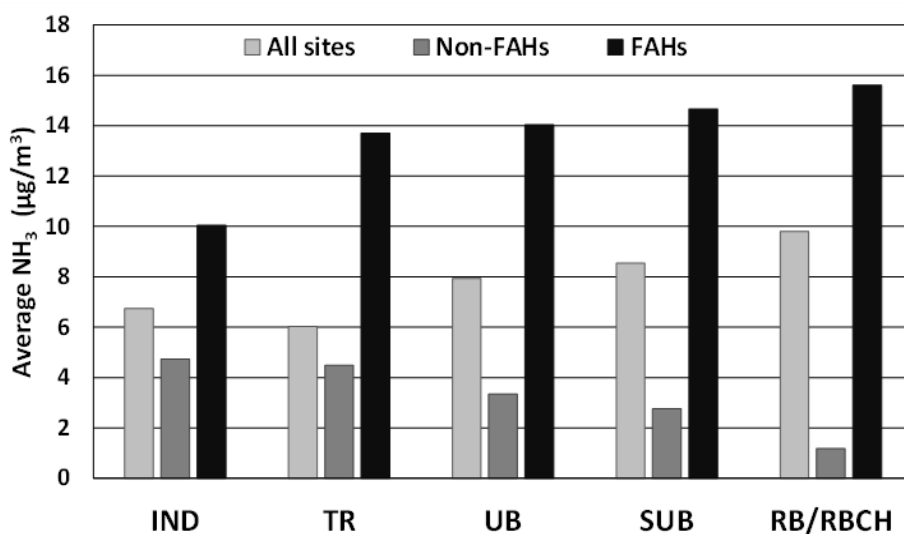


Figure 7.2: Average NH_3 concentrations for all (69) sites, outside (non-FAHs) and inside (FAHs) farming/agricultural hotspots, according the type of environment: industry, IND; traffic, TR; urban background, UB; suburban background, SUB; regional background, RB, and regional background close to hotspots, RBCH. Figure modified from Liu et al. (2024a).

For the **non-FAHs sites**, the **trend analysis** showed the following results (Figure 7.3):

- Trends were very variable for the different sites in all types of environments (UB, TR, RB, IND) and this yielded to non-statistically significant trends in the analysis of each type, and for all types.
- Regarding UB and TR sites (N=7), three sites followed a statistically significant decreasing trend, while other three sites followed a statistically significant increasing trend.

- For the RB sites, a slight non-significant decreasing trend was observed.

For the **FAHs sites**, the **trend analysis** showed the following trends (Figure 7.3):

- A statistically significant decreasing trend was obtained at two of the UB sites (N=3, Figure 4), yielding to an overall non-statistically significant trend for all UB sites.
- For the RBCH sites, a statistically significant increasing trend was obtained for seven sites. Aas et al. (2024) attributed the NH₃ increasing trends of RB to their progressively decrease in the NH₃ consumption to generate (NH₄)₂SO₄ and NH₄NO₃ associated with the marked decreases in the emissions of SO₂ and NO_x. However, the articles referred to background NH₃ concentrations, while the RBCH sites (with extremely high NH₃ concentrations), were located in NH₃ FAHs, where an increase in emissions of this pollutant cannot be discarded in addition to the cause above.

It is important to consider these trends, with those on emissions and atmospheric processes to assess the current situations and to devise effective NH₃ abating policies.

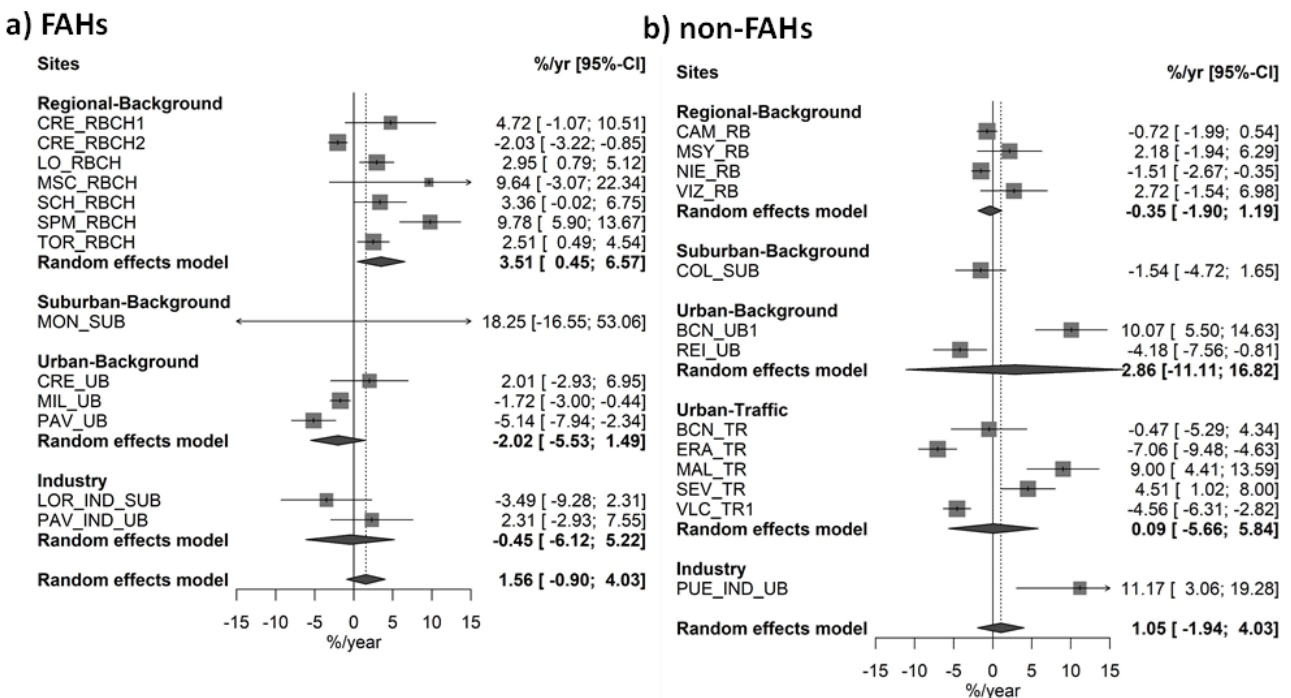


Figure 7.3: Annual NH₃ trends at (a) FAHs and (b) non-FAHs. Values represent change per year (%/yr) with 95% confidence level range in square brackets. Modified from Liu et al. (2024a).

8. VOCs IN URBAN EUROPE

8.1 The complexity of measuring VOCs

Based on the EU Directive 1999/13/EC of 11 March 1999, volatile organic compound (VOC) means any organic compound having an initial boiling point less than or equal to 250°C measured at a standard pressure of 101,3 kPa. VOCs exhibit a variety of functional groups and can be categorized by certain structural and reactive features, according to the way carbon bonds to itself or another element, e.g. carbon double bonded to oxygen. These different ways of bonding will lead to different reactivities with ambient oxidants (OH, NO₃, O₃). Table 8.1 presents the different families of VOCs based on their functional groups.

Table 8.1: Chemical families of VOCs.

Family	Molecular formula	Functional group (R=Alkyl group)
Alkanes	C _n H _{2n+2}	-C-C-
Alkenes	C _n H _{2n}	-C=C-
Alkynes	C _n H _{2n-2}	-C≡C-
Halocarbons	C _n H _{2n+1} X	-X: F, Cl, Br, I
Alcohols	C _n H _{2n+2} O	-OH
Ethers	C _n H _{2n+2} O	R-O-R
Aldehydes	C _n H _{2n} O	R-CH(O)
Ketones	C _n H _{2n} O	R-C(O)-R
Carboxylic acids	C _n H _{2n} O ₂	R-C(O)OH
Esters	C _n H _{2n} O ₂	R-C(O)-OR
Amines	C _n H _{2n+1} NH ₂	-NH ₂

For benzene, three different reference methods are available (EN 14662-1–3). In addition, two other CEN standards (EN 14662-4–5) have been published that can be used for e.g. indicative measurements of benzene. For other VOCs, standardisation work is ongoing in the CEN working group TC264/WG13.

Typically, abundant compounds observed in ambient air and commonly reported in the literature include non-methane (NM) hydrogenated VOCs (HVOCs) such as alkanes (ethane, propane, and higher compounds), alkenes (ethylene, propene, etc.), aromatics (benzene, ethylbenzene, toluene, C₈- and C₉-aromatics, styrene), biogenic compounds (isoprene, monoterpenes, sesquiterpenes), and oxygenated VOCs (OVOCs) such as alcohols (methanol, ethanol, etc.), ketones (acetone, methyl ethyl ketone, etc.), aldehydes (formaldehyde, acetaldehyde, etc.), carboxylic acids (formic, acetic, etc.) and other families reported in Table 8.1. Terpenes are in general highly reactive and their oxidation leads, among others, to the formation of oxygenated VOC of various volatilities and chemical structures with different properties (reactivity, stickiness, etc.). OVOCs also play an active role in the chemical reactions chain of the atmosphere and are precursors of photochemical O₃ and SOA, as all the VOC chemical families. These compounds (OVOCs including formaldehyde, and terpenes) are among the recommended World Meteorological Organization (WMO) Global Atmosphere Watch (GAW) measurement variables (GAW-WMO, 2017). The measurement of these

compounds is challenging due to their reactivity, as these compounds interact with surfaces, leading to possible artefacts during the sampling stage due to adsorption and desorption effects or to the ozonolysis of unsaturated VOCs in the sampling lines.

The VOCs list in Annex VII of the NAQD 2024/2881 include 45 VOCs from different chemical families including non-methane hydrogenated VOCs (NM hydrocarbons or HVOCs), OVOCs and terpenes. The NAQD mentions that measurement of O₃ precursors shall include at least nitrogen oxides (nitrogen monoxide NO and nitrogen dioxide NO₂), and as appropriate, methane (CH₄) and VOCs. The selection of the specific compounds to be measured will depend on the objective sought and may be completed by other compounds of interest.

The RI-URBANS/ACTRIS [ST5](#) on Measurements of VOCs supply guidance on the different techniques that might be used for measuring concentrations of the VOCs included in the NAQD, including chemical ionization mass spectrometry (CIMS), proton transfer mass spectrometry (PTR-MS), selected ion flow tube mass spectrometry (SIFT-MS), and atmospheric pressure interface CIMS (API-CIMS), together with chromatography associated with various detection methods. On the one hand, a technique using mass spectrometry can offer a very good temporal resolution (few seconds to few minutes) compared to gas chromatography (GC) and high-performance liquid chromatography (HPLC) techniques (1 h in general), but on the other hand these techniques are limited in the number of compounds that can be speciated. In contrast, GC techniques provide a better speciation for a large number of compounds at the expense of time resolution. These techniques have to be chosen depending on the application. The use of online instruments with a high temporal resolution is particularly useful in studies where probing fast processes is the main point of interest, such as emissions of pollutants and possible chemical reactions and/or transformations. Online GC and offline methodologies (i.e., HPLC, canister or tube sampling/offline analysis by GC) permit the measurement of a large pool of compounds with a time resolution ranging from 1 h to several days, which is of particular interest for source apportionment, trend analysis or exposure studies. The NAQD indicates that Member States may use the method which is considered to be suitable for the monitoring objective sought, however, once available, standardised reference methods shall be applied. RI-URBANS guidance on tools to implement VOCs source apportionment analyses are also available in [ST11](#).

8.2 Emissions of VOCs

The current knowledge on VOCs origins as reviewed by the UK Air Quality Expert Group (AQEG-UK, 2020) is summarised here.

VOCs from natural gas production, distribution and use include methane, ethane, propane, butane. Many of them have a limited O₃ formation potential but should still be considered as significant O₃ precursors due to their high concentrations.

VOCs from fuels such as gasoline (production, distribution, engine emissions and evaporation) include i/n-butane and i/n-pentane, hexane, mono-aromatics (such as benzene, toluene, and m/p-xylene) and a fraction of unsaturated hydrocarbons (alkenes and alkynes). In recent decades, the amount of ethanol added to gasoline (up to 5–10%) has increased, while its content in PAHs (<30%), benzene (<1%) and di-enes (<1%) has been reduced to comply with the European standard EN 228 (2012 and A1:2017). In addition to these measures, the reduction of emissions by refineries, VOC traps at petrol stations, 3-way catalysts, together with the reduction in the use of direct petrol injection (AQEG-UK, 2020), have contributed to a very marked reduction in emissions from road transport and associated products. In addition to road traffic, benzene

emissions can be partly attributed to off-road machinery, aviation, gas and biomass boilers, as well as forest fires and agricultural waste burning (Lewis et al., 2013).

Solvent VOCs include those emitted from industrial processes (manufacturing and application of paints and varnishes) to domestic use of products (personal hygiene, cleaning, adhesives, inks, paints, sealants, air fresheners and varnishes, among others). Species emitted by solvents include toluene, m,p,o-xylene, ethylbenzene, trimethyl-benzenes, acetone, methanol, ethanol, isopropyl alcohol, formaldehyde, and halogenated alkanes (dichloromethane, among others). The introduction of the European Commission Paints Directive 2004/42/EC may have had a major effect on reducing VOC emissions.

Biogenic VOCs (BVOCs) are isoprenoids that are emitted by wild and cultivated plants (e.g. isoprene in deciduous forests, and monoterpenes in evergreen forests). In addition to being emitted in large volumes during the summer in regions with high levels of sunlight, their potential for the formation of O₃ and secondary organic PM is very high. Although BVOC emissions are much lower than anthropogenic VOC (AVOCs) emissions on an annual basis, their relative importance is much greater during the critical O₃ pollution season. In addition, the spatial distribution of BVOCs and AVOCs (as well as NO_x) emissions is different, and the former may determine the O₃ formation regime (controlled by the VOC/NO_x ratio) across large areas.

Furthermore, a large proportion of VOCs in ambient air is of secondary origin, and they are generated from reactions such as ozonolysis and oxidation of hydrocarbons to OVOCs (aldehydes, ketones, among others). There are species such as formaldehyde that can have both primary and secondary origins, and some species that are both AVOCs and BVOCs. Thus, in regions with high solar radiation and O₃ concentrations, OVOC concentrations can be very high, due to their fast generation from primary HVOCs. In urban environments, OVOCs reach higher concentrations than the HVOCs normally measured by AQMNs.

8.3 The added value of measuring VOCs in urban Europe

8.3.1 Concentrations of VOCs

In the framework of RI-URBANS, Liu et al. (2025b) compiled 21 VOC datasets across mostly urban Europe, including Belgium (7 sites), Finland (2), France (7), Switzerland (1), Spain (1), and the UK (3). The dataset comprised 3 industrial (IND), 2 traffic (TR), 15 urban background (UB), and 1 suburban background (SUB) sites. Furthermore, Liu et al. (2025c) included an additional UB site in Greece in a study focusing on BTEX in urban Europe.

Measurements of VOCs were carried out using a variety of methodologies and instrumentation, because there is not a standard or reference method to this end. Accordingly, there is a limitation to data comparison due to the different protocols used for VOCs, but also because the disparity of VOCs species measured at each site. Furthermore, some of the techniques used are not able to trap specific VOCs for subsequent desorption and analysis, and other tools are not specific for a number of VOCs but for ions from a group of VOCs (such as in some cases for PTR-MS and specific groups). In this compilation, all monitoring stations monitored benzene since it is regulated, as well as toluene, ethylbenzene, and xylene species. However, none of the supersites yielding the 21 datasets cover all 45 VOCs of the NAQD 2024/2881/EC. The studied sites included at most 29 VOCs while most of them measured more than 21 VOCs. This is reflecting the difficulty in measuring the 45 VOCs species.

It was observed that the 20 most commonly analysed VOCs at the monitoring sites were n-butane, n-pentane, i-pentane, n-hexane, n-heptane, n-octane, i-octane, 1,3-butadiene, 1-butene, trans-2-butene, cis-2-butene, 1-pentene, benzene, toluene, ethylbenzene, m,p-xylene, o-xylene, 1,2,4-trimethylbenzene, 1,3,5-trimethylbenzene, and isoprene.

For facilitating the comparison of these VOCs' datasets, the Maximum O₃ Formation Potential (MOFP) was calculated for each site by multiplying the Maximum Incremental Reactivity (MIR) of each species by its concentration at that site (Venecek et al., 2018). The secondary organic aerosol (SOA) Formation Potential (SOAP) was calculated in a similar manner, by multiplying VOC concentrations by the SOA yield (YSOA) of each species obtained from Gu et al. (2021). Average values for all sites and species included are ranked in Figure 8.1.

The results evidenced that toluene, m,p-xylene, 1-butene, n-butane, and isopentane collectively contributed on average over 50% to the total MOFP (calculated as the sum of the individual 20 MOFPs) for the sites studied, with individual contributions of 15% ± 9%, 13% ± 7%, 9% ± 8%, 9% ± 6%, and 7% ± 5%, respectively. This is primarily attributed to their relatively high concentrations and high MIR values. In parallel, aromatic hydrocarbons accounted for most of the SOAP (>85%), with toluene (55% ± 16%), benzene (20% ± 10%), m,p-xylene (7% ± 3%), and o-xylene (4% ± 2%) being the major contributors.

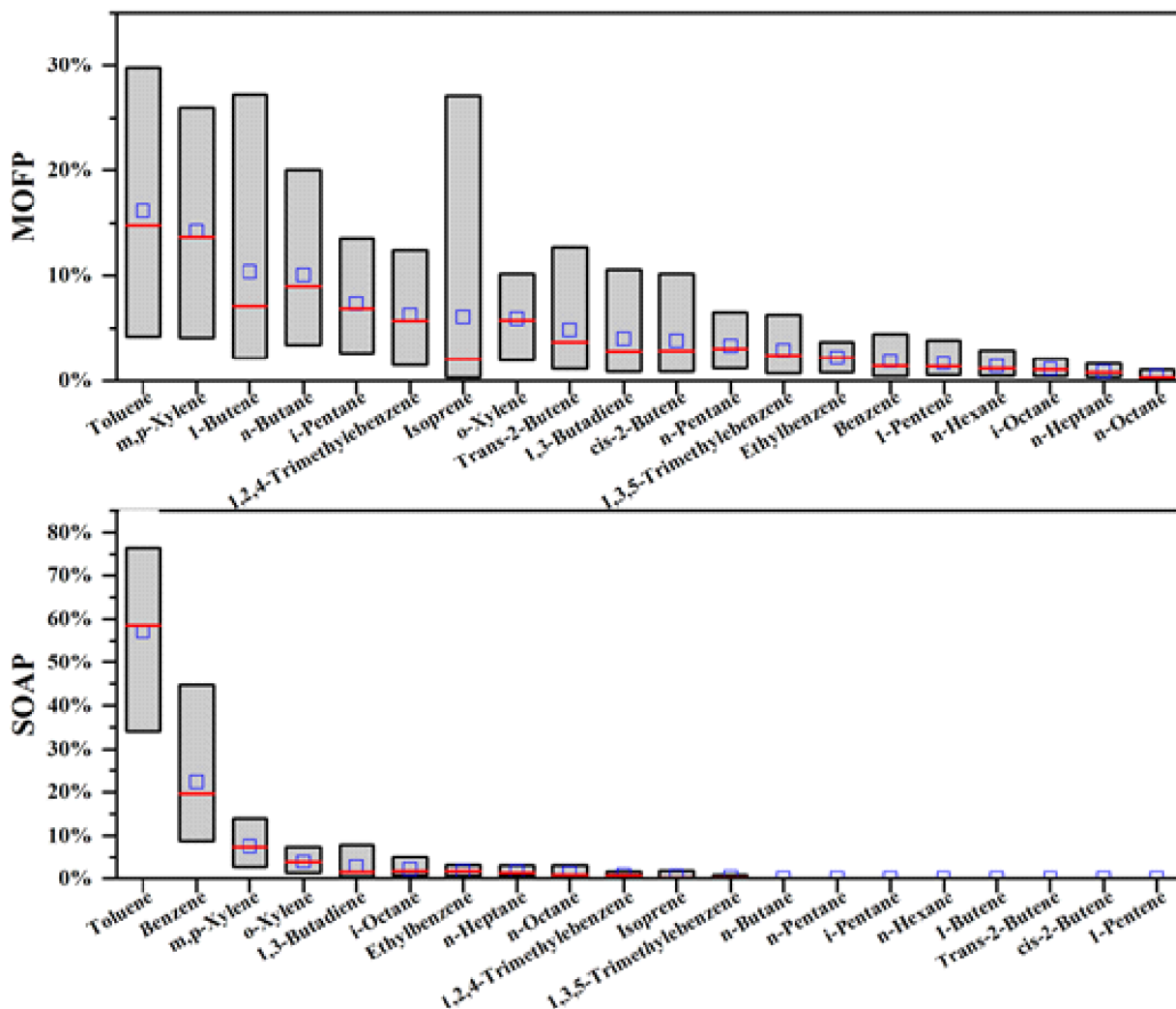


Figure 8.1: Individual contributions of 20 VOCs to (lower) the total (sum of the 20) SOA formation potential (SOAP), in $\mu\text{g SOA}/\text{m}^3$ and (upper) the maximum O₃ formation potential (MOFP), in $\mu\text{g O}_3/\text{m}^3$, as averages for the collected datasets.

The box represented the 5th–95th percentiles of ratios. The middle line and middle square represented the median values and mean values of ratios, respectively. Adopted from Liu et al. (2025b).

Liu et al. (2025c) reported that BTEX can be ranked according to their 2017–2022 average concentrations as toluene > benzene > m,p-xylene > o-xylene > ethylbenzene, with mean concentrations of 1.5 ± 1.7 , 0.8 ± 1.0 , 1.0 ± 1.3 , 0.4 ± 0.5 , and $0.3 \pm 0.5 \mu\text{g}/\text{m}^3$, respectively. Figure 8.2 shows the average concentrations observed at each site.

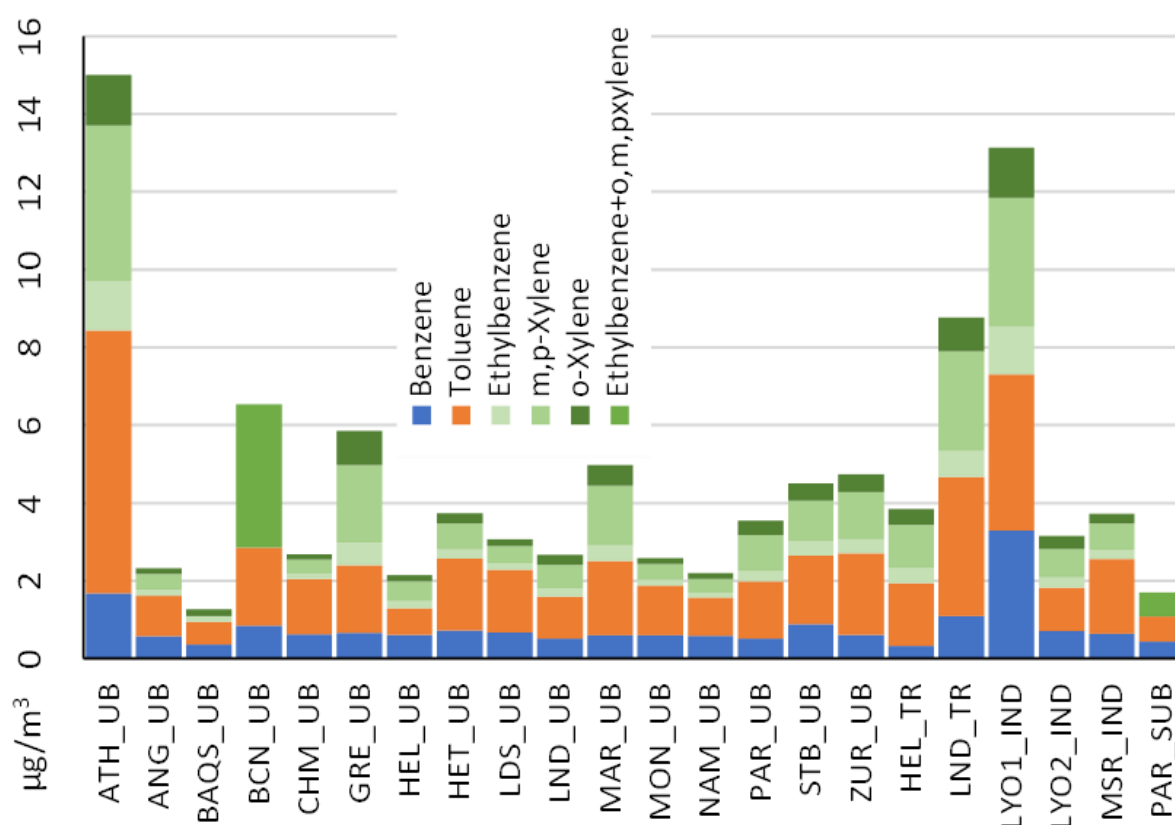


Figure 8.2: Average 2017–2022 concentrations for specific BTEX in the 22 study sites. The abbreviations stand for the following European cities: ATH for Athens, ANG for Angleur, BAQS for Birmingham, BCN for Barcelona, CHM for Charleroi, GRE for Grenoble, HEL for Helsinki, HET for Herstal, LDS for Lodelinsart, LND for London, LYO1 for Lyon (Feuzin stade), LYO2 for Lyon (Vernaison), MAR for Marseille, MON for Mons, MSR for Mouscron, NAM for Namur, PAR for Paris, STB for Strasbourg, and ZUR for Zürich. Modified from Liu et al. (2025c).

8.3.2 Source apportionment studies of volatile organic compounds in Europe

The literature review on the source apportionment of VOCs in UB and SUB sites showed that, to our knowledge, 18 studies have been performed in Europe. PMF receptor modelling was used in most of the cases to perform the source apportionment either on seasonal basis when long term data is available, or on specific campaign's data. PMF with EPA 5.0 software is the most suitable as it does not require previous knowledge on the source composition profile.

A variety of sources were identified (some in some specific periods, such as biomass burning in winter) in the urban environment, which are described with their common tracers/markers below.

- Natural gas source was mostly identified by high contributions of ethane and propane, with minor contributions from butane.
- Wood-burning source was traced by acetonitrile, acetylene, ethylene, and benzene.
- The biogenic source was identified by isoprene and its oxidation products (methyl vinyl ketone (MVK) and methacrolein (MACR)). Although isoprene has a biogenic origin, its anthropogenic origin is rarely described. The addition of monoterpenes can potentially aid in identifying its biogenic origin, although they are often emitted from other vegetation (potentially being identified as a separate factor), and also monoterpenes can be emitted from anthropogenic sources.
- Motor vehicle exhaust was characterized by high contributions from C4–C5 alkanes, especially butane and pentane, and BTEX (benzene, toluene, ethylbenzene, and xylenes) compounds. The exact tracers highly depend on the type of traffic and engines most commonly used in the urban area, and depending on the VOCs included in the study. The traffic exhaust was either separated or combined with fuel evaporation related to traffic.
- Solvent source markers often had high contributions of OVOCs and aromatics in these studies.
- Some specific industry sources were found, but this highly depended on the type of industry and on which VOCs were used to identify this source.
- Various studies found a secondary source composed of OVOCs mainly, although some studies identified this source as long-lifetime VOCs.

Within RI-URBANS, three source apportionment studies were performed after data collection at two urban/urban background sites with different VOC datasets in Marseille, France (Dufresne, 2022), Zurich, Switzerland, and Barcelona Spain (in 't Veld et al., 2023b). As an example, Figure 8.3 shows the results of the PMF source apportionment for Marseille and Zurich. These have some common VOC sources, such as road traffic, natural gas, heating/wood burning, and other local emissions (one source related to solvent use was identified only in Zurich thanks to OVOC that were measured, and additional sources in Marseille related to industrial sources). Since the two datasets did not cover the same VOCs, having a wide range of VOCs with varying volatility, including both primary NMHVOCs and secondary origins (OVOCs), is essential. This broader spectrum can aid in identifying the sources and assessing their contribution. Additionally, the measurement of OVOCs is important as it is an indicator of the impact of photochemistry and covers some markers of solvent use emission source.

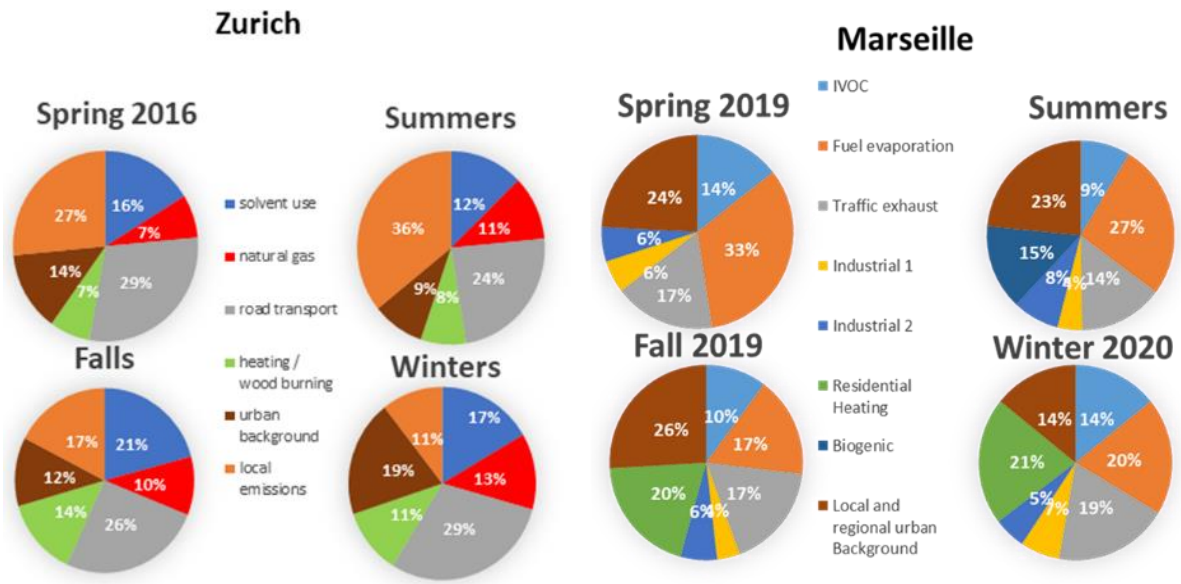


Figure 8.3: Source apportionment results at Marseille (Dufresne, 2022) and Zurich.

9. VERTICAL PROFILES

Although measurements of vertical profiles of advanced AQ parameters are not required or recommended in the NAQD 2024/2881, RI-URBANS, ACTRIS and IAGOS demonstrated that these are very useful for an advanced AQ assessment, forecast and validation of modelling tools.

RI-URBANS has produced three STs on vertical profiles in collaboration with ACTRIS or IAGOS. Thus, [ST7](#) contains guidance on measurements that allow to determine the atmospheric boundary layer (ABL) height (ABLH), a key parameter for forecasting, for example, exceedances of daily and hourly limit values; and [ST8](#) on aerosol profiles, which are very useful for detecting and demonstrating desert dust outbreaks, long transport of PM from anthropogenic or forest fires, over European cities. Finally, [ST9](#) shows the products from IAGOS on vertical profiles of AQ pollutants (NO₂, O₃, etc.) measured in commercial aircrafts and that can be openly accessed in the IAGOS website.

We provide here some examples on the added value of implementing these STs.

9.1 Atmospheric boundary layer

The ABL is the lowest part of the atmosphere that is directly affected by the Earth's surface at time scales of <24 h. When the ABL is not well mixed, which may frequently be the case during the day-night transition and several hours around those times, multiple sublayers can have distinctly different composition characteristics. In clear sky conditions, buoyant mixing during the day dilutes pollutants within the so-called convective boundary layer (CBL) that increases in height during the morning and decays around sunset. At night, the vertical buoyancy is absent or weak, leading to a relatively shallow nocturnal layer close to the ground. The air diluted within the daytime CBL remains aloft and forms the residual layer. The height of the total atmospheric boundary layer (ABLH) represents the height of the residual layer at night and during morning while the CBL extends over the entire ABL in the afternoon. To define the volume for pollution dispersion and distribution near the ground, the continuum of the shallow nocturnal layer and the daytime CBL can be considered as the mixed layer height (MLH). The cloud-topped ABL can generate its own turbulent mixing which may be sufficient for a deep MLH to persist whether day or night.

Transport processes in the ABL can significantly affect the spatial distribution (horizontal and vertical) of aerosols and trace gases. While the horizontal wind is an important variable that drives horizontal advection between neighbourhoods or between the city and its surroundings, atmospheric turbulence is responsible for the mixing of the atmosphere, the vertical dilution of pollutants as well as the potential entrainment into the CBL. If fresh air is entrained, this can improve near-surface AQ, while entrainment of residual layer air or pollutants from elevated aerosol layers (e.g. Saharan dust, forest fire plumes) may have negative effects.

[ST7](#) guides on how to characterise the above parameters of the ABL using measurements with automatic lidars and ceilometers (ALC), and Doppler wind lidars (DWL). As an example, results are shown here for long-term MLH measurements by the ABL testbed project at the RI-URBANS pilot cities. The variability of ABL dynamics can be assessed at different temporal scales, from diurnal cycles to monthly or seasonal variations to inter-annual differences. As an example, the ABL testbed demonstrator project is currently processing data from 17 measurement sites (21 ALC) across Europe, including several sites relevant to RI-URBANS pilot cities: Bucharest (2 sites), Helsinki (2 sites), Aosta - St Christophe that is influenced by Milan (1 site), Paris (2 sites), and Rotterdam (2 sites), with daily quicklooks freely accessible (ABL testbed – European: <https://observations.ipsl.fr/aeris/e-profile/>). Multiple years of measurements have been processed by the

ABL testbed spanning from 2018–present for most sensors. Figure 9.1 shows an example of the MLH daily variability in Paris.

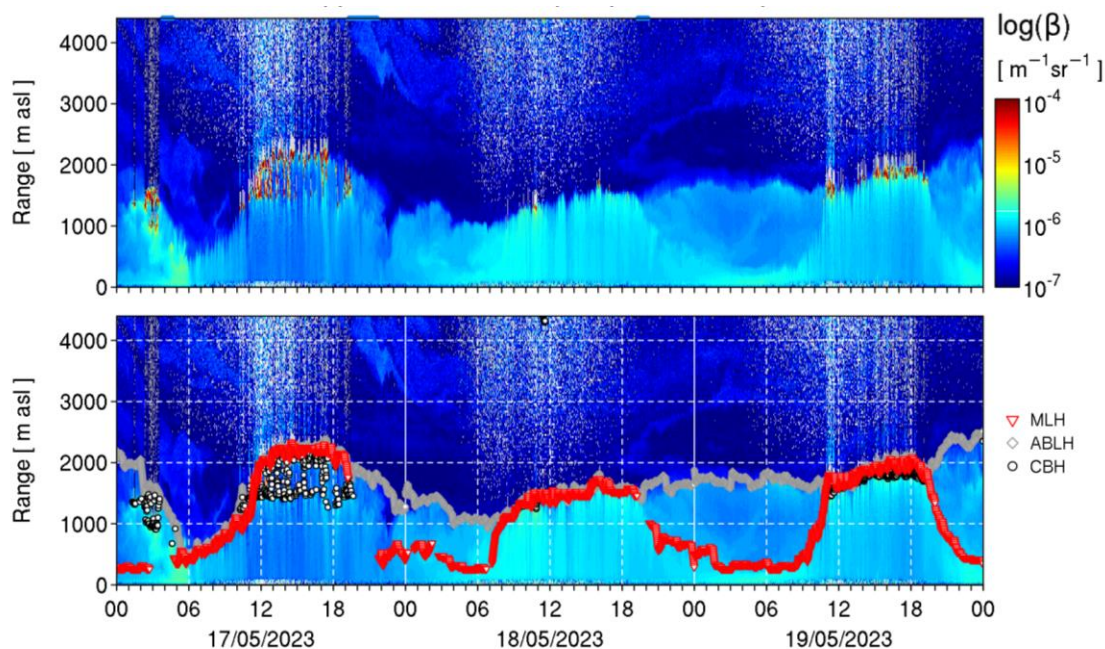


Figure 9.1: Daily quick look from the ABL testbed: overlap-corrected and calibrated attenuated backscatter observed with an ALC (Lufft CHM15k) at the SIRTA observatory at Palaiseau near Paris over a three-day period. Bottom figure also shows the cloud base height (CBH) and the mixed layer height (MLH) and atmospheric boundary layer height (ABLH) detected with the STRATfinder algorithm.

9.2 Vertical profiles of aerosols

Surface based remote sensing measurements can yield to vertical profiles of the variation of the aerosol concentrations. These measurements coupled with the ones of the ABL can be very useful to detect long range-transport of PM (including dust, forest fires, anthropogenic pollution) and to evaluate the impact on surface levels by the growth of the MLH.

Aerosol profiling quantities are typically measured through range-resolved optical remote sensing, so that optical properties are the quantities measured and are typically dependent on the chemical composition and shape of the particles and on their concentration (e.g. aerosol extinction coefficient profiles). Some intensive parameters can then be directly obtained (typically through calibrated ratio of optical properties, e.g. depolarization ratio). Finally, some quantities can be retrieved from the previous quantities, such as the mass concentration.

Aerosol properties (known as quantities) measured are aerosol backscatter, aerosol extinction, volume depolarization ratio, among others. From these, the following intensive properties are obtained: lidar ratio, Angstrom exponent, backscatter Angstrom exponent, particle linear depolarization ratio, and aerosol type, among others.

As an example, results on the aerosol optical properties climatology over Europe 2000–2019 is shown. This study is based on EARLINET long term observations performed in 2000–2019, namely the Level 3

climatological products (EARLINET Level 3 Data Product Catalogue, 2022). In the following, examples for stations identified as of interest for urban conditions considering their population in the area are reported, and compared to stations in clean conditions to be considered as a reference/background. As representative of urban conditions, the following stations are reported: Madrid (ES), Barcelona (ES), Ispra (IT), Naples (IT), Athens (GR), Thessaloniki (GR), Warsaw (PL), and Bucharest (RO). As reference for clean conditions, Granada (ES), Leipzig (DE) and Lecce (IT) stations are also reported.

Figure 9.2 reports normal months average profiles at 532 nm for each station, showing the seasonal dependence as observed during the last 20 years and relative differences between the stations. The false colour images of backscatter coefficient provide a direct insight of the presence in the atmospheric column of the aerosol particles: warm colours indicate the presence of high aerosol concentrations, while cold ones are for lower concentrations, until reaching the blue where the aerosol concentration can be considered below the detection limit.

Apart from signatures of aerosol presence above 6 km, due to special events of long range transported aerosol particles, most of the aerosol content is confined up to 4–5 km of altitude. The presence of aerosol up to higher altitude during warm periods is common to all the reported sites. Anyhow, it is observed a tendency of more pronounced trapping of aerosol closer to the surface at big cities locations (first two columns). This is clearly evident in the case of Naples, a metropolitan area located close to sea. Comparing the false colour maps in Figure 9.2 with the corresponding Lecce one (smaller city on the sea) it is clear the presence of intense red area close to ground for Naples while the yellow dominates with different nuances for Lecce, even if all the 3 show the same general pattern with higher altitude affected by aerosol in June–August period.

The same behaviour is observed for Iberian region (Barcelona and Madrid compared to Granada) and for central-East Europe (Bucharest and Warsaw vs. Leipzig). To be noted that the high aerosol content observed over Granada is probably related to the considerable presence of dust being in a very arid region and strongly affected by desert dust.

Thus, these measurements coupled with the ones of the ABL can be very useful to detect long range-transport of PM (including dust, forest fires, anthropogenic pollution) and to evaluate the impact on surface levels by the growth of the MLH.

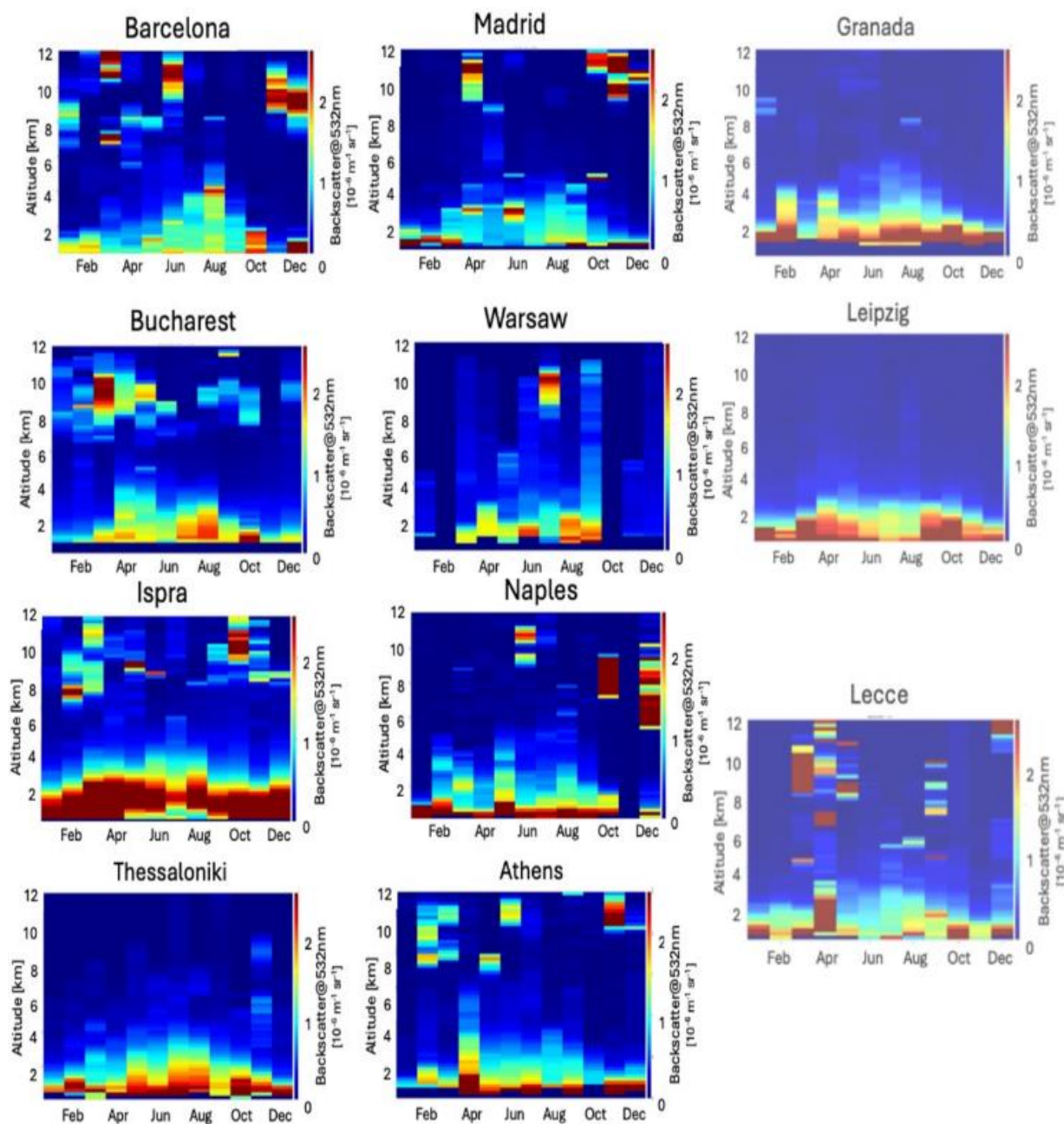


Figure 9.2: Climatological monthly averages of the aerosol backscatter profile at 532 nm in suburban locations close to eight big cities: Barcelona, Madrid, Bucharest, Warsaw, Ispra, Naples, Thessaloniki and Athens. In the third column the same quantity is reported, as partially transparent, for three sites far from big cities located in the same macro-area of the previously reported eight sites.

9.3 IAGOS vertical profiles of pollutants

Using compact and automated in-situ sensors on board of passenger aircraft, the European Research Infrastructure IAGOS (Petzold et al., 2015, Thouret et al., 2022; www.iagos.org) monitors vertical profiles of trace gas concentrations (incl. CO, O₃, NO_x, and H₂O) near airports during take-off and climb-out as well as during descent and landing flight phases between the ground and 10–12 km altitude. These profiles characterise the vertical distribution of trace gases from the free troposphere down to the regional-scale and urban background boundary layer that interacts with the urban pollution layer. In addition, elevated layers

of polluted air that are often advected via regional or long-range transport can be identified with the help of IAGOS profiles and are assessed for their impact on urban AQ.

The IAGOS profile data provide valuable information that is otherwise not accessible, and complement the data provided by surface-based AQMN stations (Petetin et al., 2018), facilitating the link to high-resolution models and satellite observations particularly in the vertical dimension. Above the planetary boundary layer, the correlation between the IAGOS in-situ and the urban background observations decreases rapidly, while increasingly high correlations with remote Global Atmosphere Watch (GAW) stations. The representativeness of the IAGOS airborne measurements for the general conditions of the lower troposphere are carefully analysed by Petetin et al. (2018).

In the middle of 2024, IAGOS counted a fleet of ten aircraft equipped with automatic instruments operated by eight international airlines. Of these, six regularly sample the European troposphere with ozone and CO since 2002 and two of them provide additional NO_x data since 2015 and 2023, respectively. A third one providing NO_x is planned for the end of 2024. Thanks to several equipped aircraft landing or taking off over the same airport, it may be possible to access the diurnal cycle of those parameters, as has been shown for O₃ in Petetin et al. (2016).

A visualisation service is available at www.iagos.org/products. This service displays the most recent profiles at worldwide airports as compared with the Copernicus Atmosphere Monitoring Service (CAMS) models on both global and regional scales. A subset of profiles over the RI-URBANS pilot cities is accessible under the category RI-URBANS (see Figure 9.3). Currently, the pilot cities available are Milano, Barcelona, Paris, and Zurich. In the first instance, they are compared with the CAMS global models, but will soon include the CAMS European AQ models on the regional scale. At the time of writing this guidance, profiles available are for O₃ and CO and a similar service is under development for NO_x.

Figure 9.3 also illustrates the vertical profile of O₃ as observed over Barcelona during the morning profile (a) with around 15 ppb of O₃ at the surface and the second profile b) with and around 55 ppb by noon.

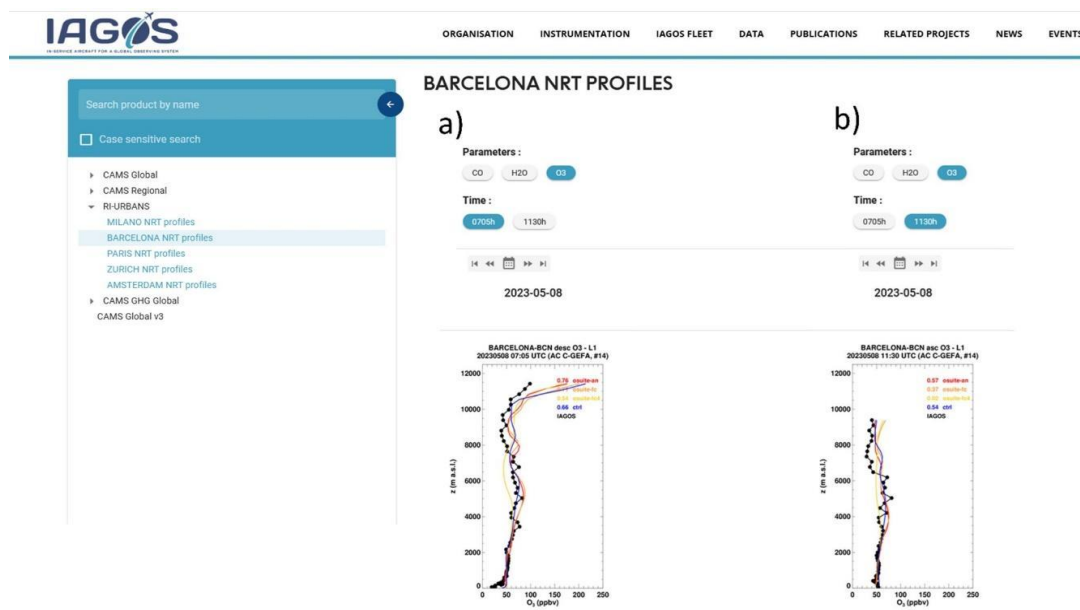


Figure 9.3: Combined screenshots of the visualisation service for profiles (available at www.iagos.org/products) over Barcelona. The diurnal O_3 profile as observed during the morning (a) and around noon (b).



10. URBAN MAPPING AND CITIZEN SCIENCE

Spatial mapping of novel AQ pollutants in urban areas can be done by using fixed and/or mobile measurements and by different types of modelling approaches. In RI-URBANS, the suggested urban mapping approaches are summarised in [ST12](#) (on deterministic modelling for mapping PM and UFP at urban scale), [ST13](#) (on mapping UFP and citizen science), and [ST16](#) (on mapping UFP using multiscale modelling approaches). The approach suggested by [ST12](#) and [ST16](#) has been commented on in the chapter on UFP-PNSD of this document. In this section only mapping according to ST13 recommendations are reviewed.

10.1 Mapping of novel AQ parameters

Different approaches can be used to assess urban variability of ambient concentrations of AQ pollutants at high spatial resolution for epidemiological studies and other applications. Mobile sensing platforms (equipped with high-, middle or low-cost sensors) and fixed (low-cost) sensor networks can be used as complementary tools to data from fixed regulatory AQMNs to map pollutant concentrations at a higher spatial density.

A distinction between mobile/fixed measurements and experimental designs with/without citizens, has been made in [ST13](#). The collected data can be processed and analysed using only measured data or using interpolation/modelling techniques like Land Use Regression (LUR)-based or machine learning models. The selected techniques used for data processing may have an impact on the required data collection approach. Each of the approaches has strengths and weaknesses. When selecting a method, the user needs to define the aim of the data collection and other considerations e.g. one may prefer to engage citizens as part of awareness training on AQ (Figure 10.1). Deliverables [D13](#) and [D14](#) from RI-URBANS show in more detail the methodologies and examples of mapping exercises done in the project (two examples are shown below).

Mobile monitoring can be used to map pollutants at a high spatial resolution with a limited number of instruments (in contrast to stationary monitoring) and can also use high-end or mid-end instruments exhibiting higher data quality than sensors. Mobile monitoring has some challenges because of the spatiotemporal nature of the collected dataset. Care should be taken during data collection and/or data processing in order to obtain representative results.

Low-cost fixed sensor networks have several limitations, especially for the real-time sensors which have shown varying performances. Good performance has been documented for low-cost diffusive (or passive) samplers. Diffusive samplers only provide weekly to monthly averages, but this may be sufficient for specific use cases. If so, diffusive samplers are the method of choice. While real-time sensors are able to provide very frequent measurements, they lack the accuracy of the substantially more expensive regulatory grade instruments and are greatly affected by extreme meteorological conditions (mainly high relative humidity). Therefore, a proper calibration and validation approach is needed. We recommend co-location performance evaluation to evaluate intra- and inter-sensor uncertainty and continuous calibration/validation under representative pollutant and meteorological conditions to compensate for seasonal effects from e.g. temperature and relative humidity. Regardless of that, they provide sensing opportunities that were not feasible before due to their portability and low cost. Using a spatially dense network can help in measuring and understanding the effect of sources that are usually “lost in the big picture”, such as the effect of hyper-local sources of pollution.

Figure 10.2 shows an example of the urban mapping of the concentrations of UFP and BC using mobile platforms and coupling these with LUR modelling for the city of Bucharest.

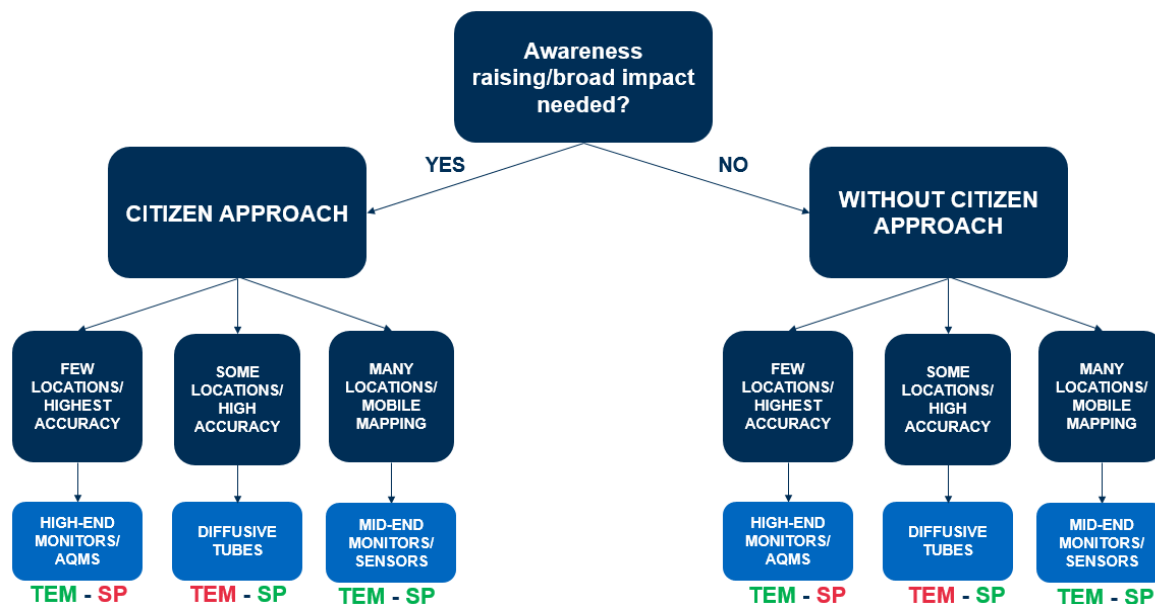


Figure 10.1: Pathways for selecting methods for urban mapping. TEM refers to temporal and SP to spatial. Green implies that the method performs well, red that it performs poorly for the spatial or temporal aspect.

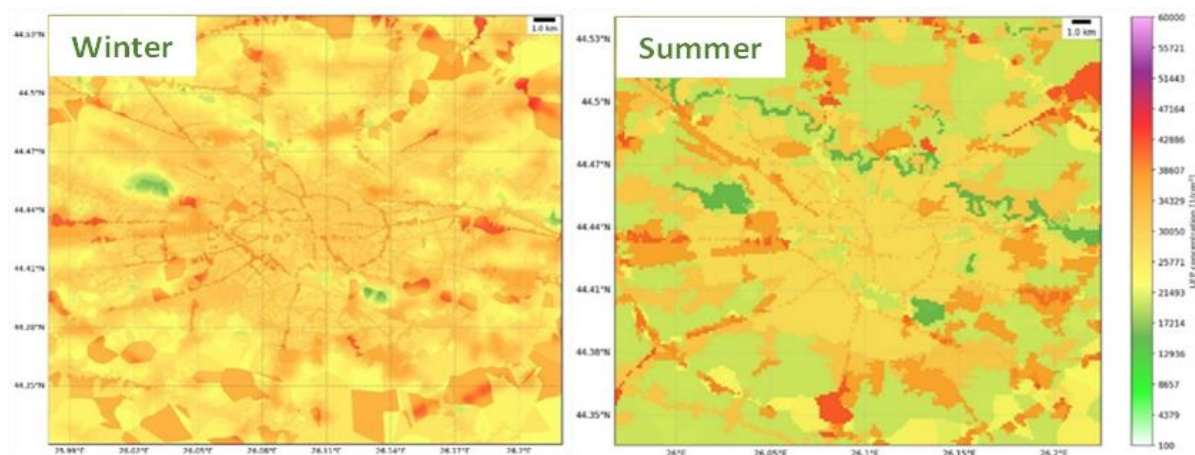


Figure 10.2: Model-measurement maps of UFP concentrations in Bucharest during winter and summer.

Overall conclusions are:

- Mobile monitoring can collect more datapoints but gives a snap-shot (no time trends). Repeated measurements, and associated sensitivity analysis, are needed to obtain representative results.
- Post-processing (data cleaning, rescaling) and model approaches have shown to be viable approaches to translate mobile measurements into actionable long-term exposure data.
- Targeted mobile monitoring makes it easier to compare different locations (collected at the same time) compared to opportunistic approaches (but are often more constrained in space and time).

- Opportunistic approaches mostly require less effort in data collection, result in large datasets but need proper processing to obtain representative results.
- Involving citizens can significantly contribute to awareness raising and obtain impact from the collected results, but will require more time and effort for communication, logistics and dissemination.
- Sensors can be deployed at a lower cost compared to mid- and high-end instruments but suffer from lower data quality. If a high temporal resolution is no requirement, diffusion samplers may be the preferred low-cost approach.
- Sensor calibration and compensation can significantly improve data quality.
- Different approaches for sensor calibration are used, varying from co-location calibrations with reference methods, or purely data-driven models including known covariates (e.g. temp, RH, O₃).

10.2 Mapping and involvement of citizen science

In RI-URBANS, the citizen science approach is summarised in **ST13** (Mapping UFP and citizen science). This approach can raise awareness of the urban citizens to air pollution issues. The **ST13** provides a comprehensive guidance on motivating the citizens to take part in AQ monitoring and provides best practices and recommendations. It further elaborates the added value of complementing stationary sensor networks with mobile measurements and provides analysis of the lessons-learned from the RI-URBANS pilot studies.

The NAQD (2024/2881) on ambient AQ and cleaner air for Europe connects to the European Union's objective towards zero pollution by 2050 facilitating a marked abatement of premature deaths due to air pollution. The NAQD merges the 2004 and 2008 legislation and responds to the recommendations from the WHO AQ Guidelines and to monitor additional air pollutants, such as UFP, PNC, NH₃, and BC concentrations. The European Member States have two years to transpose the requirements of the NAQD. The NAQD is aligned with “The European Green Deal”, which is an ambitious roadmap towards resource-efficient and competitive European society, which protects the well-being of the citizens e.g. from negative health impacts caused by poor AQ.

The EU set up stricter AQ standards and expanded the network of AQ observations, including the AQ supersite concept as well as separate requirements for the member countries to quantify the importance of air pollution hotspots. The NAQD further requires improved public involvement with informing the citizens about the AQ issues and their health implications and encourages and empowers community participation in AQ improvement efforts.

The added value of citizen observations comes from the capacity to supplement the official monitoring. The citizens can contribute e.g., by operating low-cost sensors to measure local AQ in their local neighbourhood, which increases spatial coverage and can identify pollution hotspots. These data can complement official AQMNs, filling gaps in areas lacking sufficient coverage. A specific weight should be placed on quality control of the data, for example allowing side-by-side measurements in official AQ monitoring sites, when applicable and feasible. Figure 10.3 shows, as an example, the mapping of the concentrations of BC in Rotterdam using mobile measurements with citizen involvement.

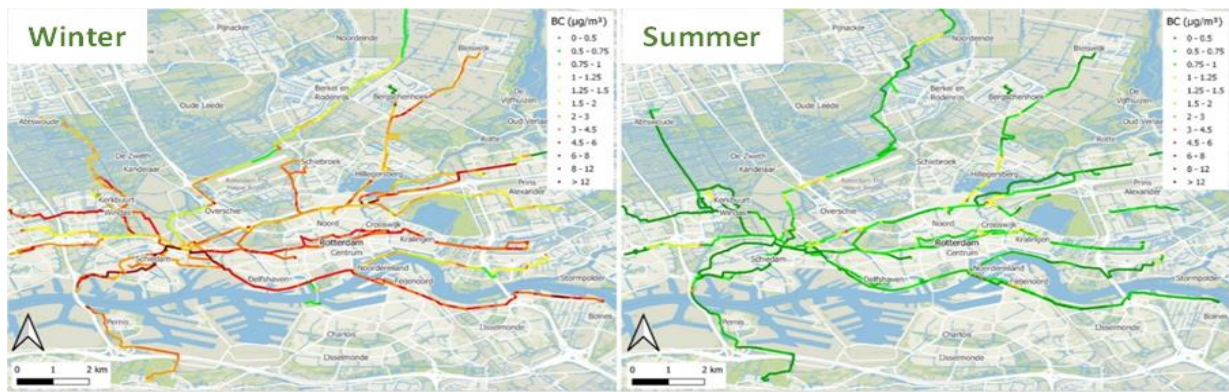


Figure 10.3: Average BC concentrations ($\mu\text{g}/\text{m}^3$) from mobile monitoring involving citizens in Rotterdam.

The citizen science activities foster awareness of pollution levels and its health impacts. This can drive personal behavioural changes, such as reduced car use or reduced waste burning. At the same time, citizen involvement empowers local communities as a whole. The citizen-generated data can empower communities to hold governments accountable for meeting AQ standards enabling grassroots movements to advocate for cleaner transportation, industry regulations, or urban greening. Citizen science should be connected to data validation and collaborative scientific activities with AQ experts. In an ideal case, citizen science projects can work alongside researchers and policymakers for example to validate AQ models. The collaboration with AQ scientists supports that the citizen-generated data meets scientific standards for reliability and usability.

In summary, citizen involvement in AQ monitoring supports AQ policy implementation by connecting the urban citizens with the decision makers in local, regional and national levels. This facilitates transparency of AQ policies. The citizen science projects can help policymakers fine-tune local strategies by providing hyper-local data that complements official AQMNs. The new data can lead to behavioural change in individual and community levels while allowing grassroots participation and sense of influencing steps towards cleaner air, improved public health, and a more engaged society.

11. FINAL CONSIDERATIONS

Concentrations of most air quality (AQ) pollutants decreased markedly in urban Europe during the last 20 years as a consequence of the European, national, regional and local AQ policies implemented since the first AQ EU Directive (1996/62/EC). Specific AQ directives, such as the ones on Industrial Emissions, Large and Medium Scale Combustion Plans and the ones fixing EURO emission standards for vehicles, among others, had a high impact in abating AQ pollutants. National and regional actions took place to implement these directives, as well as additional policies. At the local scale, low emission zones, congestion charges, policies on domestic sources, among others, contributed also to abate pollution in urban areas. These marked decreases of pollutants were reached mostly by reducing emissions of primary pollutants (those emitted directly from emission sources), although some secondary pollutants (those formed into the atmosphere from the reactions of primary ones), such as ammonium sulphate $(\text{NH}_4)_2\text{SO}_4$ also decreased.

Continuing decreasing current concentrations of AQ pollutants is a more complex target than before, because the need to decrease secondary pollutants, which is a difficult issue due to the non-linearity of many of their formation processes. Thus, to devise cost-effective AQ pollution measures a closer collaboration between the scientific community (including European Research Infrastructures, ESFRIs, but not only), AQ monitoring networks (AQMN) and policy makers is needed. RI-URBANS focuses on this gap between science and policy to support developing an advanced AQ assessment to improve AQ in urban Europe.

To abate AQ pollutants there are important scientific, technological and policy challenges that vary according to the specific pollutant.

Policy challenges: An example is NO_2 . The abatement technologies and measures to be implemented to abate this pollutant are known and available. No need for further research or technology developments, it is a matter of implementation of policies with cost-effective technological and non-technological measures. Another policy challenge is that major AQ policy is developed at European level, but implementation (such as measurements and AQ plans) takes place at national level. EU bodies such as AQUILA and ESFRIs (e.g. ACTRIS) are basic to maintain a harmonised implementation of AQ measurements. However, the policy relevance given in the different EU-17 states to AQ issues varies widely and this should be also harmonised.

Technology challenges: For some sectors, technology development to abate emissions is still a challenge. Examples are i) developing and implementing technologies to burn domestic biomass without causing AQ impairments, and ii) idem for the emissions of volatile organic compounds (VOCs) in biomass-combustion based industrial and power plants.

Scientific challenges: Examples are i) the elaboration of cost-effective measures for abating secondary pollutants (such as O_3 , and 70% of $\text{PM}_{2.5}$ in urban background of European cities, Amato et al., 2016) in an environment where VOCs, NO_x and O_3 concentrations are changing in time and space, under different climate scenarios; and ii) abating secondary $\text{PM}_{2.5}$ under an urban increase of O_3 (that generate more oxidation of gaseous pollutants and, accordingly, more secondary PM).

There is a number of advanced AQ pollutants/parameters that might contribute to a cutting-edge AQ assessment for tackling the above AQ scientific challenges, and also, in some cases, to adapt AQ monitoring

for a better protection of human health and to support further reviews of AQ standards and parameters to be included in the future AQ legislation.

In the 2021 proposal, RI-URBANS suggested as advanced AQ parameters the measurement of ultrafine particles (UFP=nanoparticles), particle number size distribution (PNSD), black carbon (BC), PM speciation, oxidative potential (OP) of PM, VOCs and ammonia (NH₃). These were included in the proposal for a new AQ Directive in October 2022, and moreover in the recently published new Directive on Ambient Air Quality for Europe (2024/2881/EC, NAQD).

RI-URBANS has produced [ST1](#) to [ST6](#) guidelines to help implement measurements on these advanced AQ pollutants/parameters. Furthermore, guidance on how to perform source apportionment analyses of these pollutants/parameters is provided in ST10 and ST11. Also, the first emission EU inventory for UFP-PNSD, non-exhaust vehicle PM emissions, and guidance on improving multiscale emission inventories, and on multiscale modelling and assessing the impact of emission sources in criteria and novel pollutants, are provided by ST15 and ST16. All these STs will support an advanced AQ assessment based on an accurate source apportionment of criteria and new pollutants, to identify causes of exceedances, and to evaluate the effect of policy measures implemented and assess future policies.

The measurement of novel air quality pollutants/parameters described in [ST1–ST6](#) shall be implemented at urban and rural air quality supersites in the EU, as outlined in Article 10 of the NAQD. AQUILA, the European network of National AQ Reference Laboratories, supports the implementation of existing EU air policy, and accordingly RI-URBANS and ACTRIS interacted with AQUILA and DG ENV from the European Commission for knowledge transfer and the co-design of the STs. It is also very important to connect these AQ monitoring efforts with those for urban greenhouse gases, and, when possible, using the same supersites for both types of measurements in connection with the RI-URBANS twin project PAUL-ICOS-cities (<https://www.icos-cp.eu/projects/icos-cities>).

Furthermore, RI-URBANS also recommends implementing measurements of vertical profiles in [ST7–ST9](#), which are not recommended in the NAQD, but might provide essential data for AQ assessment, forecasting and management. These include the boundary layer dynamics (including mixing layer height, among others), the vertical aerosol profiles to detect external PM contributions, and the available IAGOS vertical profiles of pollutants measured in several European cities by using equipped commercial aircrafts. Furthermore, [ST12](#) and [ST13](#) provide guidance on the urban mapping and citizens involvement to obtain accurate spatial and time urban variations of pollution and increase awareness of the problem.

We have presented these STs in numerous stakeholders' meetings and discussed the contents of many of these with AQUILA, and in a number of cases produced them with ACTRIS. This document demonstrates how to access the guidance documents and provides examples of the added value generated by implementing these STs. We hope that the AQMNs and other air quality stakeholders will find these Service Tools helpful in implementing the NAQD and further improving air quality across Europe.

12. REFERENCES

- Aas, W., Fagerli, H., Alastuey, A., Cavalli, F., Degorska, A., Feigenspan, S., ... & Yttri, K.E., 2024. Trends in Air Pollution in Europe, 2000–2019. *Aerosol Air Qual. Res.* 24, 230237. <https://doi.org/10.4209/aaqr.230237>.
- Amato, F., Alastuey, A., Karanasiou, A., Lucarelli, F., Nava, S., Calzolari, G., Severi, ... & Querol, X., 2016. AIRUSE-LIFE+: A harmonized PM speciation and source apportionment in five southern European cities, *Atmos. Chem. Phys.*, 16, 3289–3309; <https://doi.org/10.5194/acp-16-3289-2016>.
- AQEG-UK, 2020. Non-methane Volatile Organic Compounds in the UK. UK Air Quality Expert Group. DEFRA, 91 pp. https://uk-air.defra.gov.uk/library/reports.php?report_id=1003.
- Argyropoulos, G., Besis, A., Voutsas, D., Samara, C., Sowlat, M.H., Hasheminassab S., 2016. Source apportionment of the redox activity of urban quasi-ultrafine particles (PM_{0.49}) in Thessaloniki following the increased biomass burning due to the economic crisis in Greece. *Sci. Total Environ.*, 568 124-136, <https://doi.org/10.1016/j.scitotenv.2016.05.217>.
- Bates, J.T., Weber, R.J., Abrams, J., Verma, V., Fang, T., Klein, M., Strickland, M.J., ... & Russell, A.G., 2015. Reactive Oxygen Species Generation Linked to Sources of Atmospheric Particulate Matter and Cardiorespiratory Effects. *Environ. Sci. Technol.* 49, 13605–13612. <https://doi.org/10.1021/acs.est.5b02967>.
- Bond, T.C., Doherty, S.J., Fahey, D.W., Forster, P.M., Berntsen, T., DeAngelo, B.J. ... & Zender, C.S., 2013. Bounding the role of black carbon in the climate system: A scientific assessment. *J. Geophys. Res. Atmos.*, 118, 11, 5380-5552, <https://doi.org/10.1002/jgrd.50171>.
- Bones, D.L., Henricksen, D.K., Mang, S.A., Sionsior, M., Bateman, A.P., ... & Nizkorodow, S.A., 2010. Appearance of strong absorbers and fluorophores in limonene O₃ secondary organic aerosol due to NH₄⁺ -mediated chemical aging over long time scales, *J. Geophys. Res.*, 115, D05203, <https://doi.org/10.1029/2009JD012864>.
- Cape, J.N., Van der Eerden, L.J., Sheppard, L.J., Leith, I.D., Sutton, M.A., 2009. Evidence for changing the critical level for ammonia. *Environ. Pollut.*, 157, 1033-1037. <https://doi.org/10.1016/j.envpol.2008.09.049>.
- Canonaco, F., Slowik, J. G., Baltensperger, U., Prévôt, A. S. H., 2015. Seasonal differences in oxygenated organic aerosol composition, 2015. Implications for the emissions sources and factor analysis, *Atmos. Chem. Phys.*, 15, 12, 6993–7002, <https://doi.org/10.5194/acp-15-6993-2015>.
- Cassee, F.R., Morawska, L., Peters, A., 2019. Ambient ultrafine particles: evidence for policy makers. Thinking Outside the Box Report. [https://efca.net/files/WHITE%20PAPER-UFP%20evidence%20for%20policy%20makers%20\(25%20OCT\).pdf](https://efca.net/files/WHITE%20PAPER-UFP%20evidence%20for%20policy%20makers%20(25%20OCT).pdf).
- Diesch, J.M., Drewnick, F., Klimach, T., Borrmann, S., 2013. Investigation of gaseous and particulate emissions from various marine vessel types measured on the banks of the Elbe in Northern Germany. *Atmos. Chem. Phys.*, 13, 3603–3618, <https://doi.org/10.5194/acp-13-3603-2013>.
- Duminutti, P.A., Borlaza, L.J.S., Sauvain, J.J., Thuy, V.D.N, Houdier, S., Suarez, G., & Uzu, G., 2023. Source apportionment of oxidative potential depends on the choice of the assay: insights into 5 protocols comparison and implications for mitigation measures. *Environ. Sci.: Atmos.*, 3, 1497, <https://doi.org/10.1039/D3EA00007A>.
- Duminutti, P. A., Jaffrezo, J.-L., Marsal, A., Mhadhbi, T., Elazzouzi, R., Rak, C., Cavalli, F., Uzu, G., 2024. An interlaboratory comparison to quantify oxidative potential measurement in aerosol particles: challenges and recommendations for harmonisation. *Atmos. Meas. Tech. Discuss.*, <https://doi.org/10.5194/amt-2024-107>.
- Dufresne, M., 2022. Sources et déterminants des composés organiques volatils à Marseille [École des Mines de Douai] <https://theses.hal.science/tel-04018229>
- EEA, 2021. Sources and emissions of air pollutants in Europe. <https://www.eea.europa.eu/publications/air-quality-in-europe-2021/sources-and-emissions-of-air>
- EEA, 2022. Sources and emissions of air pollutants in Europe. <https://www.eea.europa.eu/publications/air-quality-in-europe-2022/sources-and-emissions-of-air>.
- EEA, 2023. Europe's air quality status 2023 Briefing no. 05/2023; <https://www.eea.europa.eu/publications/europes-air-quality-status-2023>.
- Garcia-Marlès, M., Lara, R., Reche, C., Pérez, N, Tobías, A., Savadkoohi, M., Beddows, D., ... & Querol X., 2024a. Inter-annual trends of ultrafine particles in urban Europe. *Environ. Int.*, 185, 108510, > <https://doi.org/10.1016/j.envint.2024.108510>.
- Garcia-Marlès, M., Lara, R., Reche, C., Pérez, N, Tobías, A., Savadkoohi, M., Beddows, D., ... & Querol X., 2024b. Source apportionment of ultrafine particles in urban Europe. *Environ. Int.*, 194, 109149, <https://doi.org/10.1016/j.envint.2024.109149>.
- GAW-WMO, 2017. WMO Global Atmosphere Watch (GAW) Implementation Plan: 2016-2023, Report, 228; https://library.wmo.int/?lvl=notice_display&id=19823#.X8ZYImhKhPY.
- Goldsmith, C.-A., Frevert, C., Imrich, A., Sioutas, C., Kobzik, L., 1997. Alveolar Macrophage Interaction with Air Pollution Particulates. *Environ. Health Perspect.* 105, 1191. <https://doi.org/10.2307/3433531>

- Grange, S.K., Uzu, G., Weber, S., Jaffrezo, J.L., Hueglin, C., 2022. Linking Switzerland's PM 10 and PM 2.5 oxidative potential (OP) with emission sources. *Atmos. Chem. Phys.*, 22, 10, 7029-7050. <https://doi.org/10.5194/acp-22-7029-2022>.
- Gu, S., Guenther, A., and Faiola, C., 2021. Effects of anthropogenic and biogenic volatile organic compounds on Los Angeles air quality, *Environ. Sci. Technol.*, 55, 12191-12201, <https://pubs.acs.org/doi/10.1021/acs.est.1c01481>.
- Hettelingh, J.P., Posch, M. and Slootweg, J., 2017, European critical loads: database, biodiversity and ecosystems at risk, CCE Final Report 2017, Coordination Centre for Effects, Bilthoven, Netherlands. <https://www.rivm.nl/bibliotheek/rapporten/2017-0155.pdf>.
- Hopke, P.K., Feng, Y., Dai, Q., 2022. Source apportionment of particle number concentrations: A global review. *Sci. Total Environ.*, 819, 153104, <https://doi.org/10.1016/j.scitotenv.2022.153104>
- Hopke, P.K., Querol, X., 2022. Is Improved Vehicular NOx Control Leading to Increased Urban NH3 Emissions? *Environ. Sci. Technol.*, 56, 11926-11927. <https://doi.org/10.1021/acs.est.2c04996>.
- Hopke, P.K., Chen, Y., Chalupa, D.C., Rich, D.Q., 2024. Long term trends in source apportion particle number concentrations in Rochester NY. *Environ. Pollut.* 347, 123708. <https://doi.org/10.1016/j.envpol.2024.123708>.
- In 't Veld, M., Alastuey, A., Pandolfi, M., Amato, F., Pérez, N., Reche, C., Via, M., ... & Querol, X., 2022. Compositional changes of PM2.5 in NE Spain during 2009–2018: A trend analysis of the chemical composition and source apportionment, *Sci. Total Environ.*, 795, <https://doi.org/10.1016/j.scitotenv.2021.148728>.
- In 't Veld, M., Pandolfi, M., Amato, F., Perez, N., Reche, C., Dominutti, P., ... & Uzu, G., 2023a. Discovering oxidative potential (OP) drivers of atmospheric PM10, PM2.5, and PM1 simultaneously in North-Eastern Spain. *Sci. Total Environ.*, 857, 159386. <https://doi.org/10.1016/j.scitotenv.2022.159386>.
- In 'tVeld, M., Seco, R., Reche, C., Pérez, N., Alastuey, A., Portillo-Estrada, M., ... & Yáñez-Serrano, A.M. 2024. Identification of volatile organic compounds and their sources driving ozone and secondary organic aerosol formation in NE Spain, *Sci. Total Environ.*, 906, 167159; <https://doi.org/10.1016/j.scitotenv.2023.167159>.
- Janssen, N.A.H., Gerlofs-Nijland, M.E., Lanki, T., Salonen, R.O., Cassee, F., ... & Krzyzanowski, M., 2012. Health effects of black carbon. World Health Organization. Regional Office for Europe. <https://iris.who.int/handle/10665/352615>
- Janssen, N.A.H., Strak, M., Yang, A., Hellack, B., Kelly, F.J., Kuhlbusch, T.A.J., ... & Hoek, G., 2014. Associations between three specific a-cellular measures of the oxidative potential of particulate matter and markers of acute airway and nasal inflammation in healthy volunteers. *Occup. Environ. Med.* 72, 49–56. <https://doi.org/10.1136/oemed-2014-102303>.
- Jung, J. G., Fountoukis, C., Adams, P. J. and Pandis, S. N., 2010. Simulation of in situ ultrafine particle formation in the eastern United States using PMCAMx-UF. *J. Geophys. Res.*, 115, D03203, <https://doi.org/10.1029/2009jd012313>.
- Krupa, S.V. 2003. Effects of atmospheric ammonia (NH3) on terrestrial vegetation: a review. *Environ. Pollut.*, 124, 2, 179-221. [https://doi.org/10.1016/S0269-7491\(02\)00434-7](https://doi.org/10.1016/S0269-7491(02)00434-7).
- Lewis, A. C., Evans, M. J., Hopkins, J. R., Punjabi, S., Read, K. A., Purvis, R. M., ... & Parrington, M., 2013. The influence of forest fires on the global distribution of selected non-methane organic compounds. *Atmos. Chem. Phys.*, 13, 851-867, <https://doi.org/10.5194/acp-13-851-2013>.
- Liu, X., Hadiatullah, H., Zhang, X., Trechera, P., Savadkoohi, M., Garcia-Marlès, M., ... & Querol X., 2023. Ambient air particulate total lung deposited surface area (LDSA) levels in urban Europe. *Sci. Total Environ.* 898, 165466, <https://doi.org/10.1016/j.scitotenv.2023.165466>.
- Liu, X. Lara, R., Dufresne, M., Wu, L., Wang, T., Monge, M., Reche, C., Di Leo, A., Lanzani, G., ... & Querol, X., 2024a. Variability of ambient air ammonia in urban Europe (Finland, France, Italy, Spain, and the UK). *Environ. Int.*, 185, 108519. <https://doi.org/10.1016/j.envint.2024.108519>.
- Liu, X., Zhang, X., Wang, T., Jin, B., Wu, L., Lara, R., Monge, M., Reche, C., ... & Querol, X., 2024. PM10-bound trace elements in pan-European urban atmosphere, *Environ. Res.*, 119630; <https://doi.org/10.1016/j.envres.2024.119630>.
- Liu, X. Zhang, X., Jin, B., Wang, T., Din, V.N.T., Jaffrezo, J.-L., Uzu, G., Dominutti P., ... & Querol, X., 2025a. Source apportionment of PM10 based on offline chemical speciation data in urban Europe. Under review
- Liu X., Zhang X., Dufresne M., Wu L., Wang T., Lara R., Seco R., Monge M., Yáñez-Serrano A.M., ... & Salameh T., 2025b, Variability of ambient volatile organic compounds in European cities, Under review.
- Liu, X., Zhang, X., Dufresne, M., Wang, T., Wu, L., Lara, R., Seco, Monge, M., ..., & Salameh, T., 2025c. Exploring the variations in ambient BTEX in urban Europe and its environmental health implications, *EGUsphere* [preprint], <https://doi.org/10.5194/egusphere-2024-2309> (*Atmos. Chem. Phys.*, Accepted).
- Lorentz, H., Janicke, U., Jakobs, H., Schmidt, W., Hellebrandt, P., Ketzler, M., Gerwig, H., 2019. UFP dispersion modelling at and around Frankfurt airport (FRA), Germany. 19th Int. Conf. on Harmonisation within Atmospheric Dispersion Modelling for Regulatory Purposes, Bruges, H19-082, https://www.harmo.org/Conferences/Proceedings/_Bruges/publishedSections/H19-082%20Helmut%20Lorentz.pdf.

- Mészáros, E., 1993. *Global and Regional Changes in Atmospheric Composition*, CRC Press 1st edition, ISBN-13:978-0873716628, 192 pp.
- Paatero, P., Tappert, U., 1994. Positive matrix factorization: A non-negative factor model with optimal utilization of error estimates of data values, *Environmetrics*, 5, 111–126; <https://doi.org/10.1002/env.3170050203>.
- Paatero, P., Hopke, P. K., 2009. Rotational tools for factor analytic models. *J. Chemometrics*, 23, 2, 91–100. <https://doi.org/10.1002/cem.1197>.
- Paciga, A. L., Riipinen, I., and Pandis, S. N., 2014. Effect of Ammonia on the Volatility of Organic Diacids, *Environ. Sci. Technol.*, 48, 13769–13775, <https://doi.org/10.1021/es5037805>.
- Pandolfi, M., Amato, F., Reche, C., Alastuey, A., Otjes, R.P., Blom, M.J., Querol, X., 2012. Summer ammonia measurements in a densely populated Mediterranean city. *Atmos. Chem. Phys.*, 12, 7557–7575. <https://doi.org/10.5194/acp-12-7557-2012>.
- Paraskevopoulou, D., Bougiatioti, A., Stavroulas, I., Fang, T., Lianou, M., ... & Mihalopoulos, N., 2019. Yearlong variability of oxidative potential of particulate matter in an urban Mediterranean environment. *Atmos. Environ.* 206, 183–196. <https://doi.org/10.1016/j.atmosenv.2019.02.027>.
- Patoulias, D., Fountoukis, C., Riipinen, I., and Pandis, S. N., 2015. The role of organic condensation on ultrafine particle growth during nucleation events. *Atmos. Chem. Phys.*, 15, 6337–6350, <https://doi.org/10.5194/acp-15-6337-2015>.
- Petetin, H., Thouret, V., Athier, G., Blot, R., Boulanger, D., Cousin, J.-M., ... & Cooper, O., 2016. Diurnal cycle of ozone throughout the troposphere over Frankfurt as measured by MOZAIC-IAGOS commercial aircraft, *Elem. Sci. Anth.*, 4:000129; <https://doi.org/10.12952/journal.elementa.000129>.
- Petetin, H., Jeoffrion, M., Sauvage, B., Athier, G., Blot, R., Boulanger, D., Cl... & Thouret, V., 2018. Representativeness of the IAGOS airborne measurements in the lower troposphere, *Elem. Sci. Anth.*, 6, 23; <https://doi.org/10.1525/elementa.280>.
- Petzold, A., Thouret, V., Gerbig, C., Zahn, A., Brenninkmeijer, C.A.M., ... & IAGOS-Team, 2015. Global-Scale Atmosphere Monitoring by In-Service Aircraft – Current Achievements and Future Prospects of the European Research Infrastructure IAGOS, *Tellus B*, 67, 28452; <https://doi.org/10.3402/tellusb.v67.28452>.
- Pietrogrande, M.C., Dalpiaz, C., Dell’Anna, R., Lazzeri, P., Manarini, F., Visentin, M., Tonidandel, G., 2018. Chemical composition and oxidative potential of atmospheric coarse particles at an industrial and urban background site in the alpine region of northern Italy. *Atmos. Environ.* 191, 340–350. <https://doi.org/10.1016/j.atmosenv.2018.08.022>.
- Reche, C., Viana, M., Pandolfi, M., Alastuey, A., Moreno, T., Amato, F., Ripoll, A., Querol, X., 2012. Urban NH₃ levels and sources in a Mediterranean environment. *Atmos. Environ.*, 57, 153–164. <https://doi.org/10.1016/j.atmosenv.2012.04.021>.
- Reche, C., Viana, M., Karanasiou, A., Cusack, M., Alastuey, A., Artiñano, B., ... & Rodríguez, S., 2015. Urban NH₃ levels and sources in six major Spanish cities. *Chemosphere*, 119, 769–777. <https://doi.org/10.1016/j.chemosphere.2014.07.097>.
- Reche, C., Perez, N., Alastuey, A., Cots, N., Pérez, E., Querol, X., 2022. 2011–2020 trends of urban and regional ammonia in and around Barcelona, NE Spain. *Chemosphere*, 304, 135347. <https://doi.org/10.1016/j.chemosphere.2022.135347>.
- Rivas, I., Beddows, D.C., Amato, F., Green, D.C., Järvi, L., Hueglin, C., Reche, C., & Kelly, F., 2020. Source apportionment of particle number size distribution in urban background and traffic stations in four European cities. *Environ. Int.*, 135, 105345, <https://doi.org/10.1016/j.envint.2019.105345>.
- Sandradewi, J., Prévôt, A.S.H., Szidat, S., Perron, N., Alfarra, M.R., Lanz, V.A., Weingartner, E., Baltensperger, U.R.S., 2008. Using aerosol light absorption measurements for the quantitative determination of wood burning and traffic emission contribution to particulate matter. *Environ. Sci. Technol.*, 42, 3316–3323. <https://doi.org/10.1021/es702253m>.
- Sarnat, S.E., Chang, H.H., Weber, R.J., 2016. Ambient PM_{2.5} and Health: Does PM_{2.5} Oxidative Potential Play a Role? *Am. J. Respir. Crit. Care Med.*, 194, 530–531. <https://doi.org/10.1164/rccm.201603-0589ED>.
- Savadkooji, M., Pandolfi, M., Reche, C., Niemi, J. V., Mooibroek, D., Titos, G., ... & Querol, X., 2023. The variability of mass concentrations and source apportionment analysis of equivalent black carbon across urban Europe. *Environ. Int. J.* 178. <https://doi.org/10.1016/j.envint.2023.108081>.
- Savadkooji, M., Pandolfi, M., Favez, O., Putaud, J., Eleftheriadis, K., Fiebig, M., Hopke, P.K., ... & Querol, X., 2024. Recommendations for reporting equivalent black carbon (eBC) mass concentrations based on long-term pan-European in-situ observations. *Environ. Int.* 185. <https://doi.org/10.1016/j.envint.2024.108553>.
- Scotto, F., Bacco, D., Lasagni, S., Trentini, A., Poluzzi, V., & Vecchi, R., 2021. A multi-year source apportionment of PM_{2.5} at multiple sites in the southern Po Valley (Italy), *Atmos. Pollut. Res.*, 12(11), 101192; <https://doi.org/10.1016/j.apr.2021.101192>.

- Shen, J., Taghvaei, S., La, C., Oroumijeh, F., Liu, J., Jerrett, M., Weichenthal, S., ... & Paulson, S.E., 2022. Aerosol Oxidative Potential in the Greater Los Angeles Area: Source Apportionment and Associations with Socioeconomic Position. *Environ. Sci. Technol.* 56, 17795–17804. <https://doi.org/10.1021/acs.est.2c02788>.
- Stacey B., Harrison R.M., Pope F., 2020. Evaluation of ultrafine particle concentrations and size distributions at London Heathrow Airport. *Atmos. Environ.*, 222, 117148, <https://doi.org/10.1016/j.atmosenv.2019.117148>.
- Sutton, M. A., Howard, C. M., Mason, K. E., Brownlie, W. J., Cordovil, C. M. d. S. (eds.), 2022. Nitrogen Opportunities for Agriculture, Food & Environment. UNECE Guidance Document on Integrated Sustainable Nitrogen Management. UK Centre for Ecology & Hydrology, Edinburgh, UK. https://unece.org/sites/default/files/2022-11/UNECE_NitroOpps%20red.pdf.
- Thouret, V., Clark, H., Petzold, A., Nédélec, P., Zahn, A., 2022. IAGOS: Monitoring Atmospheric Composition for Air Quality and Climate by Passenger Aircraft, in: *Handbook of Air Quality and Climate Change*, edited by: Akimoto, H., and Tanimoto, H., Springer Nature Singapore, Singapore, 1-14, ISBN 978-981-15-2527-8; https://doi.org/10.1007/978-981-15-2527-8_57-1.
- Trechera, P., Garcia-Marlès, M., Liu, X., Reche, C., Pérez, N., ... & Querol X., 2023. Phenomenology of ultrafine particle concentrations and size distribution across urban Europe. *Environ. Int.*, 172, 107744, <https://doi.org/10.1016/j.envint.2023.107744>.
- UNECE, 2007. Review of the 1999 Gothenburg Protocol. Report on the Workshop on Atmospheric Ammonia: Detecting Emission Changes and Environmental Impacts. Report to the 39th Session of the Working Group on Strategies and Review. ECE/EB.AIR/WG.5/2007/3. http://www.ammonia- ws.ceh.ac.uk/documents/ece_eb_air_wg_5_2007_3_e.pdf.
- Uzu, G., Sauvain, J.J., Baeza-Squiban, A., Riediker, M., Hohl, M.S.S., Val, S., Tack, K., Denys, S., Pradère, P., Dumat, C., 2011. In vitro assessment of the pulmonary toxicity and gastric availability of lead-rich particles from a lead recycling plant. *Environ. Sci. Technol.* 45, 7888–7895. <https://doi.org/10.1021/es200374c>.
- Van Damme, M., Clarisse, L., Whitburn, S., Hadji-Lazaro, J., Hurtmans, D., Clerbaux, C., Coheur, P., 2018. Industrial and agricultural ammonia point sources exposed. *Nature* 564, 99-103. <https://doi.org/10.1038/s41586-018-0747-1>.
- Venecek, M.A., Carter, W.P. & Kleeman, M.J., 2018. Updating the SAPRC Maximum Incremental Reactivity (MIR) scale for the United States from 1988 to 2010, *J. Air Waste Manage. Assoc.*, 68, 1301-1316; <https://doi.org/10.1080/10962247.2018.1498410>.
- Via, M., Minguiñón, M.C., Reche, C., Querol, X., Alastuey, A., 2021. Increase in secondary organic aerosol in an urban environment. *Atmos. Chem. Phys.* 21, 8323–8339, <https://doi.org/10.5194/acp-21-8323-2021>.
- Visentin, M., Pagnoni, A., Sarti, E., Pietrogrande, M.C., 2016. Urban PM2.5 oxidative potential: Importance of chemical species and comparison of two spectrophotometric cell-free assays, *Environ. Pollut.*, 219, 72–79, <https://doi.org/10.1016/j.envpol.2016.09.047>.
- Vörösmarty, M., Uzu, G., Jaffrezo, J. L., Dominutti, P., Kertész, Z., Papp, E., and Salma, I., 2023. Oxidative potential in rural, suburban and city centre atmospheric environments in central Europe. *Atmos. Chem. Phys.*, 23, 22, 14255-14269, <https://doi.org/10.5194/acp-23-14255-2023>.
- Vörösmarty, M., Hopke, P. K., Salma, I., 2024. Attribution of aerosol particle number size distributions to main sources using an 11-year urban dataset, *Atmos. Chem. Phys.*, 24, 5695–5712. <https://doi.org/10.5194/acp-24-5695-2024>.
- Weber, S., 2021. Source apportionment of the Oxidative Potential of aerosols, A visualisation tool and supplementary information, <http://getopstandop.u-ga.fr/>.
- Weber, S., Uzu, G., Favez, O., Borlaza, L.J.S., Calas, A., Salameh, D., Chevrier, F., ... & Jaffrezo, J.-L., 2021. Source apportionment of atmospheric PM10 oxidative potential: synthesis of 15 year-round urban datasets in France. *Atmospheric Chem. Phys.* 21, 11353–11378. <https://doi.org/10.5194/acp-21-11353-2021>.
- WHO, 2007. Health risks of heavy metals from long-range transboundary air pollution; <https://www.who.int/publications/i/item/9789289071796>.
- WHO, 2013. Review of evidence on health aspects of air pollution – REVIHAAP Project Technical Report. <https://doi.org/10.1007/BF00379640>.
- WHO, 2021. WHO global air quality guidelines: particulate matter (PM2.5 and PM10), ozone, nitrogen dioxide, sulfur dioxide and carbon monoxide. World Health Organization. 273 pp, <https://apps.who.int/iris/handle/10665/345329>.
- Wu, Y., Li, G., Yang, Y., An, T., 2019. Pollution evaluation and health risk assessment of airborne toxic metals in both indoors and outdoors of the Pearl River Delta, China, *Environ. Res.*, 179, 108793; <https://doi.org/10.1016/j.envres.2019.108793>.
- Zotter, P., Herich, H., Gysel, M., El-Haddad, I., Zhang, Y., Mocnik, G., Hüglin, C., ... & Prévôt, A.S.H., 2017. Evaluation of the absorption Ångström exponents for traffic and wood burning in the Aethalometer-based source apportionment using radiocarbon measurements of ambient aerosol. *Atmos. Chem. Phys.* 17, 4229–4249. <https://doi.org/10.5194/acp-17-4229-2017>.